FPL Energy
Seabrook Station

Root Cause Analysis for CR 02-08166

Evaluation Of "D" Steam Generator Tube Cracking

Team Manager	R. White
Team Leader	R. Lieder
Team	H. Legally (Westinghouse)
	R. Gold (Westinghouse)
	T. McGee (Westinghouse)
	W. McBrine (Altran)
	T. McKrell (Altran)
	T. Esselman (Altran)
	R. Ballinger (MIT)

FPL Energy

Seabrook Station

Root Cause Analysis for CR 02-08166

Evaluation Of "D" Steam Generator Tube Cracking

Team Manager	R. White
Team Leader	R. Lieder
Team	H. Legally (Westinghouse)
	R. Gold (Westinghouse)
	T. McGee (Westinghouse)
	W. McBrine (Altran)
	T. McKrell (Altran)
	T. Esselman (Altran)
	R. Ballinger (MIT)

Root Cause Report For
"D" Steam Generator Tube Cracking

Brief Description Of Condition

The steam generators at Seabrook were manufactured by Westinghouse and are Model F steam generators. They have thermally treated (TT) Inconel 600 tubes and stainless steel tube support plates (TSP) with concave quatrefoil TSP/tubing intersections. The U-bend region of the first ten rows of tubes also received an additional stress relieving heat treatment following bending.

Non-Destructive examination of steam generator (S/G) tubes at the Seabrook Station during Refueling Outage 08 identified axial flaws at tube support plate locations in fifteen tubes, all in S/G D. Two tubes (R5C62 and R9C63) were removed for testing and examination to characterize the flaws and to determine the cause of cracking. Of the fifteen tubes with indications, tube fabrication and S/G assembly records indicated that thirteen were from Heat #1374 and the remaining were identified as being from Heat #1456 and Heat #1457. The pulled tubes were from Heat #1374. Eddy current examinations showed that the cracking was limited to the inner ten tube rows. No cracking has been detected in any row higher than ten, or in any other steam generator. No cracking has been detected in any region of the tube other than at the tube support plates. Both hot and cold leg locations were affected over a range of elevations. This pattern is not typical of the stress corrosion cracking observed in plants with mill annealed alloy 600 tubing, and represents the first instance of cracking in alloy 600TT tubing. In addition, with only 9.6 Effective Full Power Years of Operation, Seabrook is one of the youngest plants in the United States with alloy 600 TT tubing.

CRACKING DESCRIPTION

Westinghouse and Altran Corporation performed laboratory examinations on tube intersections that contained axial indications. Fractographic and metallurgical examination of the flaws showed that the cracks were intergranular stress corrosion cracks (IGSCC) located within the lands of the quatrefoil support plate holes. The cracks initiated on the outside diameter (OD) and are oriented axially. Intergranular attack (IGA) was present within the first few grains on the tube OD surface.

ANALYSIS

In order to initiate and propagate cracks by IGSCC, a tensile stress, an aggressive chemistry, and a susceptible material must be simultaneously present. Each of these influences is discussed below.

Material Susceptibility

The two tubes that were pulled and examined exhibited a microstructure characterized by fine equiaxed grains with a significant variation in grain size as well as a non-uniform "banded" grain distribution. The microstructure was also characterized by intergranular and extensive intragranular carbide precipitation. This structure is considered to be not optimum but within the bounds of "normal" for thermally treated tubing. Modified Huey testing, with 25 weight percent nitric acid solution, showed that the tubes were not sensitized. The tubes examined had a carbon content of approximately 0.047% which is high in the range of acceptable carbon content.

Chemistry

There is no obvious source of an abnormal chemistry condition that would place the Seabrook conditions significantly outside of the "normal" bounds of the industry. Chemistry has consistently been maintained within EPRI guidelines. Surface deposits from the land regions of the tubes removed from service were analyzed. The deposits contained magnetite, copper, and other elements expected in S/G deposits. Copper oxide and lead, known to adversely influence cracking in alloy 600, were detected in the scale, but were not at unusually high levels. The lead was detected in a limited number of samples in very small amounts. The deposit chemistry was consistent with operation of a seawater-cooled plant with some copper present in the feed train.

Due to the tight crevice between the tube support plate land and the tube, the local chemistry in the crevice can be very different and much more aggressive than the surrounding bulk water chemistry. Concentration of contaminants will occur in these areas. In addition to crevice-like conditions in these regions, heat transfer can be influenced with the consequent development of super-heat. The combination of chemical concentration and superheat results in chemistry differences in these regions that is different from the bulk regions of the generator.

Since the cracking is isolated to the TSP land region, chemistry must play a role in at least localizing the cracking. Crevice concentration is a phenomenon that cannot be eliminated despite efforts to minimize the effects in the Model F steam generators through use of a quatrefoil TSP/tube intersection design. In this case, there is no evidence that the chemistry alone dominated the cracking process. However, it is probable that it did localize the cracking that was dominated by other factors. Further, the cracking has only been detected in the inner ten rows of one generator. If chemistry were a predominant cause of cracking, cracking in such a limited region would not be expected.

Tensile Stresses

Axial IGSCC cracks require a tensile hoop stress for propagation. Sources of tensile hoop stress include operating and residual stresses. A primary source of hoop tensile stress in the Seabrook tubes is from internal pressure and thermal conditions. Combined pressure and thermal stresses result in hoop stresses of approximately 10 ksi. This stress level is not large enough to cause initiation or propagation of the observed cracks.

Residual stresses can also contribute to crack initiation and growth. Possible sources of residual stresses in the TSP region include those from tube manufacturing (straightening and polishing), steam generator fabrication (misalignment during insertion), or operation (denting and tube locking in the land due to deposit accumulation). Misalignment during S/G fabrication would be expected to leave only small axial residual stresses. There was no evidence of denting or tube locking. Stresses from tube fabrication were further investigated.

The thermal treatment process is expected to relieve tube manufacturing related residual stresses within the straight length of the tube in addition to its primary function, establishing a stabilized microstructure. Residual stress measurements on the tubes removed from service indicated that the average tensile hoop residual stresses in regions close to the cracks was approximately 22 ksi. This is larger than expected for any final tubing condition especially thermally treated tubing.

Due to a typically nonlinear through wall stress distribution, actual surface residual stresses are likely to be higher than that measured. It is highly probable that residual stresses in the neighborhood of the material yield strength (65ksi) were present during operation. Normally processed thermally treated tubing is expected to have hoop residual stresses of approximately 3 ksi.

Testing of archival thermally treated tube material, obtained from the same heats as those effected by the cracking, contained residual stress at the 1-2 Ksi level, as expected.

The threshold of stress required to initiate cracks in thermally treated tubing is at least 40 ksi. The threshold stress for crack propagation is not well defined in thermally treated tubes due to limited industry experience. However, the residual stresses of the magnitude measured combined with the normal operating stresses is considered sufficient to cause the cracking detected at Seabrook. The source of the high residual stress is either an abnormal thermal treatment that was not effective in removing the residual stresses, or a process such as tube straightening, that occurred after the thermal treatment, and that was not subsequently stress relieved as specified in the fabrication procedures.

ROOT CAUSE

The cause of the cracking detected in the Seabrook D steam generator is high residual stress caused by inappropriate tube processing. A contributing factor, although not detectable in this study, is the known concentration of secondary plant water chemistry contaminants in the quatrefoil lands. The high residual stress only causes cracking in the presence of an aggressive chemistry as typically exists at the quatrafoil lands. However, the corrosive environment that exists at Seabrook, in the lands, is not unusually high compared to other pulled tube environmental results.

EXTENT of SUSCEPTIBILITY

The residual stresses that are present are caused by cold work in the material that was not relieved by subsequent heat treatment. As eddy current (EC) signatures are influenced by cold working, these signatures can be used to help bound the number of tubes that may be susceptible to cracking. In addition to the residual stress measurements the presence of cold work is further supported by the high (above the CMTR values) measured yield stress for the pulled tubes. An examination of EC data for all tubes in the first ten rows of all four steam generators showed that all fifteen tubes that were plugged showed very distinct EC signatures. An additional four tubes exhibited similar signatures and they were also in S/G D. There were no other tubes in any of the other generators with similarly distinct EC signatures.

Tubes in rows 11-59 were not subject to U-Bend stress relief, therefore the EC signals contain a different pattern than the low row tubes, making the EC technique for diagnosing residual stress more difficult. In evaluating the EC signal in these tubes, the cold worked section in the U-Bends is utilized to discriminate between tube rows, and to identify abnormal EC signal offsets. There are no outliers identified. Absence of observed corrosion damage in the outer rows also suggests that no tubes are susceptible.

SG-SGDA-02-37
Revision 1

Seabrook Tube Cracking
Root Cause Evaluation Report

September 2002

Westinghouse Electric Co., LLC
H.O. Lagally
R.E. Gold
A.R. Vaia
W.A. Byers

Change Record

Rev.	Change	Signature
0	(Original issue)	na
1	Edit to include Seabrook/ALTRAN review comments; add Table 4.2 include Appendix B; add Appendix D	Author: [signature] 11/4/02 Verified: [signature] 11/5/02 Approved: [signature]

For/R.J. Sterdis 11/5/02

Executive Summary

Potential causes of ODSCC observed at 42 tube support plate intersections, including both hot leg and cold leg indications, on 15 tubes in steam generator D at Seabrook during the spring 2002 outage were examined. The three principal causative factors of stress corrosion cracking – environment, stress and material microstructure – were examined. Testing of two of the degraded tubes, one hot leg and one cold leg, removed from the steam generator showed an elevated residual stress in both of these tubes. A detailed review of manufacturing processes and records failed to identify the specific source of the residual stress. Metallurgical examination of the pulled tubes showed that the microstructure of the material was not optimal, but consistent with the expected range of microstructure for thermally treated tubing. Analysis of the deposits accumulated at the tube support plate intersection, on the tube surface and on the crack faces did not reveal an unusually high concentration of corrosive agents. In the absence of significant concentrations of specific corrodents, it was concluded that the stress state of the material was a significant, measurable contributor to the observed cracking in the presence of unidentified corrosives in the secondary coolant environment in the steam generators.

All of the degraded tubes exhibited a common eddy current signal that was different from all but four of the remaining tubes in rows 1 through 10 of SG-D. None of the tubes in the other three steam generators exhibited this signal. This signal provides a reasonable basis for limiting the population of susceptible tubes in rows 1 through 10 of the steam generators, and, with further development, may provide a sound basis for identifying susceptible tubes in rows 11 through 59.

Table of Contents

Seabrook Tube Cracking-Root Cause Evaluation Report

1. Introduction

When a steam generator (SG) tubing degradation mechanism is discovered that was previously unreported and is unexpected at a plant, a root-cause evaluation must be performed to determine the circumstances resulting in that degradation. Reference 1-1 requires that a root cause determination be made for degradation detected during an inspection.

In May 2002, during OR08, Seabrook reported crack-like indications, of OD origin on a number of tubes in SG-D. Destructive examination of two tubes pulled from SG-D established that the indications were, indeed, cracks originating from the OD of the tube that were characterized as stress corrosion cracking (ODSCC). Tube cracking has not previously been reported among the domestic Model F and F-type SGs that utilize Alloy 600TT tubes, many of which have operated significantly longer than has Seabrook. A root cause evaluation was performed to identify the contributing factors for the unexpected cracking at Seabrook. This report summarizes the root cause analyses performed for the Seabrook SG-D tube-cracking event.

The essential elements required for ODSCC to occur are:

- A corrosive chemistry environment
- Stress in the material
- Material microstructure susceptible to corrosion in the specific applicable environment

The root cause evaluation focused on these three areas. In addition, the root cause analysis considered the potential extent of the degradation over the longer term.

A background summary of the field inspection and other pertinent information to assist the root cause evaluation is provided in Section 3.

Two tubes removed from SG-D for destructive examination were extensively tested in the laboratory to confirm the field eddy current (EC) results, obtain visual inspection data, metallurgical data and chemical data for the tube and the deposits on the tubes. These tests are reported in Reference 1-2, and are summarized in Sections 4 and 5.

The tube manufacturing process was evaluated to determine if the tube manufacturing could have caused, or contributed to, the observed degradation. Available records were researched to assess if the steps of the manufacturing procedures were properly executed, and if any other SG in operation could provide additional operational experience to assist the root cause evaluation. Development records and prior laboratory and field studies were examined to provide a comparison basis for the results of the destructive examinations. These studies are discussed in Section 6.

Plant operations were examined over the history of the plant to determine if there were any significant operational events that could have caused, or contributed to, the reported degradation. The specific focus of this investigation was any chemistry excursion in the secondary system that might have created an aggressive environment. This examination is discussed in Section 7.

Independent testing and overview functions were provided by ALTRAN Corporation under contract to Seabrook. ALTRAN participation in the root cause evaluation provided corroborating information for various tests performed and a continuing, independent review function. The ALTRAN report of its activities is included as Appendix B.

References

1-1. EPRI TR-1003138; PWR Steam Generator Examination Guidelines: Revision 6 (Draft); May 2002
1-2. Westinghouse SG-SGDA-02-35; "Seabrook Steam Generator Tube Examination"; (to be issued)

2. Summary and Conclusions

Residual stresses, at levels higher than found in archived thermally treated tubes, in conjunction with a generally corrosive environment in the deposits at the tube support plates, are considered to have caused the cracking noted in the steam generator tubes A characteristic eddy current signatures was found in the degraded tubes, which may be used to identify the tubes that had high residual stresses in the tubes in rows 1 through 10. Four non-degraded tubes were found in rows 1 through 11 with the same eddy current signal as the fifteen degraded tubes. The eddy current signals for the tubes in rows 11 through 59 were found to be similar, without unique individual deviations; therefore, it was inferred that none of the longer tubes exhibited high residual stress.

The essential facts of the Seabrook cracking are:

- Crack-like indications were reported at 42 tube-to-TSP intersections on 15 tubes between rows 4 and 9 in SG-D. No indications were reported in the other three SGs.
- Thirteen of the fifteen degraded tubes are from one heat of material, NX1374. One of the tubes is from Heat NX1456 and another is from Heat NX1457.
- Indications were reported on both the hot leg (HL) and cold leg (CL) of the tubes. Initially identified as distorted support plate indications (DSI) in the bobbin program, these indications were confirmed by the +Point probe, and re-confirmed using the Ultrasonic Test Eddy Current (UTEC) system.
- No indications were reported at the top of the tubesheet tube expansion region where initial cracking would be expected.
- Seabrook had accumulated approximately 9.7 EFPY of operation at OR08.

Metallurgical analysis of tubes pulled from SG-D provided the following information:

- Axial ODSCC was confirmed on the two tubes with indications pulled from SG-D. The cracks occurred at the TSP intersection quatrefoil lands, in some instances at more than one land. The cracks did not extend beyond the top and bottom of the TSPs.

- The tensile properties of the pulled tubes are higher than the properties reported on the certified material test reports (CMTR). Tube pull forces indicate that this is not a result of cold work introduced during the tube removal process.
- The pulled tube material is not sensitized.
- The chemistry of the pulled tube material is within the specified limits in the applicable tubing specification.
- The microstructure of the pulled tube material (Heat NX1374) is consistent with the expected range of microstructures for material that is within the material specification requirements and processed according to the approved procedures, but is not considered an optimum microstructure.
- The pulled tubes have elevated residual hoop stress compared to expected residual stress for either thermally treated or mill annealed tubing. The residual stress is approximately the same on both the HL and CL tubes, and approximately the same along the length of the tubes.
- There is no significant variation in the hardness along the length of the pulled tubes.

Related Metallurgical Analyses:

- The microstructure of an archived tube from Heat NX1374 is similar to the microstructures of the pulled tubes.
- The residual stresses in the archived tube from Heat NX1374 are lower than those measured in the pulled tubes, and similar to those expected in thermally treated tubing.
- The microstructures of archived specimens of the other two heats of material represented among the degraded tubes, Heats NX1456 and NX1457, are well within the range of expected microstructures for thermally treated Alloy 600. The microstructure of Heats NX1456 and NX1457 is better than the microstructure of Heat NX1374.

Chemical analysis of the deposits on the pulled tubes provided the following information:

- The deposit chemistry is consistent with that determined for other pulled tubes.

- Very small amounts of lead and copper were detected on the surface of the tubes and on the crack faces. The concentration of both of these elements is consistent with that found in other pulled tube examinations.

Review of the operational history of Seabrook provided the following data:

- Seabrook secondary side chemistry has been within applicable guidelines during the history of the plant except for several instances of seawater ingress that have occurred.
- The crevice chemistry is believed to be slightly alkaline.

Review of manufacturing and inspection records provided the following information:

- Thermal treating records indicate that the tubes were thermally treated, and stress relief of the U-bends in rows 1 through 10 was performed.
- There were no documented events during the manufacture of the tubes or assembly of the SGs that could have caused high residual stresses.
- All of the degraded tubes display a characteristic eddy current trace (i.e., "signature") that is unique when compared to the eddy current signal for the remainder of the tubes in rows 1 through 10. In addition to the 15 reported degraded tubes, four other row 10 and lower tubes (1- heat NX1374, 1- heat NX1457, 1- heat NX1439, and 1- heat NX1790) in SG-D display the same EC signature characteristic. None of the row 10 and lower tubes in the other three SGs displays this characteristic.
- The EC signature does not provide conclusive information regarding the potential for degradation of the tubes in Rows 11 through 59. However, the average voltage offset of the u-bend signal compared to the straight leg signal provides a good correlation with the u-bend radius. It is not possible to estimate the level of residual stress from the eddy current signature; however the signature comparison suggests that tubes in rows 11 and higher are from a common population and do not have unusually high residual stresses.

Conclusions:

1. The residual stress in the pulled tubes is considered to be a significant contributing factor to the cracking. No specific source of the residual stress has been identified. However, the residual stress is about the same over the length of the HL and CL. Since no straightening is performed after making the u-bends and the residual stress is approximately the same over both the HL and CL, it could be speculated that the tubes may have been straightened after thermal treatment (before u-bending) without subsequent thermal treatment prior to bending the U-bends. A detailed review of the tubing manufacturing process established that there were controls in place to prevent process deviations that could result in specific issues of this type. Thus, it was concluded that the condition was an isolated incidence and not a systematic process failure.
2. After the rows 1 through 10 u-bends were formed, stress relief was performed local to the u-bends, which would have relieved the stresses in the u-bend and not the straight length. This provides the basis for the ability to detect the change in residual stresses in the rows 1-10 tubes for tubes with elevated residual stress after the straight tube manufacturing process. Other tubes from all three heats represented among the 15 degraded tubes in row 10 and lower tubes that did not show the high residual stress signature in the eddy current testing did not crack.
3. No unusual environmental conditions were identified in the deposit analysis for the pulled tubes or during the review of the operating history of the plant. Small amounts of lead and copper oxide, comparable to the level identified in other pulled tube analyses, were identified in the chemical analyses and these are known to be contributing factors in corrosion of Alloy 600TT. Historically, failure to identify specific aggressive constituents in tube deposits on pulled tubes is not unusual, and should not be construed negatively or positively. Testing has shown that Alloy 600TT will crack under the stress and specific chemical environments.
4. Although the pulled tubes exhibit elevated residual stress along the length of the tubes, another known region of high residual stress in all of the tubes is the tube expansion transition. The TTS on the hot leg is also the highest temperature region of the tubes. That the tubes did not exhibit degradation at the TTS inside the sludge collars suggests that a relatively more aggressive environment existed at the TSPs.

5. For the tubes in Rows 1 through 10, a unique characteristic of the eddy current signal is considered to be a good indicator of the tubes that may have a similar material condition to that of the degraded tubes. All 15 of the degraded tubes exhibit this signature, and 4 other tubes in SG-D also exhibit the signal characteristic. None of the low row (rows 1-10) tubes in SGs A, B and C exhibits this characteristic.

3. Background Information

Inspection Summary

In May 2002, during the OR08 outage, tubes at 42 Tube Support Plate (TSP)/tube intersections were reported with crack-like indications. Some of the intersections were reported to contain multiple indications. Originally reported as distorted support plate indications (DSI) from the 100% bobbin inspection program, these indications were confirmed as crack-like with the +Point rotating probe according to the inspection plan. Further independent confirmation was provided that these indications were crack-like by application of the Ultrasonic Test Eddy Current (UTEC) system.

The indications were reported at the intersections with the first support plate above the flow distribution baffle (FDB) (02H in the eddy current inspection database) through the fifth TSP above the FDB (06H) on the hot leg of SG-D, and between 03C and 05C on the cold leg of SG-D (See Figure 3-1). No indications were reported in SGs A, B and C, which were also 100% inspected during OR08.

Table 3.1 is a summary of the inspection results for these indications. The 42 TSP intersections were confined to 15 tubes. Some intersections had more than one indication, so the actual number of reported indications was greater than 42.

There are a number of unusual aspects to the indications:

1. Seabrook has significantly less operating time than many of the other Model F SG plants that have not observed tube cracking; thus, these indications were unanticipated.
2. Indications were detected in only SG-D.
3. Indications were found at the TSP intersections and not at the top of the tubesheet (TTS) expansion transition where initial cracking would be expected.
4. Indications were reported on both the HL and CL. In all cases where a CL indication was reported, a HL indication was also reported on the same tube. CL cracking at the same time as HL cracking is unexpected due to the lower temperature on the CL.
5. All indications were confined to rows 4 through 9 (see Figure 3-2).

6. Multiple TSP intersections on the same tube were reported in most cases. The indications on only 3 of the 15 tubes reported were confined to a single TSP intersection.

Prior EC History of Degraded Tubes

All of the 42 TSP intersections observed with cracks during the OR08 inspection were reported as NDD from the bobbin inspection during OR06 in October 1999. After the indications were identified during OR08, a lookback evaluation of the data from OR06 showed the presence of a non-callable signal at 25 of the 42 locations. The remaining 17 intersections exhibited no signal during the OR06 inspection.

Tube Pull

Two tubes were removed (pulled) from SG-D at OR08. Selection of the tubes for removal was based on recovering the largest indication, obtaining as large a population of degraded and un-degraded intersections as possible, and obtaining both HL and CL indications. The tube pull plan included removing 3 tubes, R4C63-HL, R5C62-HL and R9C63-CL; this plan was later adjusted to 2 tubes when tooling issues were encountered during the pulling of R4C63. Destructive examination of these tubes was performed and is summarized in Section 4.

After removal of the tube-to-tubesheet weld and TIG relaxation of the hydraulic expansion region, the tubes were pulled through the tubesheet. R5C62 HL tube was cut below the 6th tube support plate and removed in eight segments. The pull force for R5C62 was 3,536 lbs and dropped to essentially zero after initial breakaway. R9C63 CL tube was cut below the 5th tube support plate and removed in six segments. The pull force for R9C63 was 3,373 lbs and dropped to essentially zero after initial breakaway.

Tube Material Heat Identification

The tubes for a SG are identified at the first level by the shop order number of a specific SG. Generally, the full complement of tubes for a SG was identified by a single "set" number; however, in some cases, the full complement of tubes for a SG was assembled from several different sets. A record of the set number or set numbers that correlate to each shop order number (i.e., each SG) was maintained so that the origin of all tubes could be maintained. Each set number was related to a "test number" assigned by the SG manufacturing plant to track the tubing in a set. It is not uncommon that several different tensile values can exist for the same heat, since individual heats of material were used to manufacture tubes for several different tube sets.

During installation of the tubes in the SGs, the heat number of each tube was recorded against the location, by row and column number, in which the tube was installed. This record is called the "Tubing Log", which can be used to look up specific tube heat numbers, heat chemistry and tensile test data. In Section 8 of Reference 3-1, the row and column convention was determined by a drawing that identified the Row-1: Column-1 tube location as the innermost tube nearest to the manway side of the tubesheet. Thus, the row/column locations of the tubing logs are based on the convention in Reference 3-1. The tubing logs thus created were computerized and provided to Seabrook by Reference 3-2.

A standard convention for field inspection Row/Column reference was identified (circa 1985) after the SGs were put into service and a supplement was issued to Reference 3-1. The field inspection standard uses the nozzle side of the tubesheet primary surface as the reference for R1C1. Eddy current inspection records are maintained according to this convention. Since tubing logs were not a commonly used record at the time, the supplement ignored the inconsistency with the tubing logs. Consequently, the EC database and the tubing logs are mirror images of each other. For example, the R1C1 tube in the EC database is, in fact, the R1C122 tube in the tubing logs, and the R1C62 tube in the tubing log is, in fact the R1C61 tube in the EC database. A simple conversion algorithm can be used to convert the tube column numbers from EC notation to tube log (TL) notation (the row numbers do not change):

$$C_{TL} = 61 - (C_{EC} - 62) = 123 - C_{EC}$$

Table 3.2 summarizes the degraded tubes reported from the OR08 inspection, converts the tube references to the tubing log reference, and provides the heat numbers of the degraded tubes. Table 3.3 provides the heat chemistry and room temperature mechanical properties for the affected heats based on the certified materials test reports (CMTR) for the heats identified.

References

3-1 TTMC-1440-C316; Westinghouse Technical Manual; Vertical Steam Generator Instructions for Seabrook.

3-2 Westinghouse Letter, LTR-SGDA-01-198 "Transmittal of Seabrook Tubing Logs"; August 2001.

Table 3.1 Seabrook OR08: Tubes Reported with Crack-like Indications

Row	Col	Location	Inch	Bobbin			+Point		
				Call	Volts	Rank	Call	Volts	Rank
4	63	02H	0.02	DSI	0.84	3	SAI	1.14	2
		04H	0	DSI	0.46	9	SAI	0.57	10
		03H	-0.07	DSI	0.21	28	SAI	0.45	28
4	65	04H	0.12	DSI	0.4	12	SAI	0 63	6
		06H	0	DSI	0.37	13	SAI	0.58	9
		02H	-0.05	DSI	0.36	15	SAI	0.36	35
		03H	0.07	DSI	0.2	31	SAI	0.28	42
5	62	04H	0.13	DSI	0.91	1	SAI	1.24	1
		03H	0.27	DSI	0.59	5	SAI	0.47	20
		05H	-0.11	DSI	0.21	29	SAI	0.33	38
		03C	-0.11	DSI	0.41	11	SAI	0.32	39
5	80	03H	0.19	DSI	0.45	10	SAI	0.72	3
		04H	-0.24	DSI	0.54	7	SAI	0.56	11
		03C	0.19	DSI	0.18	36	SAI	0 47	22
5	81	03H	0.03	DSI	0.11	42	MAI	0 42	31
		04H	0	DSI	0.12	39	SAI	0.31	40
		06H	-0 46	DSI	0 2	32	SAI	0.3	41
5	82	05C	0	DSI	0.12	40	SAI	0.52	15
		04H	0	DSI	0 25	19	SAI	0.47	21
		03H	-0.08	DSI	0.22	23	SAI	0.46	24
5	83	05C	0.08	DSI	0.22	24	SAI	0.59	8
		04H	0.05	DSI	0.33	17	MAI	0.54	13
		03C	0.03	DSI	0.12	41	SAI	0.5	19
		02H	0.05	DSI	0.24	21	SAI	0.43	29
5	86	02H	-0.19	DSI	0.22	25	SAI	0.46	25
		03H	0.11	DSI	0.22	26	MAI	0.37	34
5	88	03H	-0.08	DSI	0.25	20	SAI	0.45	27
6	81	03H	0.08	DSI	0.21	30	SAI	0.68	4
6	85	03H	-0.05	DSI	0.19	34	SAI	0.43	30
9	24	04H	0.26	DSI	0.62	4	SAI	0.51	16
		03H	0.05	DSI	0.37	14	SAI	0 51	17
9	26	04H	0.24	DSI	0.5	8	SAI	0.39	33
		03H	0	DSI	0.32	18	SAI	0 36	36
9	62	05H	-0.16	DSI	0.89	2	SAI	0 65	5
		06H	-0.13	DSI	0.19	35	SAI	0.55	12
		02H	0.03	DSI	0.22	27	SAI	0.5	18
		04H	0	DSI	0.17	37	SAI	0.47	23
		03H	-0.05	DSI	0.2	33	SAI	0.46	26
9	63	04C	0.05	DSI	0.55	6	SAI	0.59	7
		05H	0.03	DSI	0.34	16	SAI	0.52	14
		03H	-0.05	DSI	0.14	38	SAI	0.4	32
		04H	0.08	DSI	0.24	22	SAI	0.35	37

Table 3.2
Degraded Tube Row and Column and Material Heat Identification

EC Database (OR08) ID		Tubing Log ID		Heat
Row	Col	Row	Col	
4	63	4	60	1456
4	65	4	58	1374
5	62	5	61	1374
5	80	5	43	1374
5	81	5	42	1374
5	82	5	41	1374
5	83	5	40	1374
5	86	5	37	1374
5	88	5	35	1374
6	81	6	42	1374
6	85	6	38	1457
9	24	9	99	1374
9	26	9	97	1374
9	62	9	61	1374
9	63	9	60	1374

Usage of the Degraded Tube Heats at Seabrook (No. of Tubes)					
Heat	SG-A	SG-B	SG-C	SG-D	Total
1374	38	18	88	50	194
1456	90	124	33	93	340
1457	153	103	115	101	472
1439 (1)	28	199	47	48	322
1790 (1)	34	1	221	68	324
Total	343	445	504	360	1652

(1) Tubing from these heats were not degraded but were found to have the distinctive EC signature common to the degraded tubes (See Section 5)

Table 3.3

Tube Heat Chemistry and Strength Properties

CMTR Properties						Westinghouse Lab. (Heat 1374)		Independent Lab (Heat 1374)	
Heat	**1374**	**1456**	**1457**	**1439(1)**	**1790(1)**				
C	0.042	0.033	0.029	0.04	0.031	0.046	0.048	0.047	0.048
Ni	76.03	74.23	74.27	74.89	75.27	74.34	74.4	75.62	75.82
Fe	8.48	9.38	9.78	9.44	8.93	8.71	8.61	8.22	7.99
Cr	14.81	15.69	15.2	14.96	14.95	15.03	15.05	15.87	15.3
Mn	0.23	0 23	0.22	0.26	0.24	0.22	0.22	0.2	0.2
Mo						0.41	0.42		
Ti	0.21	0.29	0.22	0.21	0 21	0.23	0.24	0.22	0.25
Nb						0.3	0.3		
Al	0.18	0.13	0.25	0.20	0.26	0.19	0.19	0.13	0.14
Si	0.17	0.16	0.2	0.08	0.18	0.15	0.17	0.44	0.44
Pb						<0.001	<0.001		
S	0.001	0 002	0.003	0.001	0.003	0.002	0 001	<0.001	<0.001
Cu	0.24	0.28	0.3	0.33	0.4	0.25	0.24	0.19	0.21
P	0.009	0.008	0.008	0.008	0.01	0.01	0.011	<0.010	<0.010
Co	0.05	0.05	0.06	0.05	0.06	0.05	0.05	0 06	>0.01
Mg						0.01	0.01		
N						0.0072	0.0078		
V						0.03	0.02		
B	0 003	0.004	0.003	0.002	0.003				
	Tensile Data (ksi)								
YS	56	55	53	54	56	69	71.2		
US	111	112	109	109	112	121.4	120.4		
FS	83.5	83.5	81	81.5	84	95.2	95.8		

(1) Tubing from these heats were not degraded but were found to have the distinctive EC signature common to the degraded tubes (See Section 5)

Figure 3-1
Schematic of Model F SG

Notation	
Design	EC Database
FDB	1H, 1C
TSP 1	2H, 2C
TSP 2	3H, 3C
TSP 3	4H, 4C
TSP 4	5H, 5C
TSP 5	6H, 6C
TSP 6	7H, 7C
TSP 7	8H, 8C

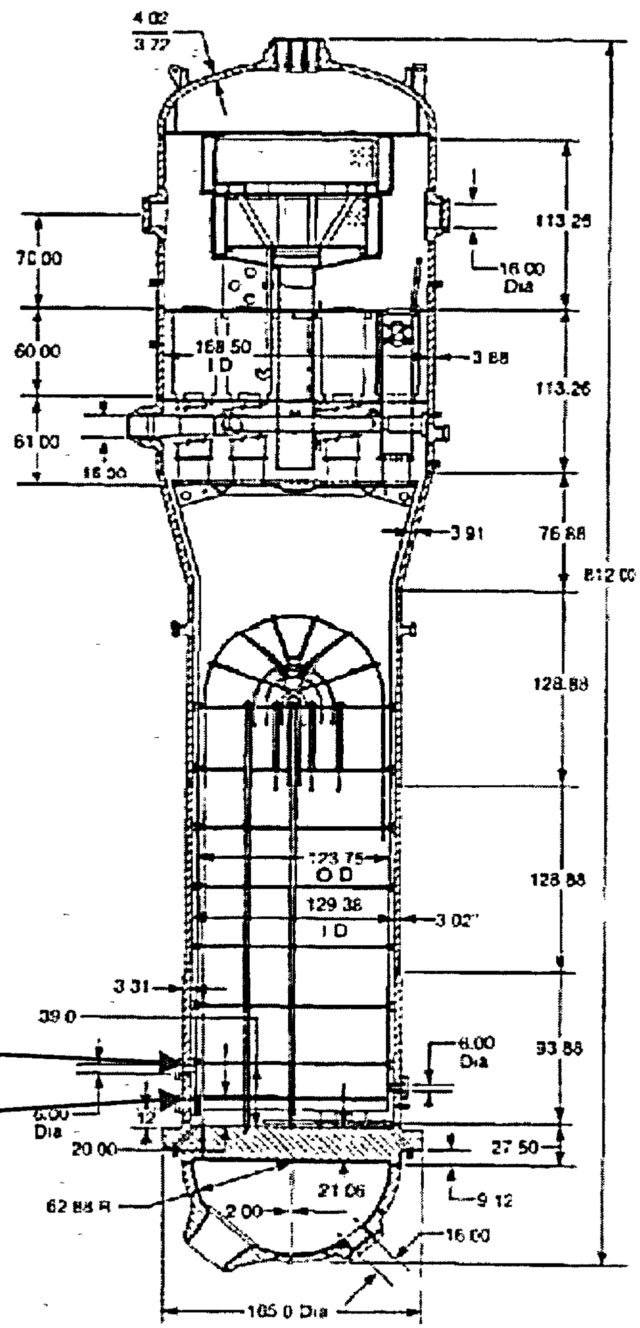

Figure 3-2 Location of Degraded Tubes

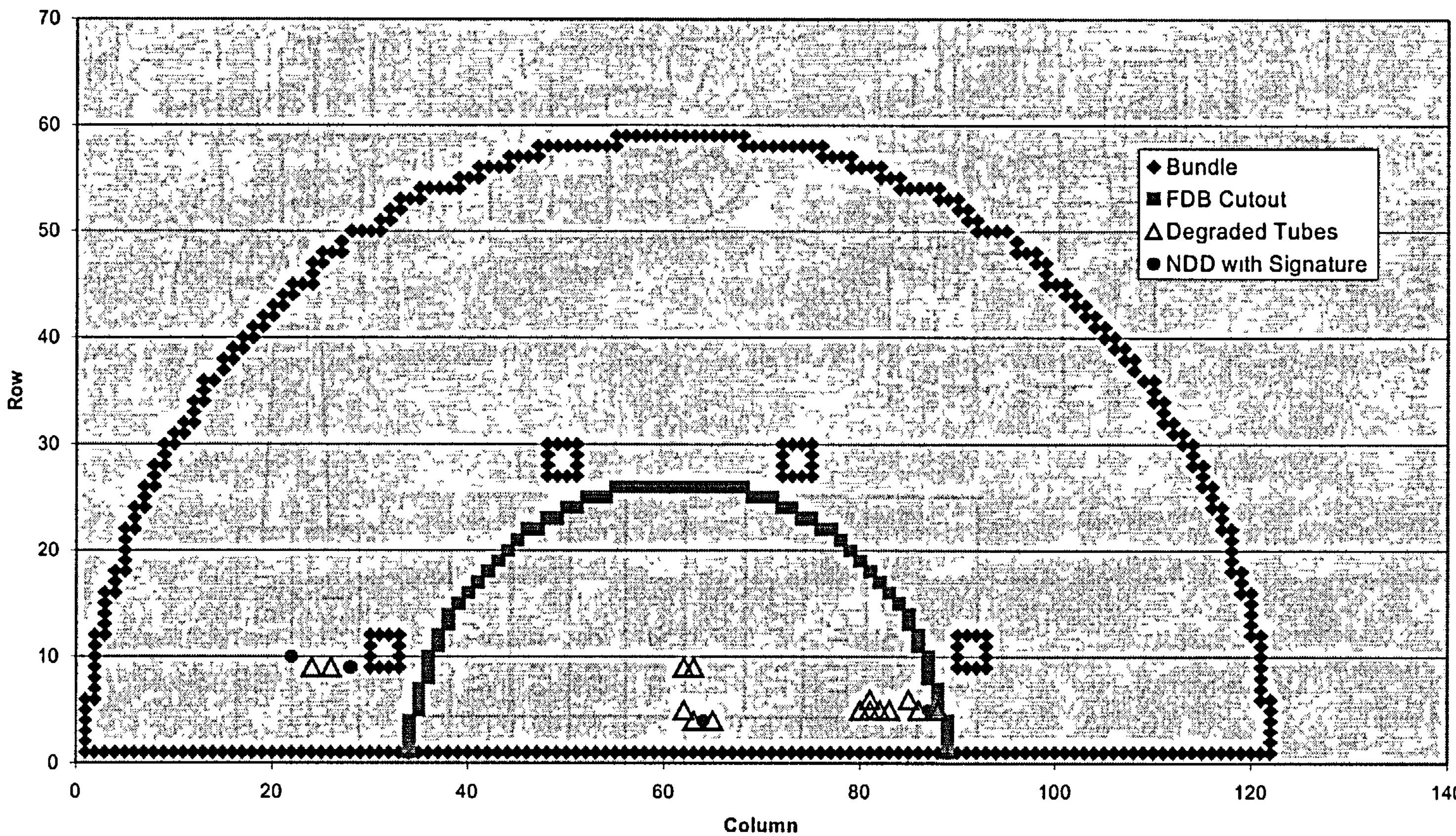

4. Pulled Tube Destructive Examination Results

Introduction

The two tubes from steam generator D of Seabrook Unit 1 (Tubes R5C62 HL and R9C63 CL) were examined at the Westinghouse Remote Metallographic Laboratory. Both of the tubes pulled were from Heat NX1374 as identified in Section 3. These tubes had field eddy current data suggestive of axial stress corrosion cracking of OD origin at the quatrefoil tube support plate intersections. The indications were originally reported as distorted support indications (DSI) in the bobbin inspection. Subsequent +Point and UTEC inspection of the DSI indications confirmed the presence of axial OD cracking.

Laboratory examination consisted of the following activities:

- Nondestructive examinations (visual, dimensional characterization, radiography, ultrasonic and eddy current testing)
- Leak and property testing (burst and tensile testing)
- Material chemistry verification
- Destructive examinations (SEM and SEM fractography, metallography, crack depth and morphology, microhardness, grain size, carbide distribution and Huey testing)
- Chemistry characterization of deposits and oxide films (EDS of OD deposits and fracture face oxides, X-ray diffraction of OD tube deposits and Auger/ESCA of OD surface deposits and fracture face oxides)

All pulled segments were photographed, dimensioned, profiled, and characterized nondestructively by radiography, UT, and eddy current examinations. Detailed metallographic and microanalytical examinations were performed to provide insight to the potential root cause of the observed ODSCC. The following discussions focus on the significant observations, supported by selected data, from this examination as well as analysis of the findings. The data presented in this summary represents only a small fraction of the obtained data and was selected to depict the conclusions drawn from the overall data collected. The complete description of tests and results is contained in Reference 4-1.

Summary results of the examinations of the following tube support plate intersections are discussed in the following sections:

Tube R5C62 H/L: Piece 3B (TSP2), Piece 4B (TSP3), Piece 5B (TSP4)

Tube R9C63 C/L: Piece 3D (TSP2), Piece 4B (TSP3), Piece 5B (TSP4)

Visual Examination

Freespan Area General Observations of R5C62 HL and R9C63 CL

In the free span regions, the tubes had a uniform gray coating around the tube. Fresh axial scratches, separated by approximately 90 degrees, were noted at the majority of the segments. The scratches occasionally were down to bare metal, and appeared to be from the tube removal process. No shiny metal was observed in any unscratched area.

Top of Tubesheet General Observations of R5C62 HL and R9C63 CL

A thick circumferential gray colored coating was observed at the top-of-tube sheet region. The gray deposit had a circumferential band of reddish brown deposit from the top of the deposit to the mid region. Fresh scratches were noted around the tube at each of the 90-degree locations. Belt polish marks were observed in the small areas where the deposit was knocked off. Shiny nicks were observed occasionally around the lower end of the deposit region.

Land Contact General Observations of R5C62 HL

A uniform whitish gray deposit was seen in each of the land contact areas. In the majority of the TSP intersections, two of the four land contact areas exhibited a thicker deposit corresponding to the land geometry. Some of the deposits were half removed with gray coating underneath the removed deposit. In some cases, a small area of reddish brown deposit was seen at the top of the white deposit. Some deep black scratches were noted just outside of the land areas. The scratches were heavily oxidized, suggesting that they preexisted and did not result from the tube pull.

Lobe Areas General Observations of R5C62 HL

The lobe areas were generally free of deposits. A few lobe areas had uniform gray thin deposit specks in each lobe. Belt polish marks were observed in the shiny areas of the lobe regions. Some vertical scratches were noted, both shiny and dull. The lobe areas were moderately shiny.

Land Contact General Observations of R9C63 CL

A uniform whitish gray deposit was seen around the land areas in the fourth and fifth support plate land contact areas. The deposits were not as thick and prominent as the hot leg deposits. The second support plate land areas did not have much of a visible deposit. Just outside the land contact areas were oxidized black scratches.

Lobe Areas General Observations of R9C63 CL

The lobe areas of the cold leg were not shiny and had a uniform gray coating. Both shiny and dull vertical scratches were seen. Belt polish marks were observed in the limited shiny regions.

Laboratory X-Ray Radiography

X-ray radiographic inspection was conducted on the hot leg TSP4 region of R5C62 to help identify the degradation morphology. This tube section was selected because it contained the largest (amplitude and apparent depth) eddy current indication of all the tube sections available. Two radiographic techniques were used. The first was a double wall film radiographic technique. To cover the entire circumference of the tube, four radiographs were taken at 0, 45, 90 and 135-degree tube rotations. The four radiographs were then evaluated. Significant indications, indicative of dense or thick deposits, were identified at the orientations associated with the land locations. A line of intermittent linear indications was identified at the 45-degree rotation. This location is consistent with the indication identified at 218 degrees by the eddy current inspection.

The second radiographic technique involved the use of a real-time display of the radiographic information. In this technique, the tube section was mounted on a rotating table that can be moved with respect to the x-ray source to allow magnification of the image. The tube section was rotated and the image monitored "real-time" on a monitor. The images were captured digitally. Figure 4-1 shows the location where linear indications adjacent to a deposit were found in the TSP4 intersection at the 210-degree orientation. The indication is composed of a series of short linear (crack-like) indications. As is generally observed for cracking, the degradation does not produce a high contrast image. As the tube was slightly rotated or translated, portions of the indication changed intensity. This behavior is consistent with observations made for stress corrosion cracks.

Sensitization Tests

Thermal treatment of Alloy 600 was implemented to improve the steam generator reliability by improving the stress corrosion cracking (SCC) resistance of Alloy 600 steam generator tubing. The thermal treatment process includes extended (8 to 15-hour) exposure of the Alloy 600 tubing in a vacuum at 1300-1320°F. In this temperature range, carbon, which has been dissolved during the final mill annealing operation and has been retained in solid solution, precipitates to form (primarily) intergranular chromium carbides. The initial precipitation – i.e., in the earliest stages of the exposure – occurs by short-range diffusion of chromium to the boundaries to effect the precipitation of the M23C6 and can result in a Cr-depleted region adjacent to the grain boundaries. This condition is typically referred to as "sensitization", and is a condition that renders the material susceptible to intergranular attack in aggressive chemical environments (but not generally in PWR primary water). To avoid this situation, the thermal treatment time is extended to permit solid-state diffusion of chromium from the matrix to the regions adjacent to the grain boundary carbides, thereby "healing" these regions.

The extent of grain boundary carbide precipitation is controlled by alloy composition (in particular carbon and chromium), diffusivity of chromium, grain size, and the availability of dissolved carbon for precipitation at the grain boundaries.

For reasons implied by the preceding, it has been Westinghouse practice in the manufacture of Alloy 600 heat transfer tubing – both mill annealed and thermally treated – to ensure that the material was not sensitized. Westinghouse, along with the industry, adopted a modified Huey test (ASTM A262 Practice C) as the principal tool for evaluation of grain boundary chromium depletion in Alloy 600. The test was modified to a single 48-hr exposure to boiling 25% nitric acid by weight. This modification was necessary to enhance the sensitivity of the test for detecting chromium depletion.

In view of this historical practice, it has been Westinghouse experience that SG heat transfer tubing in Westinghouse PWRs is not sensitized, and therefore not prone to in-service degradation in faulted secondary environments due to this condition.

The sensitization level of R5C62 HL and R9C63 CL was determined using the test practice noted above. Specimens (0.5 inch rings) were cut from both pulled tubes and exposed to a 25 weight % nitric acid solution for 48 hours. A weight loss rate of 200 mg/dm^2/day or greater is required for a tube to be classified as being sensitized. Highly sensitized samples have weight loss rates on the order of thousands of mg/dm^2/day.

As shown below, corrosion rates of 33 to 87 mg/dm^2/day were measured for the Seabrook pulled tube specimens. Therefore, the Seabrook pulled tubes are not sensitized. A specimen taken from an archived heat of Alloy 600TT tubing was also tested and showed a corrosion rate of 21 mg/dm^2/day in the modified Huey test.

Tube ID	**Corrosion rate (mg/dm^2/day)**
Archive NX 0146 1B	21.2
R9C63CL 3E2	32.6
R9C63CL 6A3	35.1
R5C62HL 9A3	41.2
R5C62HL 3C2	86.8

Microstructure

The microstructure of the R5C62 HL and R9C63 CL Seabrook tubes, and an archived tube sample from Heat NX1374, were characterized by SEM examination of a metallographic sample etched in bromine methanol.

Resulting scanning electron micrographs are presented in Figures 4-2 and 4-3. The microstructures exhibit predominantly intragranular carbides and few grain boundary carbides. The carbides were not preferentially distributed on the grain boundaries as is generally typical of thermally treated Alloy 600. The average grain size was ASTM 10 to 11. This grain size is small when compared to other Alloy 600TT tubing of this vintage.

Tensile Testing

Tubular free span (FS) segments of R5C62 HL and R9C63 CL were tensile tested at room temperature to determine the mechanical properties of the pulled tubes. The specimens, which were 10 inches long with a gage length of 6 inches, were tensile tested per ASTM Standard E8. The results, summarized in Table 4.1, indicate that the tensile strengths of the tubes were higher than the CMTR values and also were higher than the typical values for Westinghouse tubing of this vintage.

Hardness Testing

Vickers hardness measurements were made across tube wall and longitudinally at midwall for R5C63 HL. The transverse values were between 180-210 DPH (100 g load) and the longitudinal readings were between 196-202 DPH (500 g load). The hardness data are consistent both through-wall and along the tube axis and are believed consistent with the small grain size and high mechanical properties. The average microhardness of the R5C63 and R9C63 tubing was 185 VHN (500 gram load).

Destructive Examination

Post-burst test visual inspection data showed that corrosion cracks were present at the 2nd, 3rd and 4th TSP of the R5C62 HL tube and the 3rd and 4th TSP of the R9C63 CL tube. Tube cracks were limited to one or two of the tube-to-TSP land areas.

The fracture faces of all indications were opened for SEM fractographic examination. Table 4.2 presents the results of the fractographic data in the form of macrocrack[1] length and depth, compared to the field NDE data and laboratory NDE data results. More detailed data are presented in Reference 4-1. The burst openings occurred in axial macrocracks that were composed of numerous axially oriented intergranular cracks of OD origin that were aligned in a tight and narrow band corresponding to the width of the quatrefoil land. The maximum axial extent of any of the macrocracks was approximately 0.7 inches. The macrocracks had maximum depths ranging from 34% to 99% throughwall, with average depths ranging from 20% to 50% throughwall depth (TWD), and lengths ranging from 0.2 to 0.7 inches. The cracks at all TSP regions were located within and confined to one or two of the crevice regions formed by the tube and quatrefoil land intersection.

One TSP region (2H on R5C63) was initially called NDD by field bobbin. Subsequent laboratory bobbin examination showed a potential indication, while laboratory +Point examination showed NDD. Destructive examination showed a 0.2-inch long by 50% TWD crack on one of the tube to quatrefoil land intersections. The indication appeared to be centered within the width of the land and located near its the lower edge.

From the metallographic and SEM surface examinations conducted on the tube-to-quatrefoil land intersections, it was concluded that the dominant OD origin corrosion morphology was axial intergranular stress corrosion cracking (IGSCC). All cracks were axially oriented with no oblique angled cracking observed.

Figures 4-4 through 4-6 are provided to illustrate the typical nature of the cracking observed.

[1] "Macrocrack" is a term used to describe the apparent total crack that eddy current detects or that is visible after bursting the tube. Frequently, a macrocrack is a series of small cracks – "microcracks" – that are separated by un-degraded ligaments The structural performance of a macrocrack of some length that is a single continuous crack is much inferior to a macrocrack of equal length that is made up of adjacent microcracks separated by ligaments.

Metallography

A number of transverse metallographic sections were taken at different support plate locations on both the R5C62 and R9C63 tubes. The IGSCC found was always associated with the area of the tube corresponding to the land region of the quatrefoil tube support plate. Apart from the IGSCC, the tube to quatrefoil land intersections also showed the generally observed shallow IGA. Cross-sections of the free tube surfaces showed shallow IGA one to two grains deep all around the circumference of the tube, located in the quatrefoil land area.

Analysis of Oxide Films and Deposits

The deposits and oxide films which form on steam generator tubing reflect both the solution environment which was present and the corrosion processes which occurred during service. High vacuum surface analysis techniques are valuable because crack oxides and some corrosion layers are extremely thin. Most crack oxides are usually 100 nm or less in thickness, and tube OD oxides are in the vicinity of 1000 nm (1 micrometer). To characterize the deposits and oxide films on R5C62 HL and R9C63 CL tubes, X-ray diffraction (XRD) of OD deposits, energy dispersive spectroscopy (EDS) analysis of OD surface and fracture face oxides, Auger Electron Spectroscopy (AES) and X-ray Photoelectron Spectroscopy (XPS) analysis of OD surface and fracture face oxides were performed. The complete results of these efforts are included in Reference 4-1; a summary of some of the key tests is provided below.

Auger and ESCA Analysis

In order to try to get an indication of whether the environment within the tube to quatrefoil land is acid or alkaline, as well as to identify any deleterious chemical species, the surfaces of some intergranular cracks were analyzed. In general, nickel enrichment on the surface indicates an alkaline environment and chromium enrichment an acid environment.

R5C62 Hot Leg, 4th Support Plate - Crack Face Analysis:

AES depth profiling analysis was performed at 9 locations on two different crack segments. Two areas of ductile fracture produced in the laboratory were also analyzed. The first crack was approximately 50% through-wall, and the second was approximately 20% through-wall.

The AES analysis demonstrated that the crack-face oxide was quite thin in both cracks. Some oxide thickness values in the 5-10 nm range were obtained. This indicates that the cracks in this area were quite tight during power operation.

A profile showing the thin oxide composition in atomic percent is shown in Figure 4-7.

The crack-face oxide at the crack tip where little corrosion had taken place was slightly enriched in chromium relative to the bulk. This is consistent with a non-sensitized grain boundary condition. This is evident in the "metals normalized" profile shown in Figure 4-8.

The thicker crack-face oxide in crack center and towards the crack mouth was also slightly enriched in chromium. This suggests that the corrosion occurred in an acidic or near-neutral pH environment.

The impurities detected in the open crack-face were carbon, sulfur, chlorine, calcium and silicon. The calcium, sulfur and carbon were present on the lab fracture at concentrations comparable to the intergranular field fracture, so these elements could have been contaminants. The chlorine concentration was less than 1 wt%. Lead and alkali metal cations were not detected.

The ESCA analysis of the fracture surface spanned several intergranular crack segments as well as areas of laboratory fracture. The ESCA analysis detected two additional impurity elements. Lead was found at 0.05 atomic percent and sodium was detected at the 1.1 atomic percent level. This level of lead is in the lower range of what has been observed in tube examinations at other plants. The carbon signal did not show any evidence of carbonate formation, as would have been the case had the crack contained free hydroxide when it was exposed to the atmosphere in the laboratory.

R5C62 Hot Leg, 4th Support Plate - OD Analysis

The AES analysis indicated that oxides of iron calcium, aluminum and silicon were the main components of the OD deposit. Small amounts of carbon, magnesium, and sulfur were also detected. The protective oxide layer on the OD of the tubing was 0.3 microns thick and was enriched in chromium. Chromium enrichment is to be expected on the OD of tubing in all but highly alkaline crevice environments.

The ESCA analysis on the OD of the tubing detected 0.09 At% lead and 1.6% sodium in addition to the elements detected by AES. The carbon signal did not contain a carbonate component, indicating a near neutral or acidic crevice environment. The sulfur binding energy was consistent with the sulfate.

R5C62 Cold Leg, 4th Support Plate - Crack Face Analysis

AES depth profiling analysis was performed at 6 locations on the opened intergranular crack face. A profile was also done on an area of laboratory fracture near the crack tip.

Results were similar to the analysis on the R5C62 hot leg crack at the 4th support plate. The crack-face oxide was thin, especially at the crack tip, but thicker (up to 48 nm) at the crack center. The crack-face oxide at the crack tip where little corrosion had taken place was slightly enriched in chromium relative to the bulk. This is consistent with a non-sensitized grain boundary condition.

The thicker crack-face oxide in crack center and towards the crack mouth was also slightly enriched in chromium. This suggests that the corrosion film developed in an acidic or near-neutral pH environment.

The impurity elements detected on the intergranular crack face were sulfur, carbon, and silicon. Sulfur and carbon were also detected on the ductile lab fracture.

The ESCA analysis on the opened crack-face detected 0.04 At% lead and 1.7% sodium in addition to the elements detected by AES. The carbon signal did not contain a carbonate component, indicating a near neutral or acidic crevice environment. The sulfur binding energy was consistent with the sulfate.

R5C62 Cold Leg, 4th Support Plate - OD Analysis

AES profiling was performed at two locations on the protective oxide were the deposit had spalled from the surface. In addition to oxides of chromium, iron, and nickel, calcium and sulfur were detected. The protective oxide layer on the OD of the tubing was 0.8 to 1.1 microns thick and was enriched in chromium.

The ESCA analysis on the OD of the tubing detected no lead and 1.6 At% sodium in addition to the elements detected by AES. The carbon signal did not contain a carbonate component, indicating a near neutral or acidic crevice environment. The sulfur binding energy was consistent with the sulfate.

R5C62 Sample 2B2B1B

A high concentration of lead had been detected on the OD of this sample by SEM/EDS. The specimen was analyzed by ESCA to see if the lead concentration was more wide spread. Only low levels of lead were found (0.04 At% on the OD and 0.07 At% on the crack face.)

SEM Examination And Energy Dispersive Spectroscopy (EDS) Analysis

The deposits on the OD of the tubes and crack fracture faces were photographed in the SEM and were analyzed by energy dispersive X-ray spectroscopy (EDS). The EDS system used was capable of detecting elements of atomic number 11 or greater for a depth of approximately 2 micrometers below the surface. Thus, when the deposits were thin, the base metal composition strongly influenced the EDS deposit data. For the EDS analysis, regions of both relatively thick deposits and thin deposits within the OD area of interest were selected. Typical photographs and EDS analyses are shown in Figure 4-9.

<u>Residual Stress Testing</u>

Five split tube tests were performed on archived tube segments for the material heats identified for the degraded tubes. These samples were obtained from Blairsville tube mill archives on 8/22/02. In these tests, the hoop residual strain was measured using both strain gage measurements and dimensional changes. Tube samples about 2 inches long were used for these tests. Figure 4-10 shows the pre-split test sample with strain gages attached.

The results of these tests are shown on Table 4.3 (a) and (b). On 4 of the 5 specimens, the measured residual stress was low, as expected, for thermally treated tubing. The tensile stresses varied from 1.2 to 2.3 ksi with fair agreement between the two techniques. The fifth tube (Heat 1790, Lot TF8878) showed residual stresses of 12 and 11 ksi by the two methods used. This tube had no TT batch number on the tube, indicating that this archived sample had been taken at an intermediate processing step, probably after the final mill annealing and roll straightening. The results for this specimen are consistent with prior data (Reference 4-2) for MA tubing, and with the results of independent testing on MA tubing (Appendix B). This data point demonstrates the reliability of the tubing manufacturing records, and confirms the expected residual stress in a MA tube.

Similar residual stress testing was done on specimens cut from the pulled tubes, including a sample from about 14 inches above the TTS elevation of the tube to assess if there was axial variation of the residual stress. Table 4.3(b) summarizes the residual stress measurements on the pulled tube segments. The residual stress in both of the pulled tubes is greater than expected, and about the same for both pulled tubes. No significant axial variation was found based on tests of the segments from about 14 inches above the TTS and from about 189 inches above the TTS. A difference is observed in the results from contiguous test specimens, one tested using strain gages, and the other using the change in diameter technique. This difference is not considered significant, as local variations in residual stress due to a straightening process can occur.

To further evaluate the observation, based on the residual stress tests above, that the residual stress is essentially the same along the length of the tubes removed from the SG, microhardness measurements were made at several points along the length. A variation in the cold work (and therefore, residual stress) along the length of the tube would be expected to be reflected in a similar variation in the hardness of the material.

Table 4.4 summarizes the hardness test results. No significant variation of hardness is observed along the length of the tube at the OD, midwall and ID of the tube. Therefore, the axial hardness data indicate that there is no significant variation in cold work along the length of the tubes removed, which is consistent with the split ring residual stress data.

Summary of Destructive Examination Results

a) The degradation was determined to be ODSCC, with a minor presence of IGA on the OD surface. The macrocracks were formed by numerous axially oriented microcracks, typical of ODSCC. The cracks were located within the span of the tube/TSP quatrefoil intersection at one or two of the lands on both the HL and the CL.
b) The cracking is intergranular. No intragranular cracking was observed.
c) The residual stress in the pulled tubes was significantly higher than expected. Split ring tests showed the hoop residual stress was in the range of 18-22 ksi. For thermally treated tubing, the expected range of residual hoop stress is about 2-3 ksi.
d) Standard modified Huey testing showed that the pulled tube material is not sensitized.
e) At the TSP intersections, deposits were principally observed on the tubes at the land areas of the TSP vs. the lobe areas, which were generally free of deposits. The HL deposits were thicker than those on the CL. The appearance of the deposits on the freespan of the tubes was not remarkable. Some artifacts related to tube removal were observed, however, these were unrelated to the observed degradation.
f) No scratches or unusual artifacts were found during visual inspection that would suggest damage to the tubes during SG manufacturing.
g) The pulled tube material microstructure exhibited predominantly intragranular carbides, and some grain boundary carbides. The grain size of the pulled tube material is smaller than expected at ASTM 10-11.
h) The tensile test results for the pulled tubes were higher than the values contained in the CMTR for the pulled tubes (Heat NX1374).
i) The material transverse and longitudinal hardnesses are consistent with each other, and also with the elevated tensile properties and the smaller than expected grain size of the material.

References

4-1 Westinghouse SG-SGDA-02-35; "Seabrook Steam Generator Tube Examination"; November 2002

4-2 Westinghouse 77-1D2-TUCOR-R2; "Residual Stresses in Inconel 600 Steam Generator Tubes. Part II: Straight Tubes"; October 1977 (Proprietary)

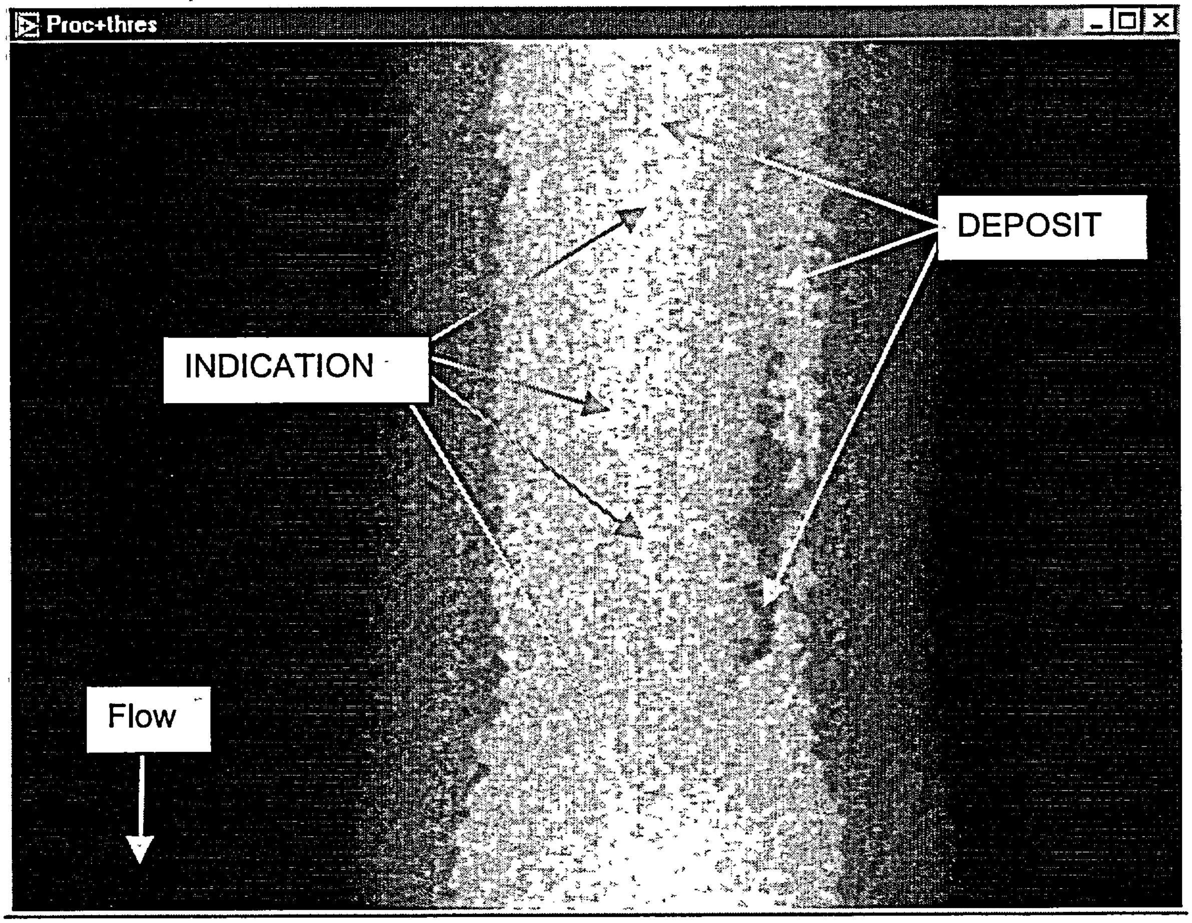

Figure 4-1 X-ray image of Seabrook tube R5C62 hot leg TSP 4 at the 210 degree orientation.

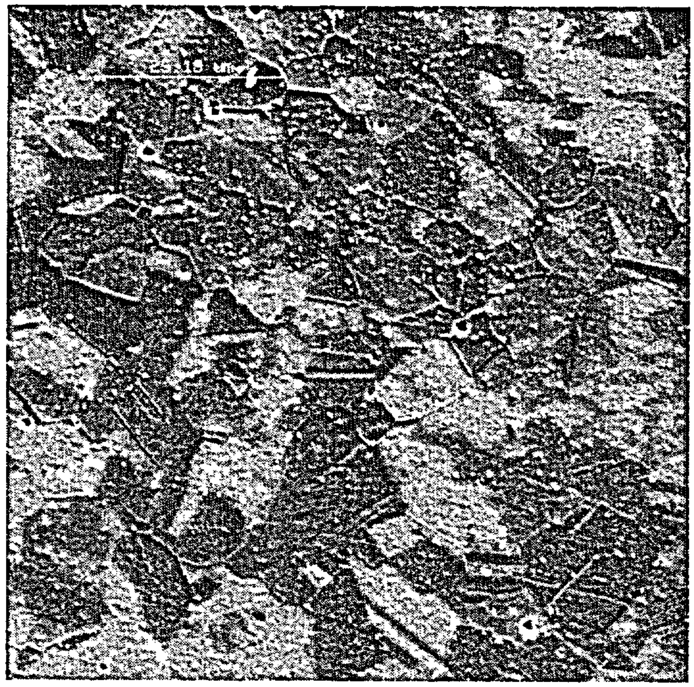

(a)

(b)

Figure 4-2 (a) R9C63 CL and (b) R5C62 HL are generally characterized by intragranular precipitation and fine grain size [ASTM 9-11]

•

•

•

•

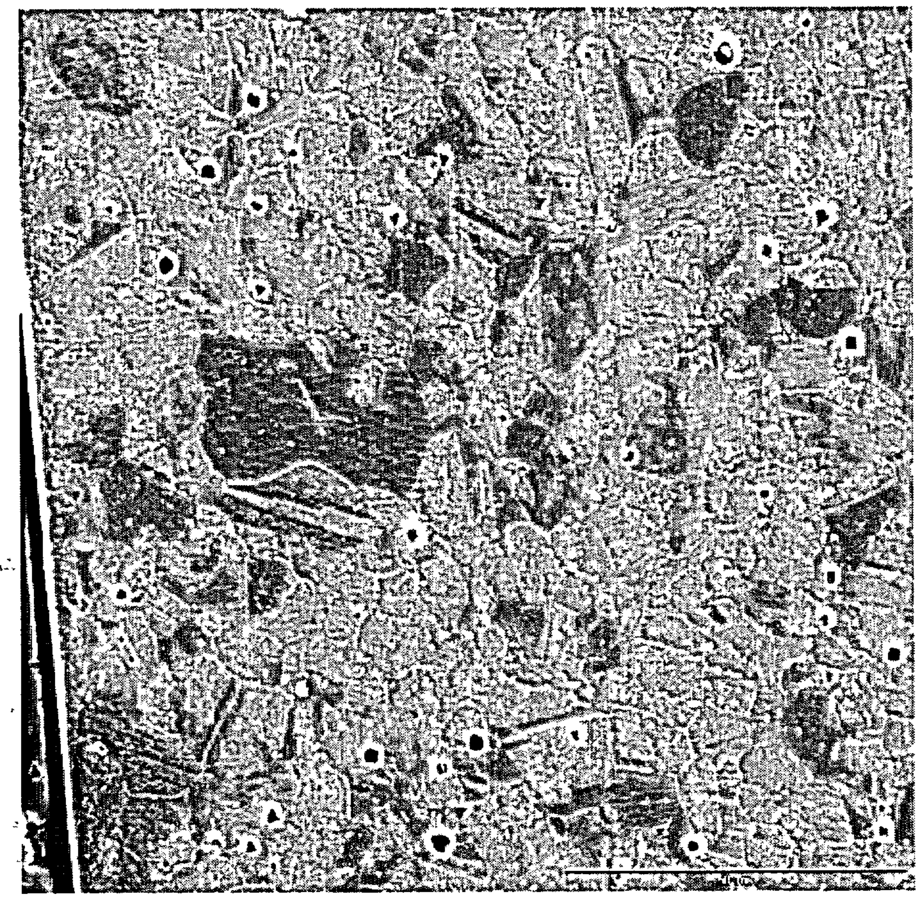

Figure 4-3 11/16" Dia. Archived Tube [Heat NX 1374] Microstructure [Lot TF6039; TT A0206D]

Figure 4-4

Fracture Face - Seabrook Unit 1 - R5C62HL (04H) - Piece 5B2A1 (120 degree) @ 25X

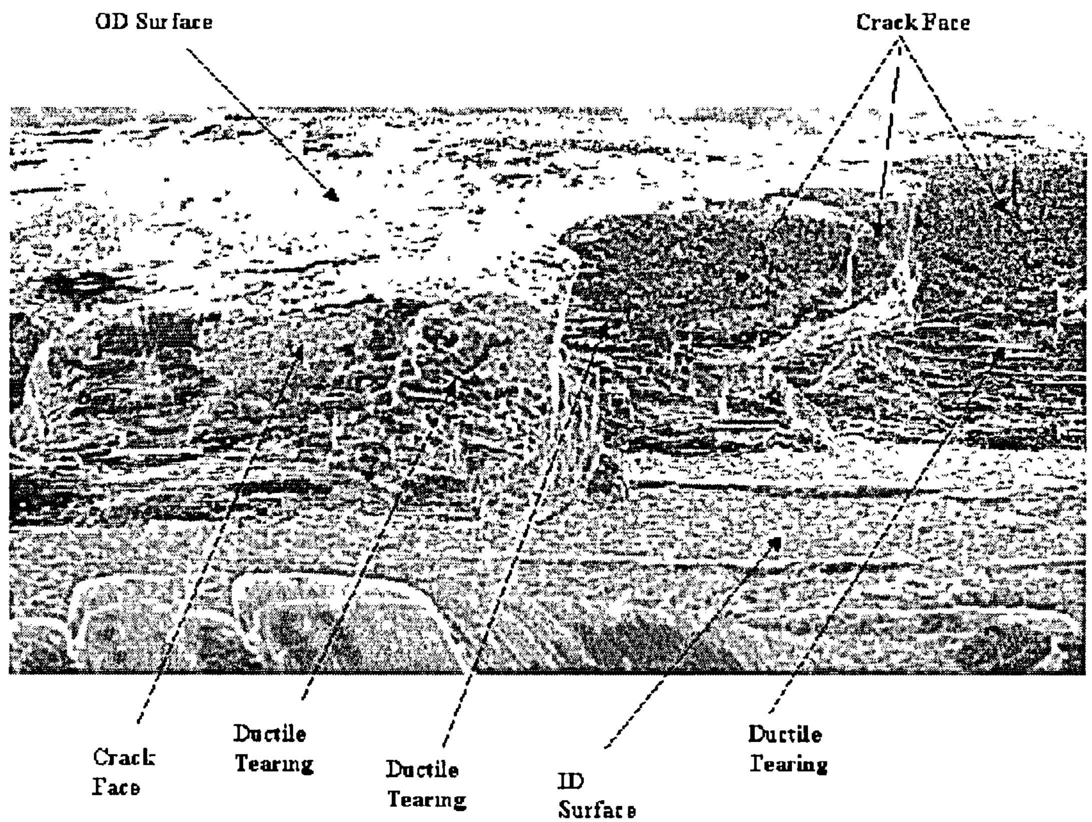

Figure 4-5

Fracture Face - Seabrook Unit 1 - R5C62HL (04H) - Piece 5B2A1 (120 degree) @ 25X

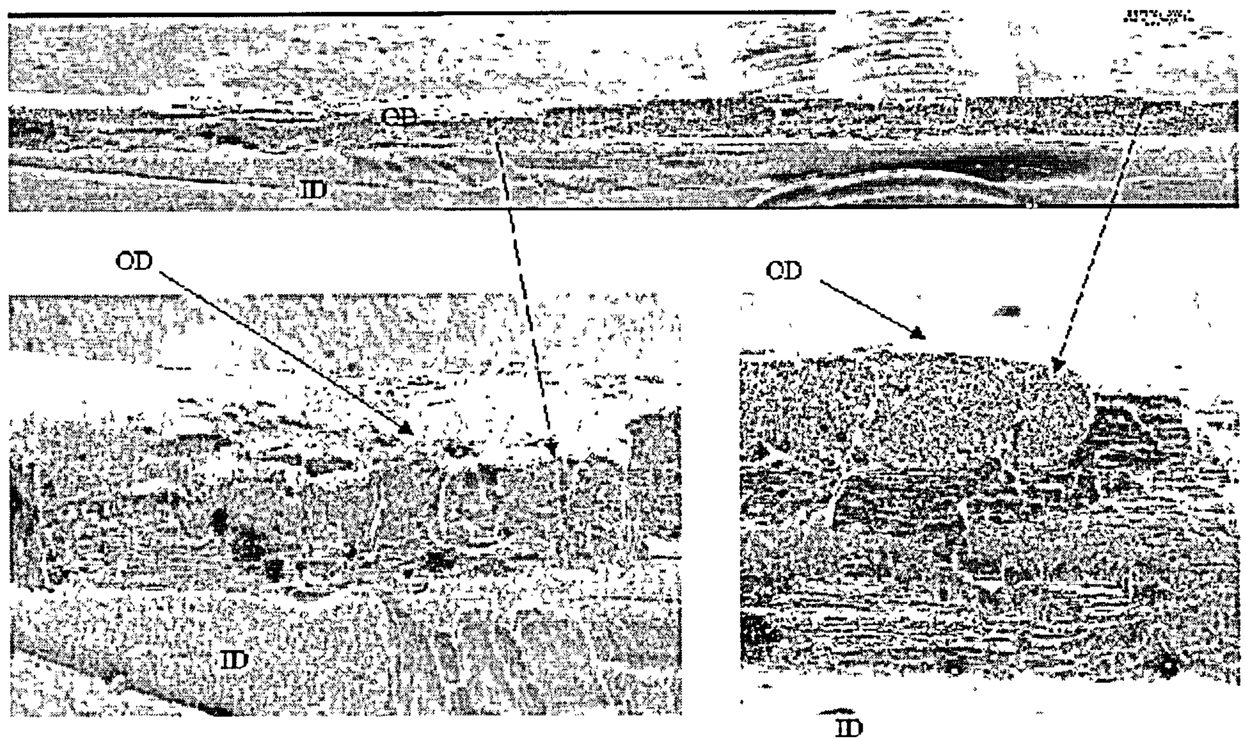

Figure 4-6

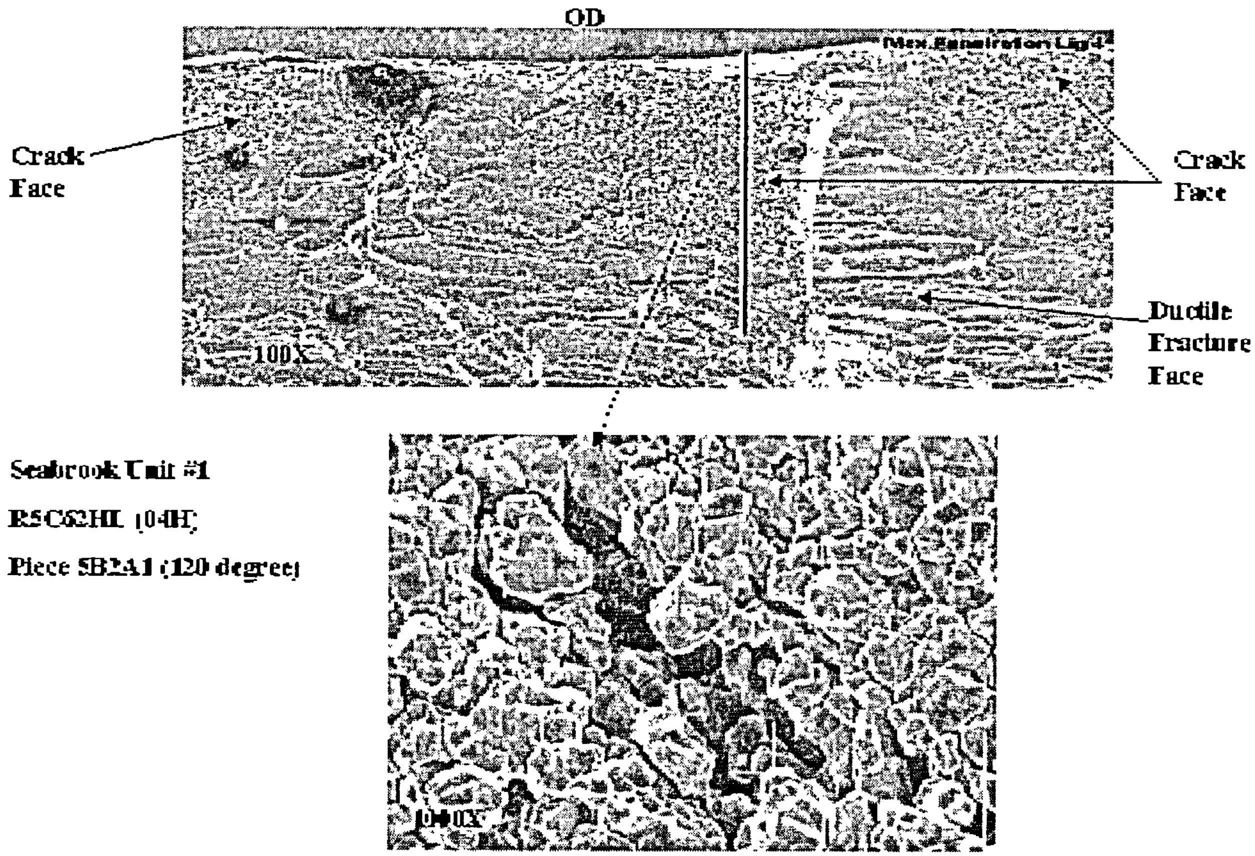

Seabrook Unit #1

R5C62HL (04H)

Piece 5B2A1 (120 degree)

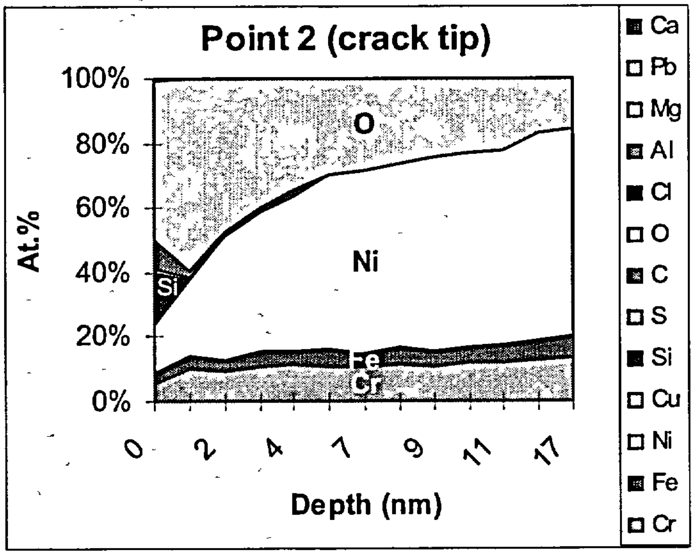

Figure 4-7 AES profile on an opened crack face from the R5C62 HL 4th TSP specimen

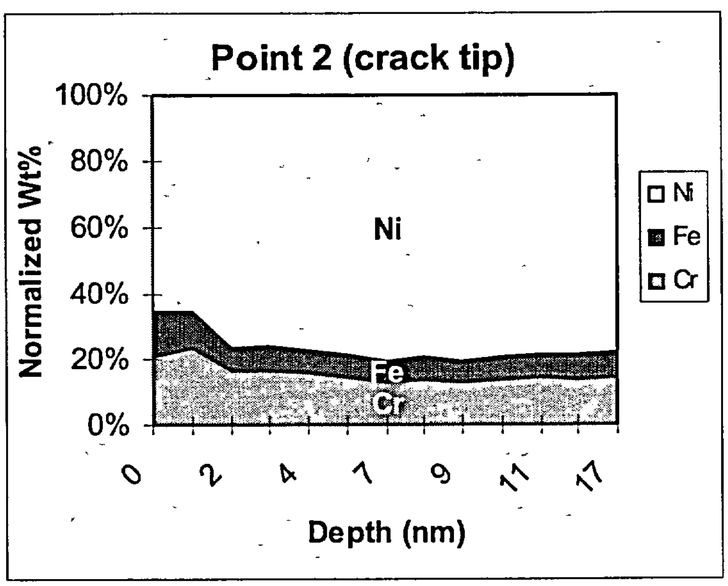

Figure 4-8. Metals Normalized AES profile on an opened crack face from the R5C62 HL 4th TSP specimen.

Figure 4-9

EDS Deposit Analysis - R5C62 (02H)

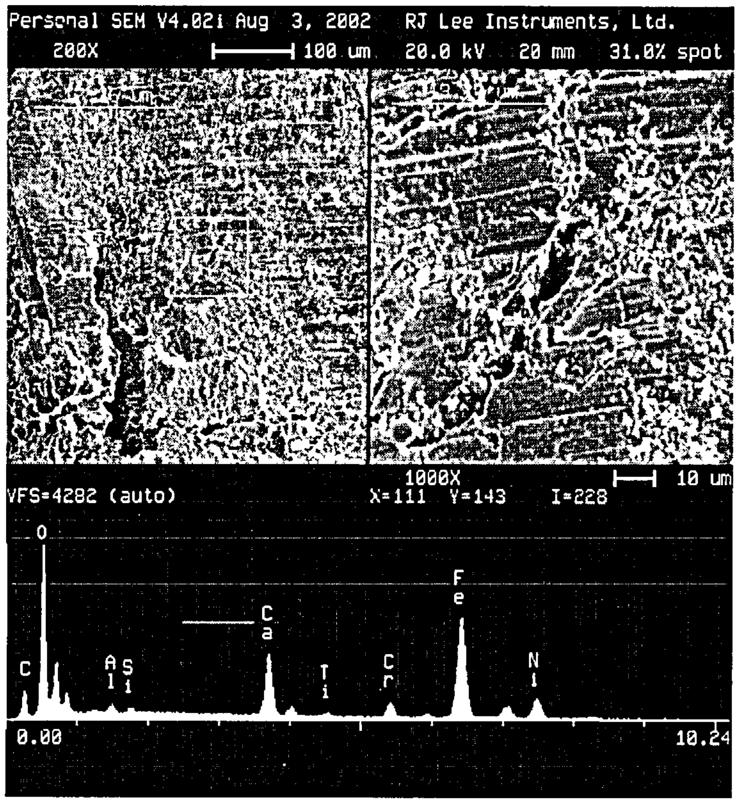

R5C62 - 02H - Piece 3B2B1@240 deg. (101EDS)
Surface deposit analysis at OD crack area

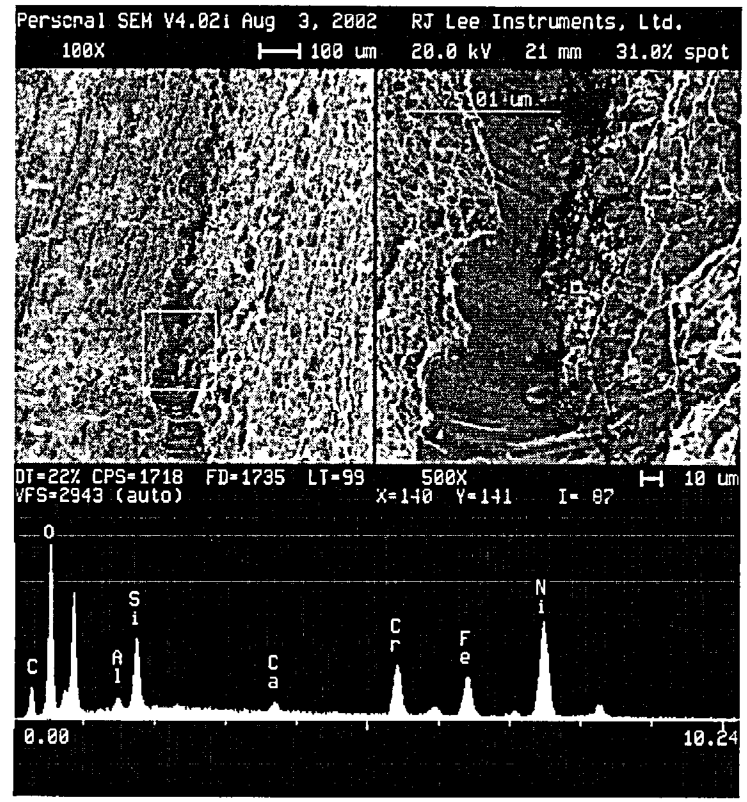

R5C62- 02H - Piece 3B2B1@240 deg. (103EDS)
Surface deposit analysis at OD crack

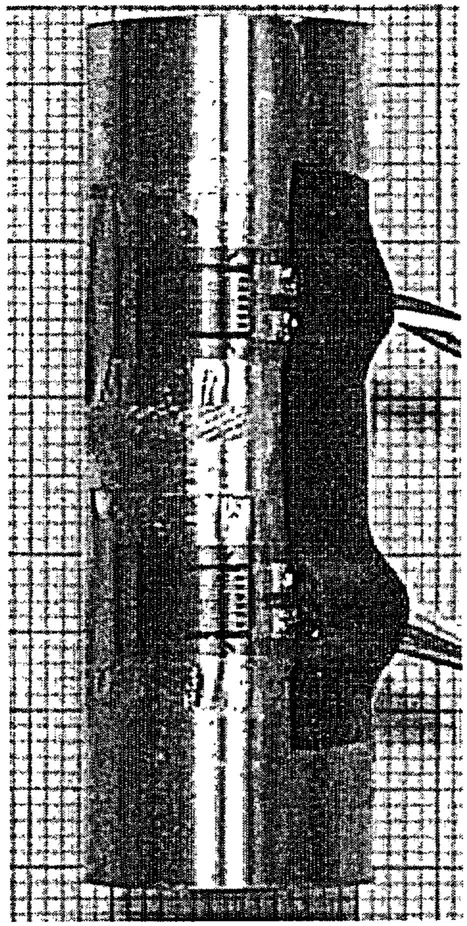

Figure 4-10 Residual Stress Test Specimen with Strain Gages Mounted

Table 4.1 Tensile Test Results

Tube	Heat No.	CMTR Value (ksi)		Tensile Test (ksi)	
		Sy	Su	Sy	Su
PT- R5C62	NX1374	56	113	71.2	120.4
PT- R9C63	NX1374	56	112	69	121.4
Archived	NX1460	49.4	107	NA	NA

Table 4.2 Crack Properties – NDE Compared to Fractography

Tube Section Identification		**Field NDE**						**Laboratory NDE**					**Fractography**		
		Bobbin Coil (1)		**+Point Probe (2)**				**Bobbin Coil**		**+Point Probe**					
Tube	**TSP**	**Volts**	**Depth (%TW)**	**Volts**	**Length (in.)**	**Max Depth (%TW)**	**PDA**	**Volts**	**Depth (%TW)**	**Volts**	**Length (in.)**	**Max Depth (%TW)**	**Length (in.)**	**Max Depth (%TW)**	**PDA**
R5C62	5H	0 21	75	0 33	0.41	64	36 3	0.34	50	0 3	0.41	48			
	4H	0.91	72	1.24	0.72	66	41.4	1.3	71	1.4 0.05	0.83 0.1 (4 in line)	67 PI	0.7470. 0.494	99.5 46.0	63 0 26 7
	3H	0.59	<20	0.47	0.6 0.42	58 55	36.5 32.8	0.68	57	036 0.53	0.47 0.69	<20 52	0.6 0.683	88.4 76 7	48 2 52.7
	2H	NDD	-	NDD	NA	NA	NA	0.05	PI	NDD	NDD	NDD	0.139	35.6	20.3
	TTS-HL	N/A	N/A	N/A	NA	NA	NA	N/A	N/A	NDD	NDD	NDD	NA	NA	NA
R9C63	4C	0.55	DSI	0 59	0.36 0.36	61 66	43.4 40.9	0 38	0 38	0.4 0.28	0.47 0.57	23 <20	0.399 0.530	60.0 60.9	29.9 33 0
	3C	NDD	NDD	N/A	NA	NA	NA	0.12	0 12	0.1	0.29	20	0 261	51.5	34.4
	2C	NDD	-	NDD	NA	NA	NA	NDD	NDD	NDD	NDD	NDD	NA	NA	NA
	TTS-CL	N/A	N/A	N/A	NA	NA	NA	N/A	N/A	0.17	0 25	77 (3)	NA	NA	NA

Notes: (1) Depth call is based on laboratory interpretation of field data.
(2) Length, depth and PDA based on post outage profiling of field data.
(3) ID indication; judged to be due to tube removal process.

Table 4.3 (a) Archived Tube Split-Tube Residual Stress Measurements

Heat No.	Lot No.	TT Batch No.	Outside Dia. (in.) 0°	90° Initial	90° Final	Inside Dia. Initial (in.)	Wall Thick-ness (in.)	Microstrain (in./in. x10^{-6}) $\Delta\text{-}\varepsilon$ Gage 1	$\Delta\text{-}\varepsilon$ Gage 2	$\Delta\text{-}\varepsilon$ Avg.	σ_{resid} (ksi) $\Delta\text{-}\varepsilon$ (2)	Δ-D (3)
1374	TF6039	A0206D	0.6903	0.6902	0.6907	0.6101	0.0401	-33	-42	-38	1.2	1.4
1456	TF6392	B0235B	0.6867	0.6867	0.6875	0.6075	0.0396	-50	-40	-45	1.4	2.3
1790	TF8878	none	0.6886	0.6884	0.6922	0.6053	0.0416	-382	-	-382	12.1	11.4
1790	TF6879	A0286	0.6890	0.6889	0.6896	0.6065	0.0412	-52	-	-52	1.6	2.3
1458	TD6374	A225C	0.6886	0.6888	0.6895	0.6061	0.0413	-73	-	-73	2.3	2.3

1. Equipment Used:
   (a) **ID micrometers:** Brown and Sharpe - RA 24-T23W5-6-1; calibration due 12/8/02
   (b) **Laser Micrometer:** Datamike 700 5-831, Checked vs NIST Standards 8/30/02, Average error = + 0.00001 inch
   (c) **Strain Indicator;** 0300, calibration due 6/21/03
2. $E_{RT} = 31.6 \times 10^6$ psi
3. $\sigma_{resid} = 34500 * W * (1/Di - 1/Df)$

Table 4.3 (b) Pulled Tube Split Tube Residual Stress Measurements
(Pulled Tubes are from Heat NX1374)

Tube (1)	Average Elevation Above TTS (in.)	Average Outside Diameter at 90° (in.)		Average Tube Wall Thickness (in.)	Microstrain (in./in. x 10^{-6})		Residual Stress (ksi)	
		Initial	Final		90° Gage	180° Gage	$\Delta-\varepsilon$ (2)	Δ-D (3)
R5C62	187.0	0.6916	0.6957	0.0399	NA	NA	NA	11.73
R5C62	189.1	NA	NA	NA	-1209	-605	19.1	NA
R5C62	14.2	0.6857	0.6924	0.0420	-626	-684	21.6	20.45
R9C63	129.6	0.6883	0.6945	0.0409	NA	NA	NA	18.30
R9C63	131.7	NA	NA	NA	-731	-682	21.6	NA

(1) Both pulled tubes are from heat NX1374 (see section 3)
(2) E_{RT}= 31.6 x 10^6 psi
(3) σ_{resid} = 34500 x W x $(1/D_i-1/D_f)$

Table 4-4 Results of Axial Microhardness Traverse
(Hardness Values in VPN)

Tube	Axial Position Along Tube from TTS	Tube Midwall					Tube OD					Tube ID				
		20 mils from wall					0.6 mils from wall					0.6 mils from wall				
		500g Load					100g Load					100g Load				
		Azimuthal Position					Azimuthal Position					Azimuthal Position				
		0°	90°	180°	270°	avg	0°	90°	180°	270°	avg	0°	90°	180°	270°	avg
Heat 0146	N/A					175					201					159
R5C62	6.45	209	189	205	196	200	158	142	190	160	163	159	140	184	143	157
	51.2					212					188					195
	92.8	196	195	202	196	197	161	172	176	142	163	144	179	177	165	166
	120.3					200					196					202
	180.44					196					223					195
R9C63	6.71	190	194	189	200	193	142	181	172	143	160	147	169	156	149	155
	48.65					199					206					194
	93.55	191	210	213	188	201	184	191	169	160	176	183	182	191	160	179
	137.75					195					199					191

5. Eddy Current Data Review

Laboratory Review of Field Data

Prior to the destructive examination of the tubes, the pulled tubes were re-tested with a number of probes. This effort was principally directed at confirming field indications and providing data for probability of detection (POD) and to support the pulled tube destructive examination. The details of the laboratory EC examinations are provided in Reference 5-1.

Table 5-1 provides a summary of the indications reported in the field compared to the indications reported during the laboratory examination. Generally, the laboratory examination confirmed the field data; however, at one TSP intersection, R5C62, TSP 2, an indication was detected with the bobbin probe that was not detected in the field. The +Point probe did not detect this indication in either the field or the laboratory.

The laboratory EC examination confirmed that the field indications were correct but did not significantly contribute to identifying the root cause of the observed cracking.

Field EC Data Review

U-bend Signal Offset

During a review of the EC data from OR08 for the degraded tubes, it was noted that the degraded tubes have a consistent and unusual signal characteristic in the low frequency (150 kHz) channel. The low frequency channel is used principally as a positioning channel since it sensitive to structures adjacent to the tubes. The low frequency channel is also sensitive to OD flaws and deposits, and to the conductivity of the tube material. The conductivity of the tube material changes when the material is strained, e.g., for bending the u-bends, thus it can be used to identify relative material condition (References 5-2 and 5-3).

The normal characteristic of the bobbin signal trace along the length of the tube that is not stress relieved in the U-bend region is generally a straight line through a null point defined by the beginning of the trace, either at TSH or at TSC, depending on the direction of the probe pull, then an excursion from null to the right through the U-bend, followed by a return to null in the opposite straight leg (Figure 5-1). The U-bending process cold works the material and changes the material state (and results in residual stresses), which is discerned by the bobbin probe.

For the rows 1 through 10 tubes, whose U-bends were stress relieved, the normal EC trace is characterized by the general absence of the U-bend signal excursion, which is replaced by a region between about 6H and 6C that is defined by entrance and exit "blips" in the signal (Figure 5-2). This region defines the heated zone for the U-bend stress relief. As noted in Section 6, stress relief is achieved by loading the low-row U-bends into the vacuum furnace apex to apex so that the U-bends are in the center of the length of the furnace, then heating the central region (of three regions) in the furnace to achieve the desired temperature in the U-bends. The "blips" in the signal define the heated region of the tube. A very small signal excursion to the left between the "blips" may indicate a stress-free state of the U-bends compared to the straight legs.

The bobbin signal characteristic of the degraded tubes in SG-D is significantly different from the normal characteristic. Instead of a signal that is essentially at the null for the entire length of the tube, the degraded tubes consistently exhibit a significant shift to the left of the null between about 6H and 6C (Figure 5-3). Based on the logic for the larger row tubes noted above, this would suggest that the residual stress state of the U-bends is significantly less than that of the straight legs. The location of the shift is consistent with the heated zone for U-bend stress relief (compare Figure 5-3 with Figures 5-2 and -1). This is also consistent with the split ring testing, which showed that the pulled tubes exhibited significant residual stress in the straight leg regions, both HL and CL (see Section 4).

The signal characteristic shown in Figure 5-3 is observed in all 15 of the degraded tubes reported in SG-D. In addition, four other tubes were identified in SG-D with this signal characteristic. The four additional tubes with this characteristic were reported with no detectable degradation at OR08. None of the tubes in rows 1 through 10 of SGs A, B and C exhibit this characteristic. Table 5.1 summarizes the tubes in Rows 1 through 10 that were found with the variation in the bobbin signal characteristic.

It is important to note that the EC signal is not a quantitative basis to evaluate the residual stress of the material or the material condition, but is a consistent qualitative indicator of relative condition. Without controlled testing of the same material in different conditions (i.e., mill annealed, thermally treated, straightening after mill annealing or thermal treatment, etc.) it is not possible to determine if a tube has high residual stress or not. The exception to this is the rows 1 through 10 tubes, because the u-bends of these tubes have been stress relieved. Because of this, the expected condition is that the entire length of the tube is in a low residual stress condition, which is verified by the signal characteristic for all but 19 tubes. Therefore, it can reasonably be concluded that only the 19 tubes in rows 1 through 10 in SG-D exhibit questionable resistance to SCC.

For the tubes in rows greater than 10, which have no U-bend stress relief, it is not possible to determine on the basis of the EC signal alone if the tubes are in a high residual stress or low residual stress condition. Since the null of the EC trace is based on the tube being tested, the only conclusion that can be drawn from the signal characteristic is that the U-bend region is at a different material state (higher strain) than the remainder of the tube.

Since the degree of strain to bend each row is less for each larger row, it can be hypothesized that, on average, the EC signal may be a discriminator of the level of residual stress in each row of tubes based on the offset of the u-bend signal from the null established by the straight legs of the tubes, measured as a bobbin voltage.

A study was performed for SG-D to measure the u-bend EC signal offset between the HL just above 8H (top tube support plate) and the adjacent U-bend signal, and similarly, for the CL. Figures 5-4 and 5-5 show the results of this study for the HL and CL respectively, superimposed with a best-fit polynomial. For each row, the average offset of all of the tubes in that row is shown. Also shown is the standard deviation of the average offset values for each row.

The hypothesis is generally shown to be true for rows up to about Row 50 since a high correlation constant is shown for the power curve fit for both the hot leg and the cold leg. The peaking in the rows greater than 50 has not been explained. However, some of the contributing effects may be deposits on the tubes in the outer rows that may influence the EC signals, a smaller database leading to greater relative variation, etc. It could be inferred from the good correlation of offset bobbin voltage and the row number that the tubes are all from the same population, however, there is no absolute standard available to differentiate an outlier from the population. Additional work would be required to establish such a standard.

Prior Industry Experience

In 1984, San Onofre experienced axial cracking and leakage in a tube. A section of the tube was removed from the SG for destructive examination (Ref. 5-2). Metallurgical analysis concluded, based on the microstructure, hardness and grain size of the material that the tube may not have received the heat treatment specified. The region of the tube that was in the condition identified by the destructive examination was identified by the field EC absolute bobbin signal as a conductivity shift that correlated with the region of the tube where the flaw occurred (Reference 5-3). This signal was utilized as a discrimination tool to test all of the tubes in the SGs. No other tubes in similar condition were identified.

Summary of EC Signature of Degraded Tubes

A summary of the logic of the eddy current signature and its application to the Seabrook SGs is contained in Appendix C

References

5-1 Westinghouse, SG-SGDA-02-35; Seabrook Steam Generator Tube Examination; November 2002.

5-2 Westinghouse, 85-5D2-SANGF-R1; San Onofre Unit 2 SG Tube R9-C151 HL; January 1985.

5-3 Combustion Engineering, S-ISI-010; "Tube Examinations for Metallurgical Anomalies at SONGS Units 2 and 3"; March 1986.

Table 5.1 Comparison of Field and Laboratory EC Results

Tube Section	Field Bobbin (Lab Review) Volts/%	Field +Pt (Lab Review) 300 kHz Volts	Laboratory Bobbin (Mix Ch) Volts/%	Laboratory +Pt 300 kHz Orientation Volts/%/Length (in.) (Deg.)
R 5 C 62 TSP 5	0.25/75	0.23	0.34/50	0 0.3/48/0.41
R 5 C 62 TSP 4	0.96/72	1.15	1.3/71	210 1.4/67/0.83 118 0.05/PI/0.1 (4 in line)
R 5 C 62 TSP 3	0.44/<20	0.3 0.39	0.68/57	101 0.36/<20/0.47 8 0.53/52/0.69
R 5 C 62 TSP 2	NDD	NDD	0.05/PI	NDD
R 5 C 62 TTS	N/A		N/A	NDD
R 9 C 63 TSP4	0.39/DSI	0.46 0.29	0.38/36	175 0.4/23/0.47 89 0.28/<20/0.57
R 9 C 63 TSP3	0.15/DSI	N/A	0.12/40	293 0.1/20/0.29
R 9 C 63 TSP2	NDD	NDD	NDD	NDD
R 9 C 63 TTS	N/A		N/A	*309 0.17/77**/0.25

* May be Tube removal artifact
** ID

Table 5.2 Tubes With U-bend EC Signatures

EC Database Reference (1)		OR08 EC Data	Tubing Log Reference (1)		Heat
Row	Column		M-Row	M- Col.	
4	65	SAI 02H-0.18 SAI 03H+0.07 SAI 04H+0.04 SAI 06H-0.14	4	58	NX1374
4	64	NDD	4	59	NX 1374
4	63	SAI 02H+0.01 SAI 03H-0.09 SAI 04H+0.10	4	60	NX 1456
5	88	SAI 03H-0.10	5	35	NX 1374
5	87	NDD	5	36	NX 1457
5	86	MAI 03H-0.03 SAI 02H-0.08	5	37	NX 1374
5	83	MAI 04H-0.12 SAI 02H+0.07 SAI 03C-0.01 SAI 05C-0.17	5	40	NX 1374
5	82	SAI 03H-0.05 SAI 04H-0.17 SAI 04H + 0.00 SAI 05C + 0.10	5	41	NX 1374
5	81	MAI 03H-0.18 SAI 04H-0.02 SAI 06H – 0.24	5	42	NX 1374
5	80	SAI 03C+0.14 SAI 03H+0.06 SAI 04H-0.12	5	43	NX 1374
5	62	SAI 03C-0.15 SAI 03H-0.06 SAI 03H+0.12 SAI 04H+0.11 SAI 05H+0.08	5	61	NX 1374

Table 5.2 - Tubes with U-bend EC Signatures (continued)					
EC Database Reference (1)		OR08 EC Data	Tubing Log Reference (1)		Heat
Row	Column		M-Row	M-Col.	
6	85	SAI 03H-0.24 SAI 03H-0.07	6	38	NX 1457
6	81	SAI 03H-0.18	6	42	NX 1374
9	63	SAI 03H+0.10 SAI 04C-0.18 SAI 04C+0.12 SAI 04H+0.16 SAI 05H-0.02	9	60	NX 1374
9	62	SAI 02H-0.02 SAI 03H+0.08 SAI 04H-0.02 SAI 05H-0.44 SAI06H-0.38	9	61	NX 1374
9	28	NDD	9	95	NX 1439
9	26	SAI 03H-0.01 SAI 04H+0.14	9	97	NX 1374
9	24	SAI 03H+0.05 SAI 04H+0.21	9	99	NX 1374
10	22	NDD	10	101	NX 1790

(1) See section 3 for explanation of difference between EC database R/C reference and tubing log R/C reference.

Figure 5-1 Normal Eddy Current Signal for a Tube in Row 11 or Greater

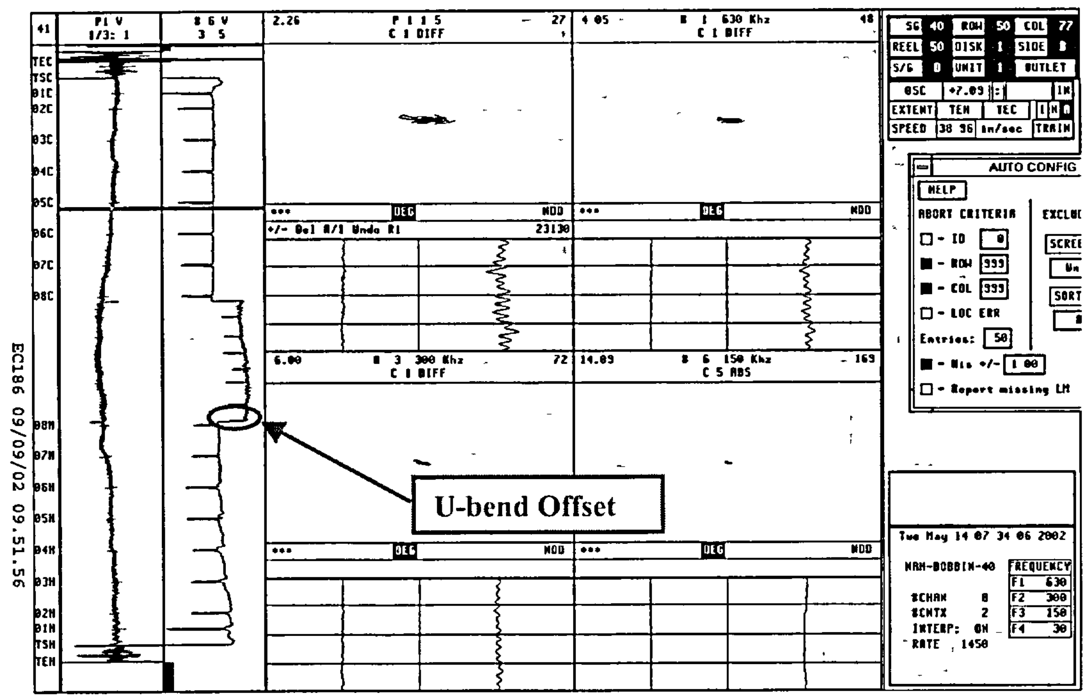

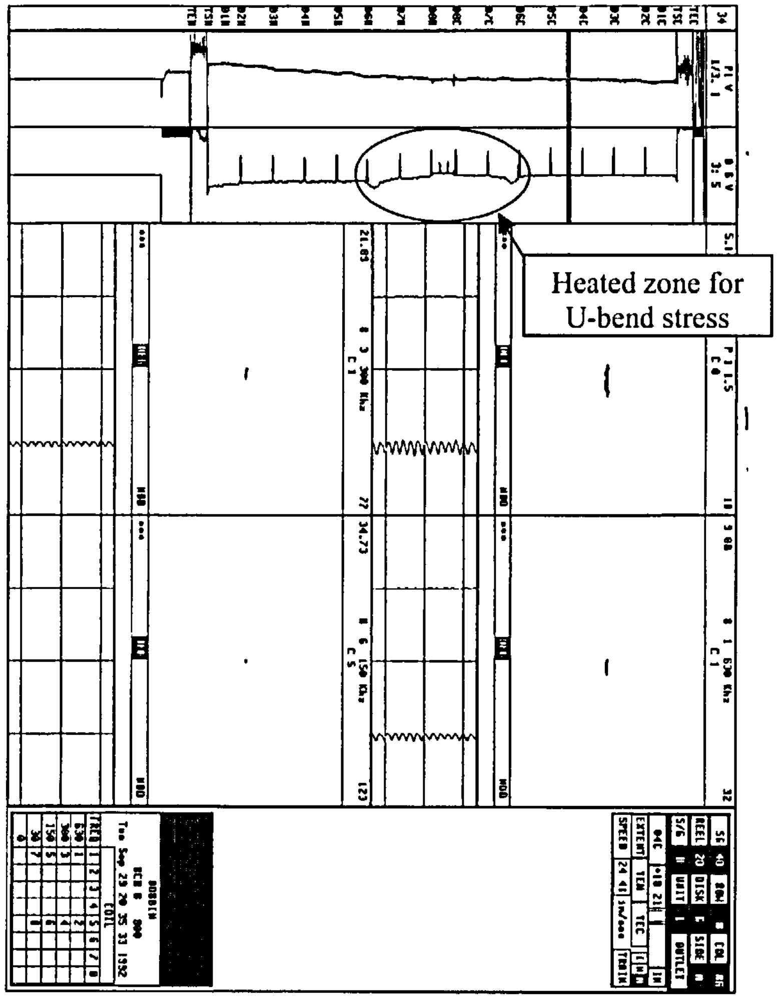

Figure 5-2 Normal EC Signal for R<11 Tube

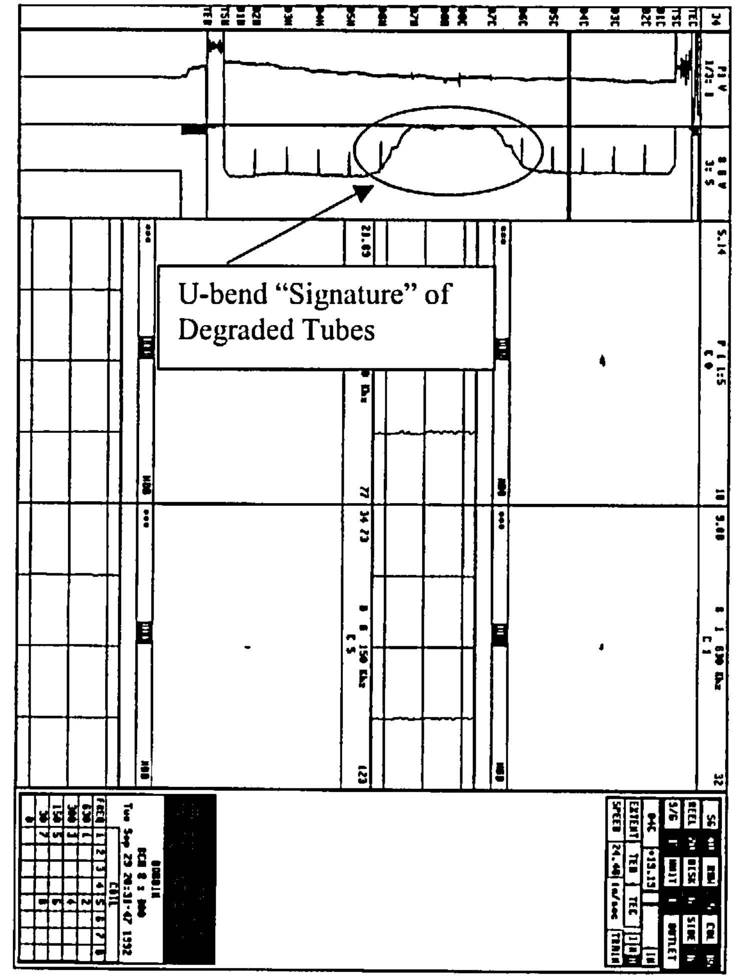

Figure 5-3 Eddy Current; Degraded Tubes

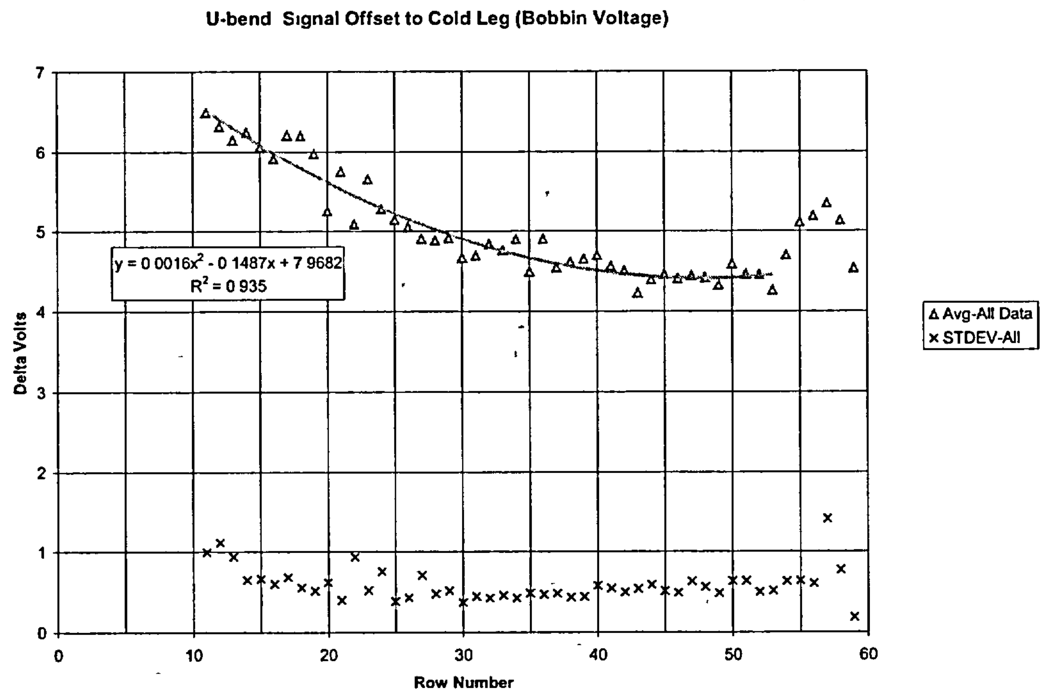

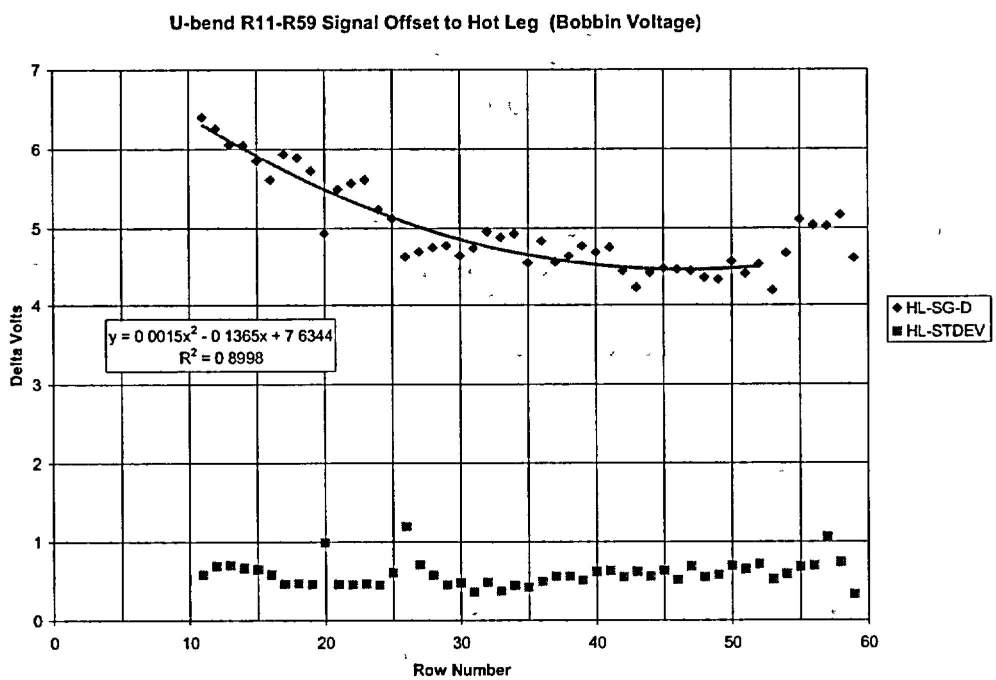

Figure 5-4 EC Signal Voltage Offset of U-bend from Straight Leg of the Tubes

6. Manufacturing Review

A manufacturing review was performed to determine if there were any deviations in the processes that may have contributed to the conditions leading to the cracking of the tubes in Seabrook SG-D. Both the tube manufacturing processes and the SG manufacturing processes were examined.

By necessity, the manufacturing review is principally a review of records maintained for the manufacturing processes. Consequently, the focus of the records search was to look for documented deviations, and a review of these to assess if they could have contributed to the observed degradation.

Tubing Manufacturing Timeline

A timeline of SG tubing manufacturing was prepared to focus the records search in the proper timeframe for the Seabrook SGs. A timeline of all of the Model F SG tubing sets manufactured is shown in Figure 6-1. This timeline shows that the Seabrook SG tubes were manufactured (delivered) between April and June 1980. The tubing sets manufactured just prior to the Seabrook sets were installed in the Napot Point SGs (never operated), and those manufactured at about the same time as the Seabrook tubing sets were installed in the Maanshan 2 and Kori 3 SGs. The nearest tube sets manufactured for domestic SGs were provided to Vogtle 1 and Millstone 3 in the timeframe about June-July, 1980. Both of the domestic plants and Maanshan 2 have operated without reporting cracking to date.

The timeline shows the time of delivery tubing "sets". A set of tubes is generally the complement of tubes for a single SG, plus spares. However, it is not unusual to find that the tube complement for some SGs is comprised of tubes from several different sets. It is presumed that this is the result of manufacturing sequence and manufacturing efficiency.

Tubing Manufacturing Process

The tube manufacturing process and procedures were examined to assess if there was a potential for a process deviation in the thermal treating process, leading to reduced corrosion resistance or to an elevated residual stress in some tubes. No documented process deviations were found; indeed, after examining the records retained for the tubing process, high confidence in the integrity of the process and its controls was achieved.

It is considered extremely unlikely that a failure to thermally treat a few tubes could occur. The process flow would dictate that a larger number of tubes, more than one steam generator, and probably more than one operating plant should be involved. For example, a single furnace load for the thermal treating process could include up to a maximum of about 625 tubes. With concurrent manufacturing of multiple sets of tubing, which share the heats of material utilized in the Seabrook SGs, it would not be expected that Seabrook would be unique in reporting crack-like indications in the tubes. Further, the microstructures of the pulled tubes and the archived tubes indicate that the tubes in question were heat-treated. Additional pulled tubes from the other affected heats would be required to completely answer this question.

Figure 6-2 shows the process flow for manufacturing the Alloy 600TT tubing utilized in the Seabrook SGs. The starting point of the process was the receipt of a "Lot" of TREXes. TREXes were ordered by weight to produce the desired length of tubes. For the later tube production- this is interpreted to include the Seabrook tubes, 90% of the TREXes in a Lot was required to be from the same heat of material. The mill practice was to process a Lot of TREXes at the same time; this is logical because the tubes produced from a single Lot of TREXes would, by plan, all be approximately the same length.

Following a cold pilgering and two cold drawing processes, separated by intermediate mill annealing for 5 minutes at 1900°F, the tubes were final mill annealed in a continuous belt, hydrogen environment furnace. Twenty-two tubes (11/16" dia.) were placed across the width of the belt, which traveled at 3.25 ft/min. Care was taken to maintain both the material heat number and the TREX Lot number that were vibro-etched into the tube at one end.

Following mechanical straightening, belt polishing, and re-marking, the tubes were binned by length, approximately 20 different lengths for the rows 1-59 u-bends. (The difference in length between a row 1 tube and a row 59 tube is greater than 15 feet.) When sufficient tubes were available in the bins, the tubes were loaded into the thermal treating furnace segregated by length in 5 different compartments on the loading rack (see Figure 6-4), longer tubes on the bottom; shorter ones on the top.

The thermal treating furnace was a vacuum furnace, electrically heated by 9 banks of heaters that were independently controlled in three regions along the length of the furnace. Figure 6-3 (a) shows one of the two furnaces utilized during tubing production; Figure 6-3 (b) shows the heater control panel for the furnace. Figure

6-4 shows the loading rack for the tubes and the identification of the loading compartments.

Records were maintained for each furnace load (number assigned that identified the furnace used, A or B, and the rack location of tube (A through E) and the heat number for each tube). The furnace load number was assigned prior to unloading the furnace. If a tube had been previously thermally treated, the records also indicated the prior thermal treatment furnace load number. Re-thermal treatment was required if straightening was performed after the initial thermal treatment. A straightening procedure was always followed by belt polishing that would remove the original vibrotooled identification. Since it was required to vibro-etch the thermal treatment batch number on each tube prior to unloading it from the furnace, each re-worked tube would display the final thermal treatment batch number. The records indicate that re-thermal treatment was not uncommon; however, the process review concluded that re-straightening was not frequently performed. Figure 6-5 shows a typical thermal treatment log record that includes tubes that were previously thermally treated, then re-thermally treated.

The thermal treatment specification limited the total time of exposure to the 1320°F environment to 30 hours; thus, it was possible to perform two thermal treatments and one stress relief of the rows 1-10 u-bends within the required time limit. If straightening was performed after the second thermal treatment, the tube could not be re-thermally treated. There is no evidence that this procedure was violated during the manufacturing cycle of the tubes.

After thermal treatment, the tubes were bent into u-bends. A tube was not bent unless it was verified and recorded that a thermal treatment lot number was evident on the tube. Following bending, the rows 1 through 10 u-bends were stress-relieved in the area of the bends. The u-bends were loaded into the vacuum furnace (the same furnace used for thermal treatment) as shown on the schematic in Figure 6-6. The u-bends were nested, and stacked about 22 tubes high, held in a modified rack that prevented relaxation of the u-bends. Only the central region of the furnace was heated, so that the heated zone on the u-bends extended from about the elevation of TSP6 hot leg to cold leg. The tubes were maintained at 1320°F for 2 hours.

The details of the tube manufacturing process were reviewed in a special, open review by a panel of experts who were active in the development and implementation of the process at the time the Seabrook tubes were manufactured.

The specific question of how high residual stress could be introduced in the manufacturing process was addressed. The review identified additional process controls that were not evident in the available records. For example, the specific control on acceptability of a tube for tube bending was identified as the presence of a thermal treatment batch number vibro-etched on the end of the tube. Based on the records review and the special experts review, the tube manufacturing process appears to have been well defined, well organized and well documented with built-in controls to prevent intermingling of mill annealed and thermally treated tubing. The available records provide verification of the process steps from original TREX to finished U-bend.

With the currently available records, it is not possible to link specific tubes in a SG to specific thermal treatment lot numbers. The Experts Review indicated that such a record was made, i.e., information contained on the data card attached to each tube. A record was made during SG tube installation of the heat number of each tube related to the specific position of that tube in the SG; however, no record relating the thermal treat batch number to the specific tube location has been found to date.

<u>SG Manufacturing Review</u>

The manufacturing records for Seabrook SG D were reviewed. No non-conformances were identified of any significance to the observed tube cracking events. The complete report of the review is included as Appendix A.

Figure 6-1
Tubing Manufacturing Timeline

Plant	J-77	J-77	A-77	S-77	O-77	N-77	D-77	J-78	F-78	M-78	A-78	M-78	J-78	J-78	A-78	S-78	O-78	N-78	D-78
Callaway	202		204, 206	208															
Wolf Creek															232, 234		237, 239		

	J-79	F-79	M-79	A-79	M-79	J-79	J-79	A-79	S-79	O-79	N-79	D-79	J-80	F-80	M-80	Note	S-82
Vandellos 2					247								253, 255				320
Kori 2			249	251				257									
Maanshan 1								257		259, 261							
Napot Point													263	265			

	A-80	M-80	J-80	J-80	A-80	S-80	F-81	M-81	A-81	M-81	J-81	J-81	A-81
Seabrook 1	267	269, 271, 273	277, 279										
Maanshan 2		273	275, 277, 279										
Millstone 3				281, 283	285, 287	288							
Kori 3	287	288	289, 290										
Vogtle 1			289, 290		291, 292, 293	294							
Kori 4			290				297		301	303			
Vogtle 2			290						301		304, 305, 306	307	
Salem 1 (Seabrook 2)			290				295, 296, 298		301	302			

	S-81	O-81	N-81	D-81	J-82	F-82	M-82	A-82	M-82	J-82	J-82	A-82	S-82	O-82
Yeonggwang 1	308		309		310									
Yeonggwang 2										315	316			317

Figure 6-2 Tube Manufacturing Sequence

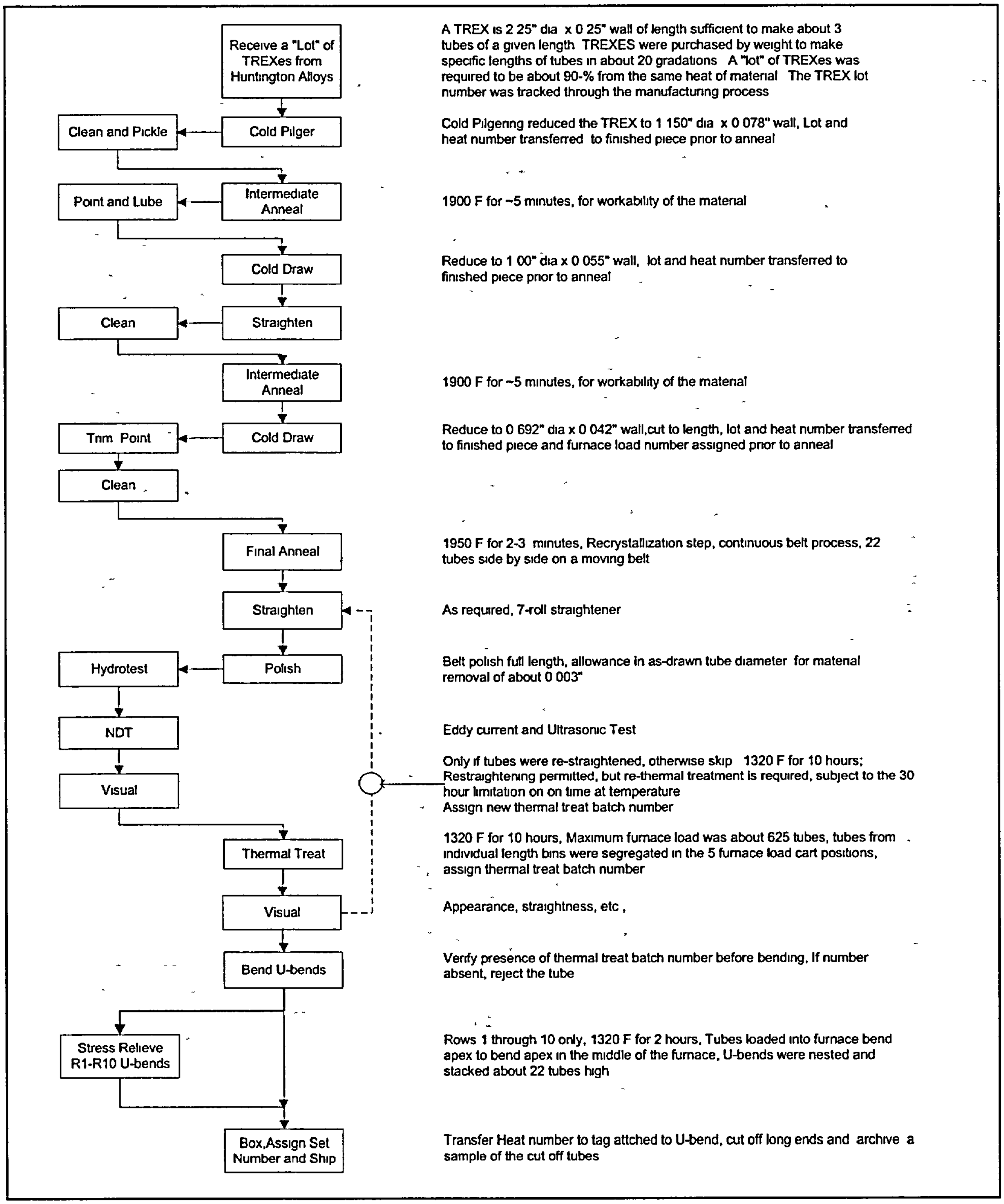

Figure 6-3 Thermal Treatment Facility (a) Vacuum Furnace

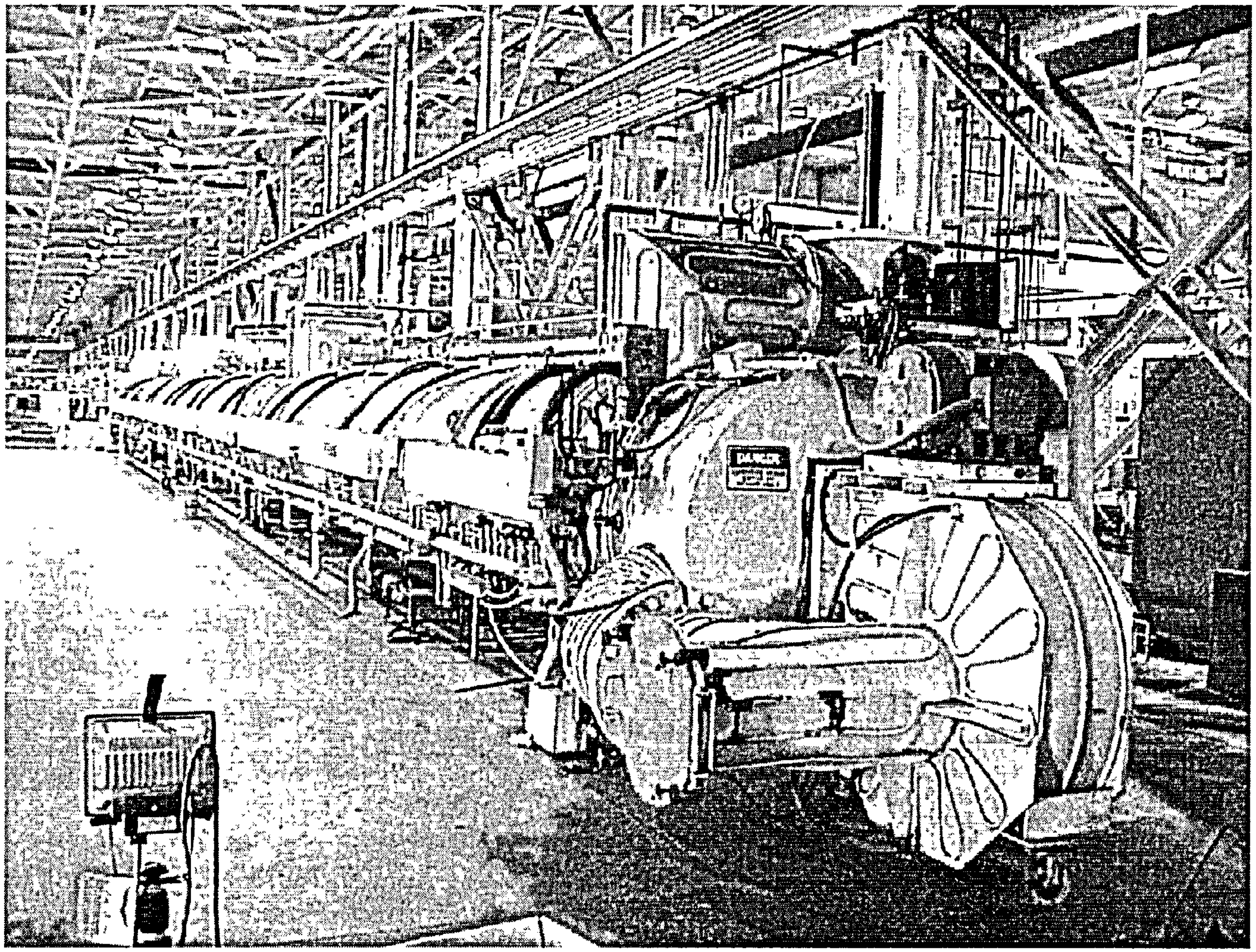

Figure 6-3 Thermal Treatment Facility (b) Furnace Controls

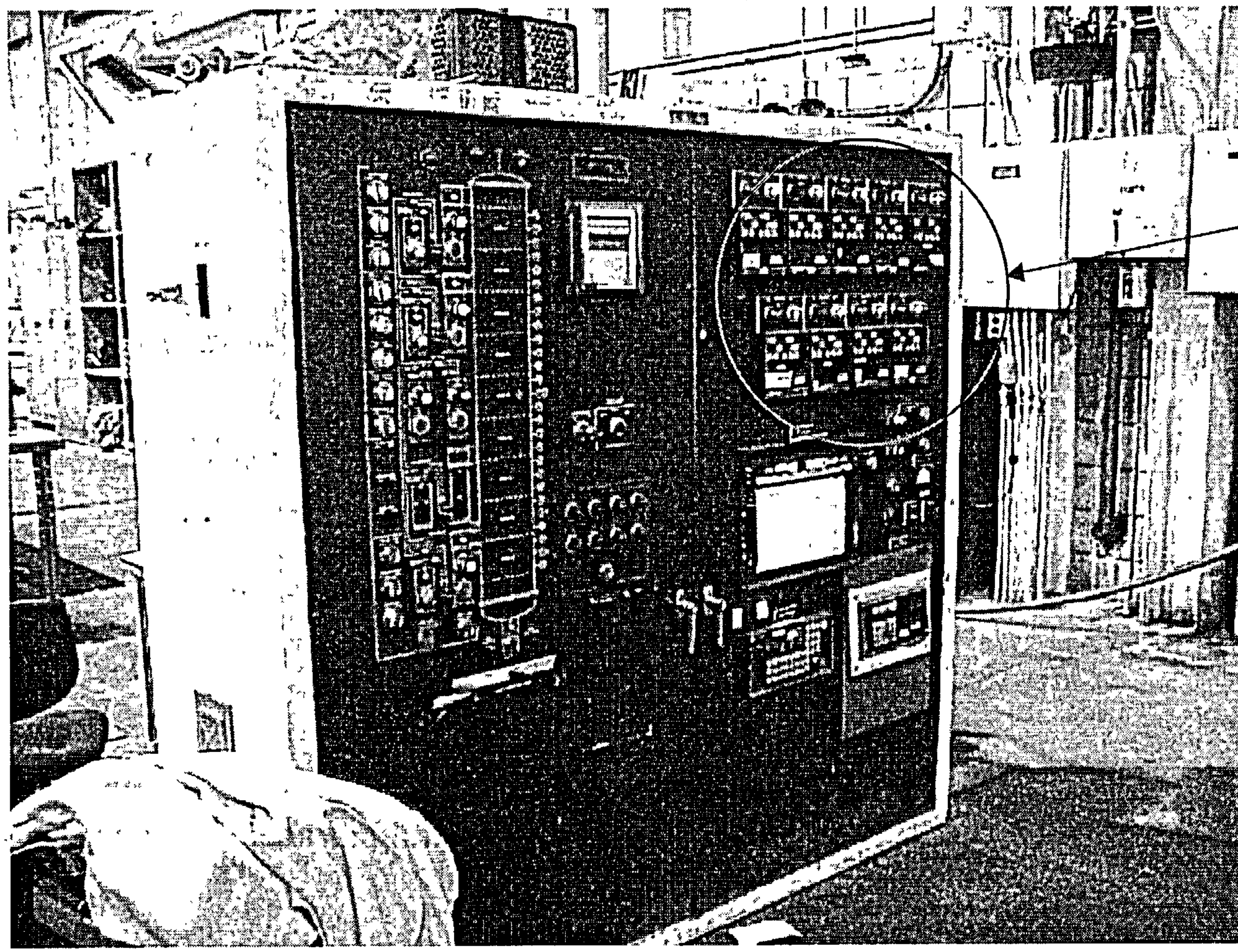

Independent heater controls – 9; three furnace zones

Figure 6-4 Thermal Treatment Furnace Loading Rack

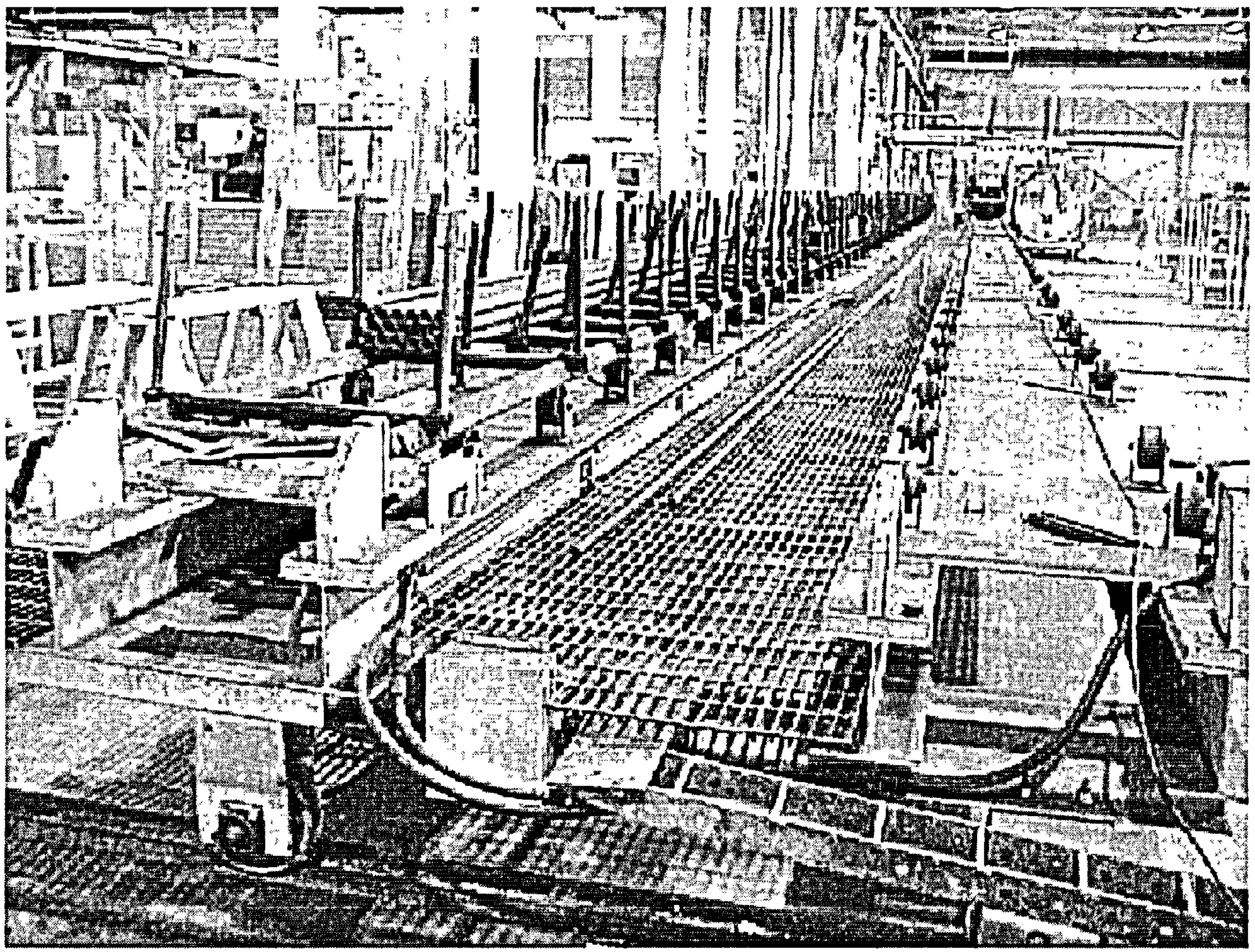

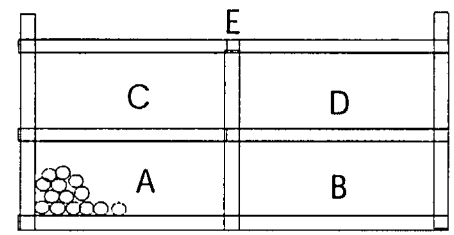

Loading Rack with

Removable Separators

Total capacity of the rack was about 625; 125 tubes per section (A,B,C,D), and about 125 tubes on top of the rack (E).

Figure 6-5 Typical Thermal Treatment Record: (a) General Record

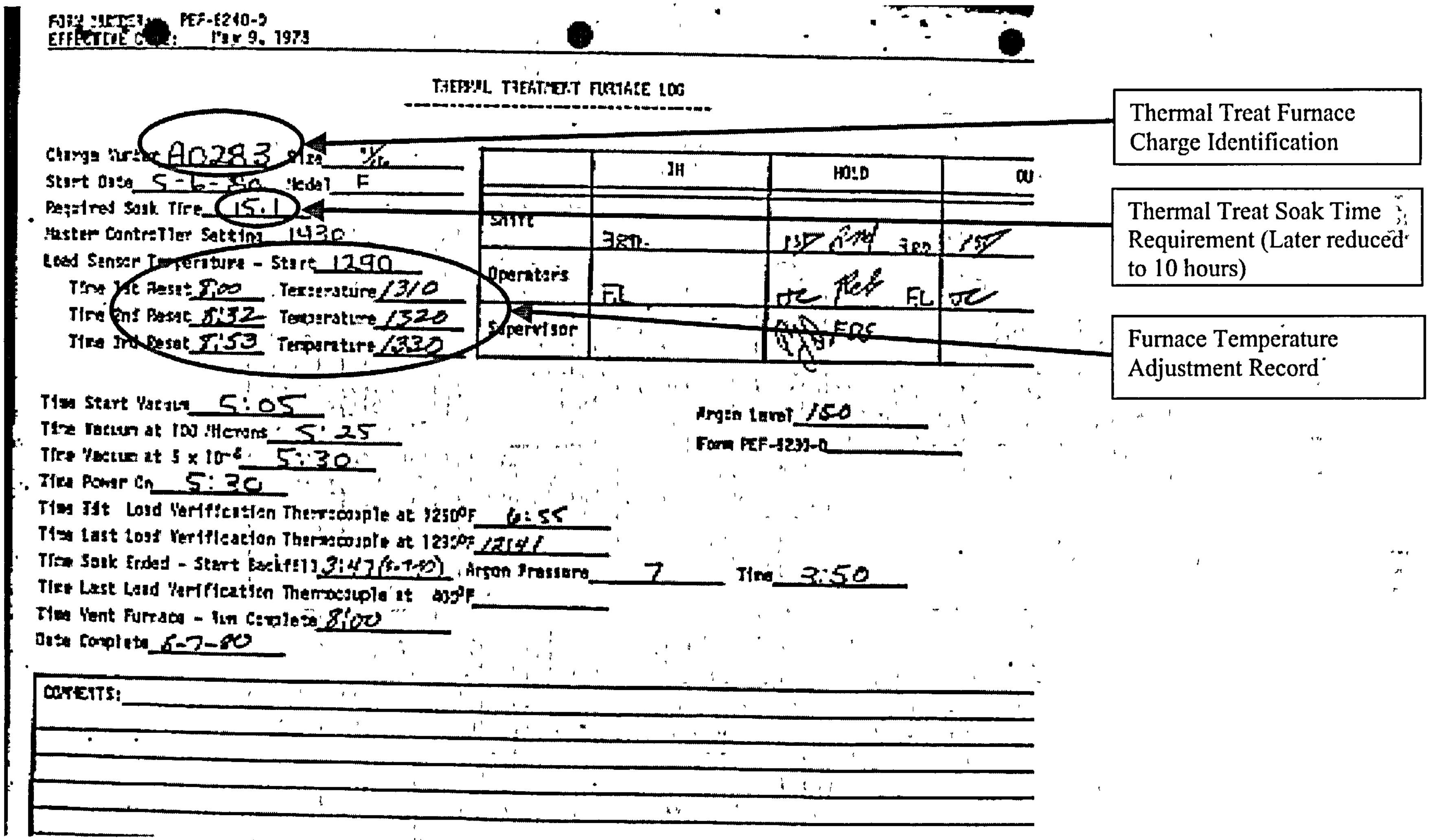

Figure 6-5 Typical Thermal Treatment Record: (b) Furnace Load Record

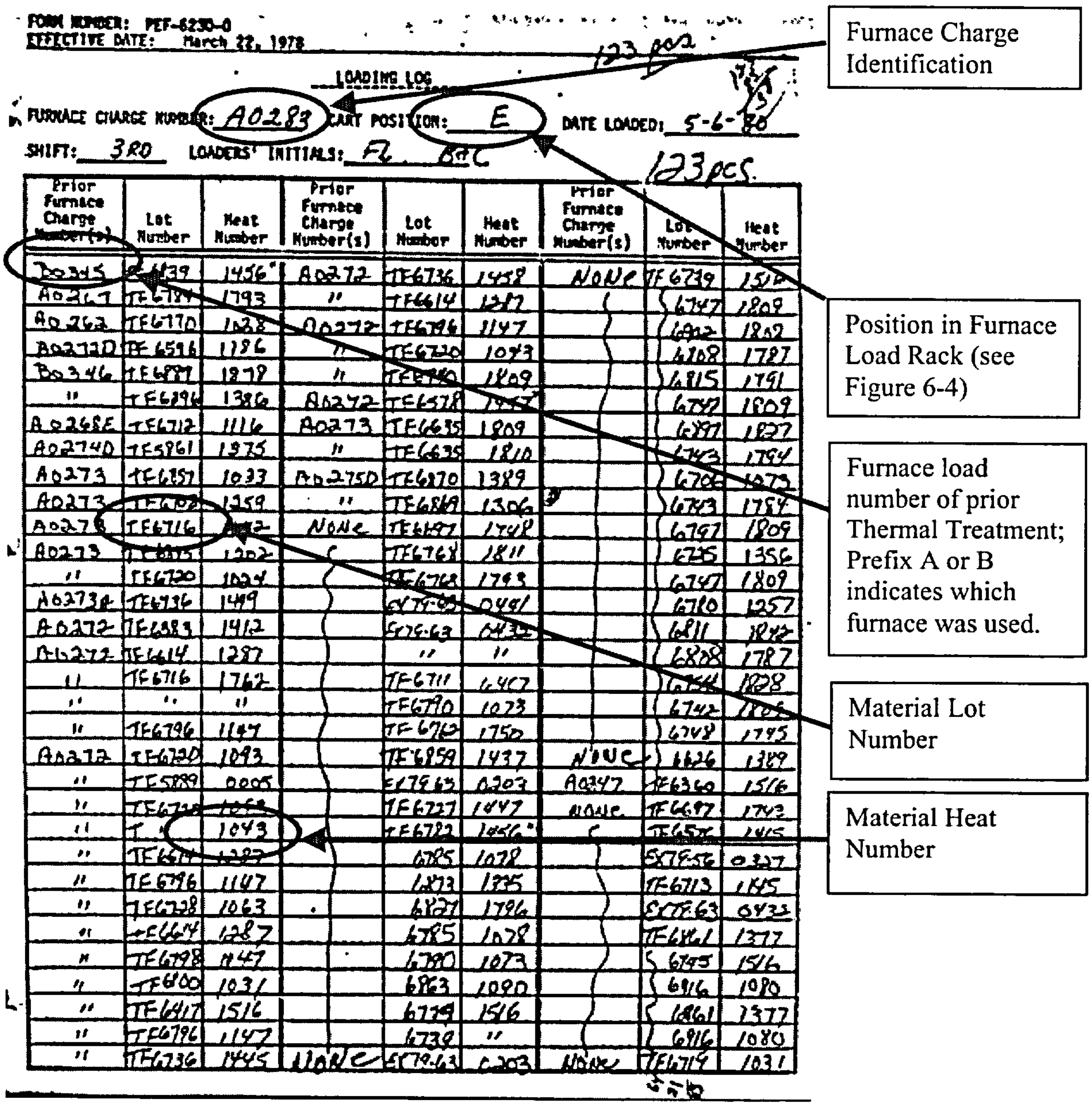

Figure 6-6 Schematic of Furnace Loading for U-bend Stress Relief

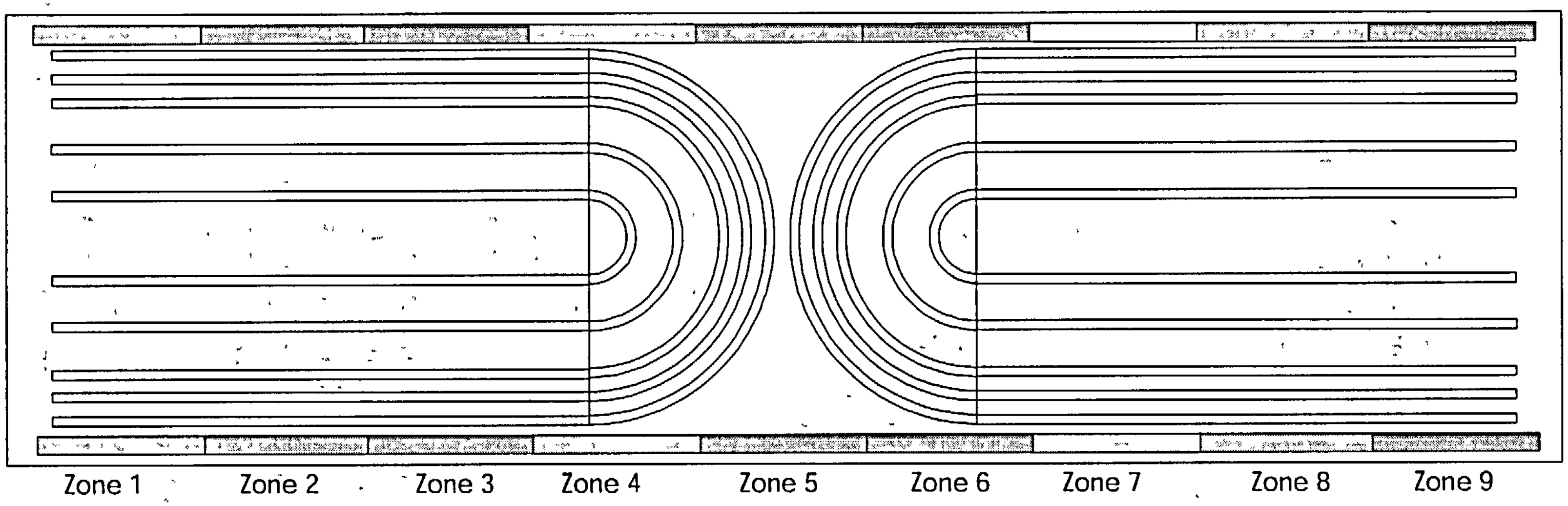

Zones 1 through 9 are heating zones in the furnace. Only zones 4, 5 and 6 were activated for stress relief of the u-bends.

7. Operations Review

A review of the plant secondary side operating chemistry was performed by a joint Westinghouse/Seabrook team. The significant events that could affect secondary side chemistry conditions were summarized (Table 7.1) and evaluated for their potential to contribution to the root cause of the ODSCC reported at Seabrook during OR08. The input data utilized during this review were:

- 1996 Chemistry Assessment
- Deposit Analysis Reports
- 1996 - Scale Profiling using OR03 and OR04 EC data
- 2000 - Scale Profiling using OR05 and OR06 EC data
- Visual Inspection Data
- 2000 - SCA Test Program
- Pri./Sec. Strategic Water Chemistry Plans (0R01 -0R05)
- Jan. 2000 Seawater Ingress Report
- June 2000 Plant Trip Report
- OR07 Hideout Return Evaluation Report.
- Seabrook Jan 2001 Startup Report
- March 2001 Condenser Leak Report

The results of the deposit analyses performed after the outages OR01 through OR05 provided the following data:

- The amine chemistry maintained during this time resulted in a decreasing trend of corrosion product transfer from 16 ppb to 2 ppb.
- The copper concentration decreased during this time from about 15-wt% to about 5 wt%. Copper oxide is known to be associated with corrosion cracking.
- Scale containing zinc, copper and silicon was first observed after cycle 3.
- In OR05, aluminum was detected in the deposits.
- At OR05, hideout return was found to be slightly caustic and MRI 1-2.
- At OR06, loose deposits displaced by the upper bundle hydraulic cleaning process were found to contain magnetite and copper metal.
- Copper was observed in the 4-8 wt% range, and lead was observed in the 120-150 ppm range after OR 06.
- Densification of the deposits and the presence of binding material were observed in the deposits removed during OR06.
- Application of EC-based scale profiling techniques indicated that significant deposit accumulation existed in SG-A (4000 lbs.) and SG-B (3400 lbs.),

distributed 46% in the hot leg, 37 % in the cold leg and 17% in the U-bend. The heaviest deposits were predicted to be between the 4th and 7th support plates, and visual inspection data supported this prediction. The EC data suggested that accumulation in the quatrefoil was beginning; however visual inspection did not confirm this.

- At OR07, analysis of the loose deposits showed the presence of magnetite and copper metal in the 2.5 wt% to 6.5 wt% range on the surfaces of the tubes in the interior of the bundle. Lead was found in the deposits between about 131-151 ppm, with a single high reading of 849 ppm in the scale from the grit tank.

During the OR07 hideout return analysis, nothing was identified that would be cause for alarm and no corrective actions were recommended. Westinghouse analyses suggested that the crevice environment was slightly alkaline. However, the low concentrations of the alkaline forming species indicate that any highly alkaline conditions would be restricted to a very localized region in the tube bundle.

Several instances of seawater ingress have occurred during the operating history of Seabrook.

- In January 2000, an error in valve alignment resulted in seawater ingress into the main condenser into the flush lines and hot wells. Sodium concentration exceeded the EPRI Guidelines Action Level III limit, but chemistry was rapidly restored to a compliant status after the incident.
- In March 2001, seawater in-leakage into SG- B and C main condenser was observed. Chemistry cleanup following this event was a lengthy process; however, conditions were restored to comply with the guideline limits.

Observations from the OR08 SG bulk deposit analysis were:

- Iron is major constituent of bulk deposits with concentrations ranging from 60 to 63 wt %
- Copper concentration ranged from 7 to 8.8 wt %
- The highest iron and lowest copper concentrations were seen in SG D sample
- Manganese concentration ranged from 0.86 to 1.1 wt %
- Nickel concentration ranged from 1.4 to 1.5 wt %
- Lead concentration ranged from 150 to 160 ppm
- Positive silver concentrations ranging from 14 to 33 ppm were detected in all samples
- The iron, nickel, lead and chromium levels seen in the OR08 SG bulk deposits are comparable to levels seen in the OR07 bulk deposits. The copper levels in

SG A, SG B and SG C were slightly elevated and the copper level in SG D was depleted somewhat compared to the OR07 samples

Summary

1) There are no obvious chemistry anomalies during the operating history of Seabrook that can be directly related to the observed cracking at OR08 from current evidence.
2) Overall chemistry conditions are good. The pH control program appears to have resulted in decreases in corrosion product transport over time. Hideout return chemistry shows good control of impurity levels.
3) While concentrations of copper and lead are typically low in sludge samples, there has been some indication of elevated lead concentration in the sludge lance grit tank and the presence of a trace of copper oxide. These observations were made only after OR07. No significant issue has been identified since there was only one sample with high lead and the copper oxide concentrations are low.

Table 7.1 Seabrook Chemistry Assessment – Chronology of Events and Results of Associated Data Reviews

Time	Event/Action
Prior to Cycle 1	• Condenser tubes staked with stainless steel shanks and bakelite wedges to reduce tube fretting from steam impingement • Tube sheets coated with epoxy on seawater side to reduce potential of galvanic attack. Performed 100 % eddy current testing of condenser tubes.
Cycle 1	• Standard AVT regime. Maintained FW pH of 9.2 at 25° C using hydrazine.
Cycle 2	• Increased FW hydrazine to raise FW pH to 9.2-9.6 at 25° C.
OR02	• Installed stainless steel impingement baffles around susceptible condenser tubes
Cycle 3	• Increased FW hydrazine to raise FW pH to 9.5-9.6 at 25° C. (The result of this pH increase over the course of cycles 1-3 was a steady decrease of iron transport from 16 to 6 ppb in the feedwater. Copper transport on the average was less than detectable). • Began an aggressive air in-leakage reduction program • Installed new corrosion transport sample boxes for improved monitoring • Injected alternate amine, Ethanolamine, at end of cycle (These initiatives improved sampling reliability for corrosion product transport, and began to further reduce the iron transport).
OR03	• Replaced water treatment system with a UF-RO-DEOX-EDI-MB unit • Changed one of the blowdown resin beds to a lead cation bed (These two initiatives reduced the introduction of contaminants, especially sodium and sulfate, into the secondary side of the plant).

Table 7.1 Seabrook Chemistry Assessment – Chronology of Events and Results of Associated Data Reviews (continued)

Cycle 4	• Increased ethanolamine injection to achieve 1.3 ppm in FW • Revised the regeneration procedures for blowdown demineralizers • Continued the elevated hydrazine addition (>100 ppb) • Maintained a FW pH of 9.5 at 25° C • Established a control band for CPD oxygen at 2-4 ppb • Pressure pulse cleaning of all 4 SGs (This cycle optimized the oxygen control band in the condensate system, and continued the monitoring of iron reduction with the addition of ethanolamine).
Cycle 5	• Maintain FW ETA at 1.0 ppm • Injected alternate amine Methoxypropylamine to achieve 5 ppm in FW • Decreased hydrazine to 80 ppb in FW once MPA addition was stable • Maintained CPD oxygen at 2-3 ppb (when possible) • Pressure pulse cleaning of all 4 SGs
OR05	• Replaced CST "delta" seal on floating lid. (Refined the oxygen control band, introduced MPA and reduced iron transport to ~ 2 ppb).
Cycle 6	• 4 forced outages • Maintained feedwater chemistry at 5 ppm MPA and 1 ppm ETA • Feedwater hydrazine maintained at 80-90 ppb, CPD oxygen at 2-3 ppb • Feedwater iron trended down to an average of 1.4 ppb at end of cycle • Mossbauer analysis of feedwater CPT sample shows that iron is 100% as magnetite

**Table 7.1 Seabrook Chemistry Assessment –
Chronology of Events and Results of Associated Data Reviews (continued)**

OR06	• Prepared condensers for tie-in to condensate polisher • Continued replacement of carbon steel extraction steam drains with chromium-molybdenum alloy which is flow erosion resistant • Performed Upper Bundle Hydraulic Cleaning (UBHC) of all four steam generators • Modified SB Flash Tank to allow blowdown flow up to 100 gpm per steam generator
Cycle 7	• Maintained feed water chemistry at 5 ppm MPA and 1 ppm ETA • Feedwater hydrazine maintained at 80-90 ppb, CPD oxygen at 2-3 ppb • Seawater intrusion event 1/8/2000 • Plant trip due to failure of Feedwater Pump circuit card (June 2000)
OR07	• Consolidated Edison Combined Inspection and Lancing (CECIL) used on the tube sheets of steam generators B and C to remove scale collars • Feedwater sample line modification initiated (MMOD 99-623) • Condensers put into a modified dry lay-up. Condenser drained and warm, dehumidified air blown through the condensers. Condensate and feedwater train drained. (This was related to an unexpected diesel problem, which extended the outage from 11/22/00 to 1/29/01).
Cycle 8	Experienced a condenser leak in March 2001

8. Root Cause Evaluation

The following information summarizes the facts derived from the prior assessments:

Chemical Conditions:

1. There is no direct evidence of unusual chemistry conditions in the crevice deposits or in the bulk sludge that can be clearly identified as causing the cracking observed at Seabrook.
2. Seabrook secondary side operating bulk chemistry has been within the EPRI guidelines for secondary coolant chemistry.
3. There have been secondary side chemistry transients, including seawater ingress at several times. Re-establishment of acceptable chemistry conditions has been relatively rapid following these events.
4. Lead and copper were identified in the bulk sludge but not in unusual quantities.
5. Traces of lead and copper were identified on the tube OD and on the crack faces.

Material Condition:

1. The degradation is principally axial ODSCC, with minor presence of IGA based on the destructive examination of the degraded intersections.
2. The microstructure of the pulled tubes, both from the same heat (NX1374), is consistent with the range of expected microstructures for thermally treated tubing, but is not considered the optimum microstructure.
3. The microstructures of archive samples of the other two material heats (NX1457, NX1456) included among the degraded tubes are typical of the microstructures expected for thermally treated tubes. No pulled tubes from these heats of material are available.
4. The microstructure of the pulled tubes compares well with that of previously pulled tubes (from other plants) that performed well with regard to corrosion.
5. Manufacturing records show that it is extremely unlikely that the tubes were not thermally treated. Detailed records exist for thermal treating and U-bend stress relieving, including position of the tubes in the furnace and records of re-thermal treating as necessary.

6. The pulled tube material is not sensitized based on multiple modified Huey tests performed in accordance with the standard industry test method.
7. The tensile properties of the pulled tubes are higher than expected for thermally treated tubing.
8. The residual stress, as measured by split ring tests, is about 20-25 ksi, significantly greater than the 2-3 ksi expected for thermally treated tubing. The source of the residual stress has not been explained.
9. The residual stress is not localized at specific axial positions but appears to extend over the length of the pulled tubes. This was determined in split ring tests on specimens from the upper, middle and lower sections of the pulled tubes. Further, hardness tests taken along the length of the tubes indicate essentially no variation in hardness along the length of the tube.
10. The tube pull forces were very low after the initial breakaway in the tubesheet region.
11. There are no documented manufacturing deviations that could have affected the tubing during SG manufacturing.

Other Data:

1. Thermal treating records indicate that the tubes were thermally treated, and stress relief of the u-bends in rows 1 through 10 was performed.
2. Thermal treatment time at temperature exposure is limited by the procedures to 30 hrs. at temperature (1320 deg. F)
3. The manufacturing process of the tubes permits straightening of the tubes following thermal treatment provided a subsequent thermal treatment is performed.
4. The EC signal for all of the degraded tubes is characteristically different from that of all except 4 of the non-degraded tubes. This observation is limited to the tubes in rows 1 through 10.
5. The EC signal for the tubes in rows 11 through 59 provides a good correlation between the signal offset for the U-bend region from the straight leg regions and the row numbers (bend radius). However, without comparison to a known standard, the EC signal does not provide conclusive information on the comparative stress state of the rows 11-59 tubes.

Root Cause Analysis

The analysis of the root cause of the cracking considered the data evolving from testing of the pulled tube material, tests performed on archived and pulled tube materials by an independent laboratory and an increasing knowledge of the tube manufacturing processes resulting from the review of manufacturing records. Various hypotheses were developed and evaluated against the known facts to assess their viability. The hypotheses considered are summarized in Appendix D.

Ultimately, residual stresses, at levels unexpected in thermally treated tubes, in the presence of an unidentified corrosive environment, were considered to have been a significant factors to cause the cracking noted in the steam generator tubes.

Collectively, the data on the material condition of the pulled tubes indicate that the tubes were manufactured in accordance with the applicable procedures. No evidence exists that the pulled tubes were not properly thermally treated. The microstructure of the pulled tubes is comparable to that of other pulled tubes and to that of archived tubes with a range of properties, all known to be thermally treated, although it is not considered to be optimal. The microstructure of an archived tube from a heat of material of one of the degraded tubes was considered "good" compared to the expected range of microstructures for thermally treated Alloy 600.

The elevated residual stress along the length of the pulled tubes is likely a significant contributor the observed cracking. The elevated tensile strength of the pulled tubes is consistent with the high residual stress measured in the tubes and the hardness of the tubes. The source of the high residual stress has not been identified.

No overtly aggressive chemical environment was identified in the cracks or on the surface of the tubes; however the presence of a corrosive chemical environment is required for cracking to occur in Alloy 600 tubing. The presence of lead and copper may be a contributing element; however, the concentration of both is not unusually high compared to other pulled tube environmental results. Although it may be speculated that an aggressive environment may have existed at some time during operation, leading to initiation of cracking, there is no current evidence of specific corrosive elements.

The particular material condition of the degraded tubes (as indicated by the elevated residual stress) provides an opportunity to identify the tubes in that condition by a distinctive eddy current signal that differentiates between the low stress condition of the stress relieved u-bends, and the apparently high residual stress condition of the straight legs. It is not known precisely what property is being measured by the eddy current probe, because detailed metallurgical and physical tests have not been performed to establish this; however, similar conditions have been observed previously at another plant as noted in Section 6.

All 15 of the degraded tubes display the EC signature and four additional tubes, all in SG D, also do. None of the tubes in SGs A, B or C display this signal.

Based on the observation for the low row tubes, a hypothesis can be made for the tubes in rows 11-59 that the difference in the material state between the straight legs and the u-bend should also be discernible by the EC signal, based on the assumption that the majority of tubes would have low residual stress straight legs, similar to the low row u-bends. Since the bending process of the u-bends significantly strains the material through the u-bends, the changed material condition of the u-bends should be visible to EC, but in the opposite direction as the low row u-bends.

A study of the u-bend bobbin voltage offset showed that the offset generally correlates well with the row number, an expected result since the strain imparted to the tubes decreases with increasing row radius. It is not possible to conclude with certainty that this correlation indicates the absence of the conditions that are believed to exist for the degraded tubes until controlled testing is performed to establish the relative behavior between low residual stress and high residual stress tubing. However, the data suggest that the tubes in rows 11 through 59 are from the same population; thus, if the incidence rate of degraded tubes is assumed to be similar to that of the low row tubes, i.e., 15 of 19 tubes with the EC signal, then, for the rows 11-59 tubes, it would be expected that a number of tubes should have been reported as degraded if all of the tubes are from the same population. None of the tubes in rows 11-59 have been found to be degraded.

THIS PAGE
INTENTIONALLY
BLANK

Appendix A
SG Manufacturing Records Review Report

Purpose:

To review the manufacturing records and associated documents for Seabrook Unit 1 Steam Generator Shop Order 2057 ("D" SG), in order to investigate whether any situation arose during manufacture of this unit that could potentially be attributed as a cause of the eddy current indications observed in 15 tubes of this steam generator. The indications were observed at support plates 2 through 6 on both hot and cold leg sides in tubes located between rows 2 and row 9. Similar indications were not observed in any of the other three steam generators.

Scope:

The following records and shop order documents were used to affect the manufacturing records review for Westinghouse Shop Order NAGT-2057 (Seabrook Plant "D" Steam Generator).

A) Model F Steam Generator Stress Report, Analysis of As-Built Steam Generators For Public Service Company of New Hampshire, WNEP 8242 Parts 1 thru 3

The Analysis of As-Built Steam Generators for the Model F Stress Report for Public Service Company of New Hampshire, Seabrook Unit 1 contains non-conformance documents (EANs & MRRs) and analysis of the as-built condition for all four steam generators manufactured for Seabrook Unit 1. The document includes copies and structural justification of the non-conformance documents. Only those non-conformance documents classified as significant variations, i.e., those variations that had an impact on the stress analysis are included in the as-built report. A review of actual manufacturing records is necessary to ensure all non-conformance documents generated during manufacture of the steam generators are considered.

B) Customer Data Package, Shop Order NAGT 2057, Microfilm Roll #700

The Customer Data Package includes:

- Purchase Order Compliance Data
- Quality Release
- Approved Deviation Notices
- ASME Manufacturers Data Report

- Letters of Compliance
- Materials
- Major Parts List
- Certified Material Test Reports
- Welding Information Chart
- Certified Welding Material Test Reports
- Heat Treatment Records

The Customer Data Package was used mainly to obtain the Heat Code Numbers for the various major parts associated with the tube bundle for subsequent review of material procurement (certifications and NDE records) information.

C) Tampa Heat Code Records

a) Tube Plate - Microfilm Roll 1731
b) Tube Support Plates - Microfilm Rolls 4024, 4026 & 4027
c) U-tubes – Microfilm Rolls 5291, 1871, & 1875

The Heat Code Records contain Material Certifications and NDE records for the major procurement items. They are used to review non-conformance generated by the material supplier.

D) Assigned Items (Routings), Microfilm Rolls #TF573 & TF574

The Assigned Items record contains the manufacturing routings used in the manufacture of the steam generator, including; manufacturing operations, Engineering Changes (G-sheets), and all non conformance documents generated during the manufacturing process.

The following are the assigned items (assembly sequence) for Shop Order NAGT-2057

TABLE 1

Assigned Items	Description
Disassembly (lower)	Lower assembly
Disassembly (Upper)	Upper Assembly
Final Assembly	General Assembly and Final Fabrication
A	Upper shell Internal Installation
AA	Upper Shell Assembly
AAA	Upper shell Barrel Cone End
AAA02	Feedwater Nozzle Mod.
AAB	Upper Shell Barrel Head End
AAC	Upper Head
AAC01DA	6.00 Inch Restraint Lug
AAC01DB	9.50 Inch Restraint Lug
AA02	Steam Outlet Nozzle Clad & Mach
AA04	Support Ring
AAI	Weld Back-up Ring
AC	Thermal Sleeve Reducer Assembly
ACA	Thermal Sleeve Detail Assembly
ACA01	Thermal Sleeve
ACA02	Safe End
AD	F. W. Ring Dr. & Nozzle Detail Assembly
ADA	Feedwater Ring Assembly
ADA05	Crossover Pipe
ADA08	Feedring Support Assembly
ADA08A	Backing Ring
ADA08B	Backing Ring
ADA08C	Support Pipe
ADA08E	Feedwater Ring Support Plate
AH	Upper Internal Detail Assembly
AHB	Moisture Separator Housing assembly
AJB	Bar
AJC	Bar
AM	Feed Ring Support Cap Detail
AMA	Cap
AN	Feed Ring Support Pipe
AS	Hatch cover
AU	Backing Ring (10.12 OD)
B	Tube Bundle Chamber Assy.
BA	Tube Bundle Assembly/Tubing
BAA	Lower Shell Structuring Horizontal
BAA01	T/P & Lower Shell Detail Assembly
BAA01A	Tube Plate and Stub Barrel Assy.

Table 1 (continued)

BAA01AB	Tube Plate Clad & Mach.
BAA01ABA	Tube Plate
BAA01AK	Blocking Plates
BAA01D	Lower Shell assembly
BAA01DE	Transition Cone
BAA01DF	Lower Shell Barrel Stub End
BAA01DG	Lower Shell Barrel Cone End
BAA01FB	Boss Plugging Alteration
BAA01FBA	Pressure Plug
BAA01FC	Boss Plugging Alteration
BAA01FCA	Pressure Plug
BAA01FD	Boss Plugging Alteration
BAA01FDA	Pressure Plug
BAA01FEA	Pressure Plug
BAA02	Flow Distribution Baffle Plate
BAA03	Intermediate Support Plate
BAA04	Intermediate Support Plate
BAA05	Intermediate Support Plate
BAA06	Intermediate Support Plate
BAA07	Intermediate Support Plate
BAA08	Intermediate Support Plate
BAA09	Intermediate Support Plate
BAA12	Handhole Closure Inner Plate Assembly
BAA12A	Handhole Closure Inner Plate
BAA12B	Handhole Closure Stud
BAA13	Handhole Closure Outer Plate Assy.
BAA13A	Handhole Closure Outer Plate
BAA13B	Handhole Closure Pipe
BAA13C	Handhole Closure End Plate
BAA17	Anti Rotation Bar
BAA25	Wrapper Canopy assembly
BAA25B	Canopy Filler Plate
BAA26	Wrapper Canopy assembly
BAA26B	Canopy Filler Plate
BAA27	Wrapper Canopy assembly
BAA27B	Spacer Model “F” Vert.
BAA28	Spacer Model “F” Vert.
BAA49	Wrapper Cone Sitdown Ring “F” Vert.
BAA50	Wrapper BBL. Final Sub-assembly
BAA50A	Wrapper BBL. Final Sub-assembly Vert.
BAA50AA	Wrapper Long BBL. Fab “F” Vert.
BAA50AAA	Wrapper Barrel Assembly Vertical

Table 1 (continued)

BAA50AB	Jack Ring Machine "F" Vertical
BAA50ABA	Wrapper Ring Bbl. Fab. Model "F"
BAA50AD	Wrapper Barrel
BAA50AE	Angle "F" Vertical
BAA50AF	Angle "F" Vertical
BAA50AJ	Handhole Wrapper Plate Model "F"
BAA53	Wrapper Position Block
BAA68	Stay rod
BAA69	Stay rod
BAD	Lower Deck Plate Detail
BAD01	Lower Deck Plate Assy "F" Model
BAD04	Divider Angle
BB	CH HD Clad/Mach Fab "F" Model
BB	Quality Data Package
BBB	Primary Nozzle Clad and Machine
BBB	Primary Nozzle (Fab – Channel Head)
BBC	Primary Manway (Fab – Channel Head)
BBC	Primary Manway Clad and Machine
D	Seal Ring
FH	Vane Cover Assembly
FHA	Cover (Vane Cover Assy)
FHB	Bar (Vane Cover Assy)
FI	Cover Plate
FM	Vane Cover
FMB	Cover
FN	Vane Cover (Final)
FO	Vane Cover (Top)
UA	Primary Nozzle shipping Cap
UB	Steam Outlet Nozzle Shipping Cap
UC	Shipping Outlet Manifold Assembly
UE	Shipping Inlet Manifold
UJ	Shipping Inlet Manifold
Transfer	"A" Barrel x "B" Barrel
Wanding	Wanding of Flow Baffle "A"
ZF	Plywood
ZR	Plywood Spacer
ZS	Plywood Spacer
ZW	Clip

Records Review:

A) Stress Report:

The Analysis of As-Built Steam Generators (WNEP 8242) was reviewed. Specifically each non-conformance document associated with Shop Order NAGT-2057 was reviewed for potential cause of the observed tube indications. The following is a complete list of non-conformance documents for Shop Order NAGT-2057 included in WNEP 8242. These include Material Review Requests (MRR) and the earlier used Error Appraisal Notice (EAN)

TABLE 2

571	32747	34760	35671
3640	32764	34784	36134
5906	33177	34788	36172
11463	33180	34889	36204
30053	33371	34942	36284
30481	33513	34945	36393
30957	33616	34946	36669
31898	33885	34948	36947
31900	33930	34953	37190
31961	34018	35172	37207
31972	34019	35175	37208
31976	34150	35178	37209
32171	34234	35196	37210
32719	34235	35197	37211
32743	34243	35426	37217

Of the non-conformance documents included in WNEP 8242, the following related to the tube bundle and were of particular interest for this review.

TABLE 3

EAN/MRR Number	Affected Part	Condition
11463	Tubesheet	Thickness
30053	Tubesheet	Flatness
30481	"D" Tube Support Plate - T08111-3	Extra hole
31961	"D" Tube Support Plate - T08111-3	Undersized ligaments & tube hole diameter
31972	"E" Tube Support Plate – T07728-2	Undersized ligaments
31976	"B" Tube Support Plate – T07998-2	Undersized ligaments
32719	"F" Tube Support Plate – 7727-1	Extra hole on plate rim
32743	Tubesheet	Undersized ligaments/hole diameter variations
33616	"B" Tube Support Plate 7998-2	Undersized ligaments
33885	Tubesheet	Flatness/Thickness
34018	"F" Tube Support Plate – T07727-1	Undersized ligaments
34019	"H" Tube Support Plate – T07726-2	Undersized ligaments
34234	"F" Tube Support Plate – T07728-2	Stayrod hole counterbore diameter
34235	Flow Distribution Baffle – T05921	Stayrod hole counterbore concentricity
34760	"F" Tube Support Plate – T07727-1	Rim gouge
34784	"D" Tube Support Plate – T08111-3	Extra hole
34788	"D" Tube Support Plate – T08111-3	Undersized ligaments
34942	"E" Tube Support Plate –T07728-2	Undersized ligaments
34945	"B" Tube Support Plate – T07998-2	Undersized ligaments
34946	"B" Tube Support Plate – T07998-2	Undersized ligaments
34948	"F" Tube Support Plate – T07727-1	Undersized ligaments
34953	"D" Tube Support Plate – T08111-3	Undersized ligaments
35178	Flow Distribution Baffle	Extra support wedges at assembly
35196	"G" Tube Support Plate – T07721-2	Undersized ligaments
35197	"H" Tube Support Plate – T07726-2	Undersized ligaments
35426	"D" Tube Support Plate – T08111-3	"D" Plate Row 17, Col 120 hole reamed to allow tube to pass

B) Material Heat Codes:

The following are the Heat Code numbers for Major Parts Associated with Tube Bundle (Reference Data Package). These were used for review of the specific Heat Code records for any potential impact of supplier non-conformances on the field observed tube indications.

TABLE 4

Description	Test Number
Tubesheet (Tubeplate)	T0 5921
Flow Distribution Baffle - Plate "A"	T0 8410-2
TSP "B"	T0 7998-2
TSP "C"	T0 8111-3
TSP "D"	T0 8210-2
TSP "E"	T0 7728-2
TSP "F"	T0 7727-1
TSP "G"	T0 7721-2
TSP "H"	T0 7726-2
U-tubes	T0 9539
U-tubes	T0 9034
U-tubes	T0 9735

C) Assigned Item Sequence (Routings):

The microfilm records for NAGT-2057 Assigned Items (Routings) were reviewed to identify any non-conformances or Engineering Changes that could be a potential cause of the observed tube indications. Only those Assigned Items determined to impact the tube bundle were reviewed. The list of assigned items reviewed is as follows:

TABLE 5

Assigned Item	Description
BA	Tube Bundle Assembly/Tubing
BAA	Lower Shell Structuring Horizontal
BAA01A	Tube Plate and Stub Barrel Assembly.
BAA02	Flow Distribution Baffle Plate
BAA03	Intermediate Support Plate
BAA04	Intermediate Support Plate
BAA05	Intermediate Support Plate
BAA06	Intermediate Support Plate
BAA07	Intermediate Support Plate
BAA08	Intermediate Support Plate
BAA09	Intermediate Support Plate
BAA50	Wrapper BBL. Final Sub-assembly

Review Results:

Review of the non-conformance documents included in the Analysis of Steam Generator As-Built condition (WNEP-8242) did not reveal any unusual non-conformances. All of the conditions evaluated (Reference TABLE 3) are typical of steam generators manufactured in the same time frame and do not indicate any condition that could be a cause for the indications observed in the small number of tubes in one of the four Seabrook Unit 1 steam generators. Most of these non-conformances involve tube support plate ligaments and oversized holes, which have more random locations and cover many areas of the tube support plates.

Review of Heat Code Packages (Reference TABLE 4) for major tube bundle parts did not reveal any unusual material issues that can be related to the indications observed. This includes tube support plate broaching which was provided by an outside vendor. Conditions addressed are typical and more random than the locations of the reported field observations.

Routing review of tube bundle related manufacturing operations (Reference TABLE 5) did not reveal any conditions that could be identified as a potential cause of tube indications in NAGT 2057 ("D" SG). Most non-conformances were included in the Analysis of the As-Built steam generator covered by WNEP 8242. Additional non-conformances, found during the routing review process, failed to reveal any manufacturing conditions to explain the observed indications.

Conclusion:

The manufacturing records contain no evidence to address the cause of the reported eddy current indications observed in the Seabrook Unit 1 "D" steam generator (Westinghouse Shop Order NAGT-2057). No conclusion, as to the potential cause of the indications, can be drawn from the manufacturing record review.

The design requirements for NAGT-2057 are identical to two of the other three steam generators (NAGT-2056 & 2058). The only design difference between the four steam generators is found in NAGT-2055, which uses tube support plates with a bolted patch plate. NAGT-2055 reflects an earlier design configuration for the support plates dictated by a vertical structuring manufacturing option. The non-conformances associated with NAGT-2057 are typical of steam generators manufactured in the same time frame and do not indicate any condition that could be a cause for the indications observed in the small number of tubes in one of the four Seabrook Unit 1 steam generators. Of particular interest in this review were the tube support plates, since they interface directly with the tubes and therefore have a higher probability of affecting the tubes than other tube bundle parts. Fabrication and installation of the support plated for NAGT-2057 are considered typical. The following outlines the NAGT-2057 and typical process for manufacturing tube support plates.

Typically, tube support plates manufactured in this time frame were stack drilled. The 0.75" thick plates were drilled in a stack of three and 1.125" thick plates were typically drilled in a stack of two. Both stayrod and tube hole pattern holes were drilled in stacked configuration with an N/C tape controlled multi spindle machine (35 or 41 spindles). Following drilling, the stack was disassembled, the plate O.D. machined, followed by removal of all burrs (rim and surface). The tube lane slots, stayrod counterbores and cutouts were then machined. Following deburring of the counterbores, slots and cutouts, the plates were broached. Many of the plates manufactured during this period were broached by an outside vendor (Hill Tool Corp. of Tampa Florida). The plates for Shop Order NAGT-2057 were broached by Hill Tool. After broaching, the plate surfaces were disc sanded, the tube holes were wire brushed to remove burrs and the plate surfaces buffed in a special machine with a buffing compound. The plates were then steam cleaned, inspected, protected and stored in vertical racks until assembly into the steam generator lower shell assembly. The above sequence of steps is that used for the Seabrook Unit 1 steam generators.

Appendix B

ALTRAN Report 02807-TR-001

Testing to Support the Root Cause Analysis of Steam Generator D Cracked Tubes

Technical Report 02807-TR-001

Revision 0

Volume 1 of 1

Prepared for:

North Atlantic Energy Service Corporation
Seabrook Station

October, 2002

altran

Altran Corporation 451 D Street Boston, MA 02210 PH: 617•204•1000 | FAX: 617•204•3080

altran

Report Record

Report No.: 02807-TR-001	Rev. No.: 0	Sheet No. 2	
QA Status: 10CFR50 ☒, 21CFR820 ☐, ISO 9000 ☐, CG ☐, Other ☐		Total Pages: 101	

Title: Testing to Support The Root Cause Analysis of Steam Generator D Cracked Tubes

Client: North Atlantic Energy Service Corporation Facility: Seabrook Station

Revision Description: Original issue

Computer runs are identified on a Computer File Index : Yes ☒ N/A ☐

Error reports are evaluated by: [signature] Date: Oct 24, 02

Computer use is affected by error notices. No ☒, Yes ☐ (if yes, attach explanation)

Originator(s)	Date	Verifier(s)	Date
Thomas McKrell, Ph.D.	10/24/02	William J. McBrine, P.E.	10/24/02
Thomas H. Service, Ph.D., P.E.	Oct 24, 2002	Ockert Van Der Schijff, Ph.D.	10/24/02
Vincent Roy	10/24/2002	Jose Magalhaes, Ph.D.	10/24/02
Van Christie	10/24/02	Peter Wronski	10/24/02
Ronald Ballinger, Ph.D.	10/24/02	Thomas H. Service, Ph.D., P.E.	Oct 24, 2002
Thomas C. Esselman, Ph.D.	10/24/02	Richard Martin	10/25/02

Verification: Verification is performed in accordance with EOP 3.4 as indicated below

☒ Design review as documented on the following sheet or

☐ Alternate calculation as documented in attachment or

☐ Qualification testing as documented in attachment or

Approved for Release: [signature] 10/25/02

Thomas McKrell, Ph.D., Project Manager Date

altran

Verification

Report No. 02807-TR-001 Rev. 0 Sheet 3

Verification Considerations (in accordance with EOP 3.4)

		Initials
1.	The inputs come from an appropriate and controlled source, and are clearly referenced.	RL
2.	The inputs from uncontrolled sources or assumptions are properly justified and documented.	* RL
3.	The inputs or assumptions that are not adequately justified are identified for later confirmation.	N/A
4.	Design, analysis, testing, examination, and acceptance criteria are specified and complied with.	RL
5.	Appropriate interface control was administered during the process of this report.	RL
6.	The computer programs used are authorized for use and/or properly verified.	RL
7.	Applicable codes, standards, or regulatory requirements are properly specified and complied with.	RL
8.	The specified tests and examinations were performed by personnel with appropriate qualifications.	RL
9.	All tests and examinations were performed in accordance with written procedures.	RL
10	Specimens are controlled by identification number and their traceability is maintained.	RL
11	The calibration of instrumentation is acceptable and properly recorded.	RL
12	The instruments that are used are recorded by name and identification number.	RL
13	The report is neat and legible and suitable for reproduction.	RL
14	The formatting and technical requirements of applicable procedures are complied with.	RL
15	Critical numerical computations have been checked in detail.	RL
16	The endorsements of all originators and verifiers have been properly recorded.	RL
17	Appropriate construction, operation, and/or maintenance considerations have been considered.	N/A
18	The conclusions satisfy stated objectives, and they are consistent with the input.	RL
19	All material specified are compatible with their service environment.	N/A
20	Procedural requirements for report revisions and subsequent reviews are complied with.	N/A

Clarify significant comments:

* Data for Tectyl 506 G does not reflect commercial grade status of the product.

All comments are resolved and incorporated into the report except as noted here:

Revised section 4.3 to clearly describe the commerical status of the Tectyl 506 G and to state that the associated ~~rults~~ results are non-safety related. TJM 10-25-02

[signature]	10/25/02	[signature]	10/25/02
Originator's Concurrence	Date	Verifier's Concurrence	Date

altran

Laboratory M&TE Index

Report No. 02807-TR-001 Rev.: 0 Sheet: 4

By.: Tom McKrell Date: Chk.: V. Christie Date:

The following laboratory test equipment was used, within the calibration periods listed, in performance of the work described in this report.

M&TE Equipment	ID No.	Calibration Date	Calibration Due Date	Operator Name	Test Procedure
Noran Voyager IV Energy Dispersive X-ray Spectrometer	3168	3/20/02	3/20/03	V. Christie	TP 11.06
Leitz Miniload Microhardness Tester	498647	4/29/02	4/29/03	V. Christie	TP 11.08
AND HR-300 Balance	13200434	6/25/02	6/25/03	Varied	As Described in Report
Instron 1332 Load Frame	137	7/5/01	7/5/02	V. Roy	TP 11.01
Instron 1332 Load Frame	137	9/6/02	9/9/03	V. Roy	TP 11.01
Load Cell	UK20	7/5/01	7/5/02	V. Roy	TP 11.01
Load Cell	UK20	9/6/02	9/9/03	V. Roy	TP 11.01
Six Channel Thermocouple Readout	5271	9/19/01	9/19/02	T. McKrell	Instrument Manual
Stage Micrometer	02B00421	1/5/98	1/5/04	Varied	TP 11.10
Mitutoyo Digital Caliper	0031482	10/3/01	10/3/02	Varied	As Described in Report
GC/MS Hewlett Packard	5971	6/28/02	9/28/02	Jack Hubball	TP 11.14
Strain Gages	CEA-06-125UT-120 Option P2	8 /27/02	12/31/02	V. Roy	As Described in Report

Computer File Index

altran

Report No. 02807-TR-001 Rev.: 0 Sheet: 5

By: Thomas Service Date: 9/16/02 Chk: Jose Magalhaes Date: 9/16/02

PROGRAM NAME: ANSYS **VERSION NO.:** 5.7

USERNAME: N/A **PROJECT MANAGER:** Thomas McKrell

QA Status ☒ **yes,** ☐ **no** **(App. B** ☒**, ISO 9000** ☐**, CGMP** ☐**)**

PROGRAM USE DESCRIPTION: Linear Elastic Finite Element Analyses of Split Tube

KEY WORDS: /PREP7, PLANE42, /SOLU, /POST1,

Run No.	Description	Input File Name	Output File Name	Run Date::Time
1	7/8" Split Tube Analysis	7-8inch.inp	N / A	9/16/02 9:56 AM
2	11/16" Split Tube Analysis	11/16inch.inp	N / A	9/16/02 9:57 AM

Altran Corporation
Technical Report 02807-TR-001
Revision 0

TABLE OF CONTENTS

APPENDIXES

List of Tables

List of Figures

1.0 INTRODUCTION

Nondestructive examination (NDE) of Seabrook station's steam generator D tubes, during the spring 2002 refueling outage (OR08), showed indications of flaws that were later determined to be outer diameter initiated cracks, resulting in the subsequent plugging of 15 tubes. These tubes were all located in rows ten and lower with NDE indications occurring in the land regions of the tube support plates. The manufacturer of the steam generator, Westinghouse, determined that the plugged tubes all came from three heats. The number of tubes from each heat being: 13 from Heat #1734, one from Heat #1456 and one from Heat #1457. The pulled tubes were shipped to the Westinghouse laboratories. A subset of the tubes were then shipped to Altran for analysis. Two free-span sections (R5C62 and R9C63) and one cracked section (R5C62 HL 7B2) were received. Altran performed analysis of these tube sections as part of a root cause analysis and to complement the analysis at Westinghouse. The focus of this testing was to determine the importance of each of the three simultaneous requirements for stress corrosion cracking: 1) presence of an aggressive environment, 2) a susceptible material and 3) a tensile stress.

The objective of this report is to document the testing and analysis performed to support the root cause analysis of the tube cracking detected during OR08.

2.0 INPUT

2.1 Sample Identities

All samples tested were Inconel 600

2.1.1 Seabrook Service/Pulled Tube Samples

2

Westinghouse provided Altran Corporation with two shipments of freespan/unflawed sections and one shipment of a cracked section. All sections having been cut from the two pulled tubes removed from the Seabrook station steam generator D. The tubes were 11/16" outer diameter (OD) with a 0.040" wall. Figure 2-1 shows the thermal/mechanical history of these samples, as stated by Westinghouse in Reference 1.

The first shipment included (Reference 2):

- A 2" piece, identified as R5C62 Pc. 5C2 hot leg, cut from the top of Westinghouse's piece 5. The centerline of this sample was 9" above the centerline of 04H tube support plate.
- A 2" piece, identified as R9C63 Pc. 4A1 cold leg, cut from the bottom of Westinghouse's piece 4. The centerline of this sample was 29" below the centerline of the 03C tube support plate.

The second shipment included:

- A 4" piece identified as R5C62 Pc. 4C3 hot leg.
- A 4" piece identified as R9C63 Pc. 4C3 cold leg.

The third shipment included:

- A cracked 4" long tube section identified as R5C62 7B2 hot leg. This tube section was reported by Westinghouse to contain, as indicated by NDE, an axially oriented crack centered in the region corresponding with one of the quatrefoil lands of tube support plate 05H, Reference 3. The angular position of the crack was marked by Westinghouse with a zero degree position line. The tube support plate intersection with the tube was located at the center of the 4-inch long sample.

All of these samples were received by Altran as radioactively contaminated. The Seabrook service samples, R5C62 and R9C63, were stated to be from Huntington heat 1374, Reference 4.

Receipt of SG Order Tampa SG Division

Place Order for Tube Bundle with SMD

Blairsville Specialty Metals Division

Trexes from Huntington Alloys		**2.25 in. OD x 0.25 in. wall**
Cold Pilger	*Wall reduction*	**1.15 in. OD x 0.078 in. wall**
Intermediate Anneal	*For workability*	**1900°F x ~ 5 min.**
Cold Draw		**~ 0.94 in x 0.052 in. wall**
Intermediate Anneal	*For workability*	**1900°F x ~ 5 min.**
Cold Draw to Final Size		**~ 0.690 in. OD x 0.040 in. wall**
Final Mill Anneal	*Recrystallization*	**1950°F x 2-3 min.**
Thermal Treatment	*Carbide precip.*	**1320°F x 10 hours**
U - bending		**All rows**
Stress Relief Anneal	*Rows 1 - 10*	**1320°F x 2 hours**

Figure 2- 1. Westinghouse's Manufacturing Sequence for the Steam Generator Tubes (Reference 1)

2.1.2 Mill Annealed (MA) Samples

The following mill annealed samples were used in testing:

- An approximately 4' long tube with a 7/8" OD and a 0.050" wall thickness. The tube material was produced by Babcock and Wilcox for EPRI and was from heat 96845, Reference 5.
- An approximately 36 inch length of 7/8" OD x 0.050" wall tube. The tube material was produced by Huntington Alloys International (now Special Metals Inc.) and was from heat 1638, Reference 6.
-

2.1.3 Thermally Treated (TT) Samples

Archive samples were received from Westinghouse that represented the three heats that comprised the 15 plugged tubes. These samples were (Reference 7):

- Heat 1456, a 0.5" long tube with an 11/16" OD and a 0.040" wall thickness.
- Heat 1457, a 0.5" long tube with a 7/8" OD and a 0.050" wall thickness.
- Heat 1374, a 0.5" long tube with an 11/16" OD and a 0.040" wall thickness.

Additionally, the following archive sample was received from Seabrook Station:

- An approximate 14 inch length of 7/8" OD x 0.050" wall tube with the vibro-etch identifier TY9402 9993 B0579B, Reference 8.

3.0 Methodology

3.1 Laboratory Heat Treatments

For comparative purposes and to provide baselines, Altran Corporation performed a number of laboratory heat treatments on some of the samples prior to testing. All heat treatments were performed in a box furnace in air. These heat treatments included:

- Thermal Treatment (TT): Treatment at 700°C for 10 hours followed by air cooling. This heat treatment is designed to ensure complete carbide precipitation followed by "healing" of carbide precipitation induced chromium depletion. If properly done the process results in a corrosion resistant or un-sensitized microstructure.
- Solution Treatment (SA): A solution treatment at 1050°C for 1 hour followed by a water quench. This heat treatment places all constituents, in particular carbon, into solution, resulting in a uniform distribution of Cr and a corrosion resistant or un-sensitized material. Based upon the highest expected carbon content, 0.050% and the known carbon solubility (Reference 9), the minimum temperature for the solution treatment was determined to be 1000°C. A temperature of 1050°C was therefore chosen for actual laboratory treatments.

- Sensitization Treatment (ST): SA treatment followed by a treatment at 700°C for 2 hours followed by air cooling. This treatment results in the formation of grain boundary carbides and Cr depleted regions adjacent to the grain boundaries. The Cr depleted regions are susceptible to corrosion leaving the samples in a sensitized state.

3.2 Bulk Chemical Analyses

Bulk carbon and sulfur content were determined by Leco combustion. Other element concentrations were determined by inductively coupled plasma/optical emission spectroscopy.

3.3 Microstructure Examination

The tube materials were sectioned, mounted, and polished for metallographic analysis per Reference 10. Longitudinal, and in some instances transverse, cross sectional faces were examined for microstructural features using a two-step electrochemical etch process as described in Reference 11. This procedure allows for the quantitative determination of the fraction of intergranular versus intragranular carbides and grain size. The process first involved microhardness indenting the sample to provide a fiduciary mark. Subsequently, the sample was electrolytically etched at 2.5 V for 15 seconds in a solution of 80 ml orthophosphoric acid mixed with 10 ml of distilled water to reveal carbides without etching grain boundaries. A micrograph containing the indent was taken and the sample was then lightly re-polished by repeating the final 0.05 micron colloidal silica polish to remove the etching but not the indent. Next, the grain boundaries were revealed using a grain boundary specific etching procedure. Namely, the sample was electrolytically etched, at 2.5 V for 15 seconds, in a nital solution (95 ml methanol and 5 ml of concentrated nitric acid) and then photographed in the area near the fiduciary mark.

3.4 Microhardness Measurements

Knoop microhardness measurements (100 g load) were taken on samples that had been mounted and polished.

3.5 Modified Huey Testing

The modified Huey testing was performed in accordance with Practice C of Reference 12 as modified by Reference 11. Specifically, Reference 11 recommends a reduction in the nitric acid solution concentration to 25 volume percent and a shortening of the exposure period to a single 48 hour period. The calculation for the 25 volume percent solution is presented in Appendix A. The specimen condition was photo documented prior to and at the end of each test. The modified Huey test evaluates the sensitivity of a material to corrosion in oxidizing environments, by attacking areas of the material with Cr content below a critical value, Reference 13. The corrosion rate is then defined as the weight loss per unit area per day, and is commonly given in the units of mg/(dm^2 day) or mdd.

3.6 Residual Stress Measurements

Residual stress measurements were performed to estimate the surface stresses in the tubing. Measurement of residual stresses was performed by axially cutting a one inch section of tube. Residual stress values were determined by two means: 1) by making residual strain measurements using biaxial strain gages, and 2) by measuring the diameter change of the tube after slitting and using this data to analytically determine residual stresses.

3.6.1 Strain Gage Measurements

Biaxial strain gages manufactured by the Micro-Measurements Division of Measurements Group, Inc. were used for the strain measurements. The use of biaxial gages provided simultaneous measurement of the hoop and axial strains. The strain gages were type CEA-06-125UT-120 option P2, and were all from lot number A44AD805. The cracks were found to be axially oriented therefore the residual hoop stress was of primary interest. The advantage of the biaxial gage was that it also allowed axial strain measurement. This provided confirmation that axial strain was minimal. Furthermore, each sample was instrumented with two gages attached 90 degrees from either side of the axial cut. The areas where gages were applied were prepared by lightly hand sanding with 600-grit paper, followed by application using the method detailed by the manufacturer, Reference 14. A hacksaw was used to make the axial cut. All measurements were made at room temperature both before and after cutting.

3.6.1.1 Strain Gage Calibration

All of the strain gages used for this work were from the same lot. Calibration of the lot was carried out by mounting two gages on the tensile specimen shown in Figure 3-1. The sample was pulled elastically and the applied stress recorded. Using the modulus of elasticity of material, the axial strain measured by the strain gages was used to calculate the expected axial stress. The percent error associated with the gages was determined by comparing the applied and calculated axial stresses. The results of the comparison, Table 3-1, show that there was a very small error associated with the gages, less than 5%.

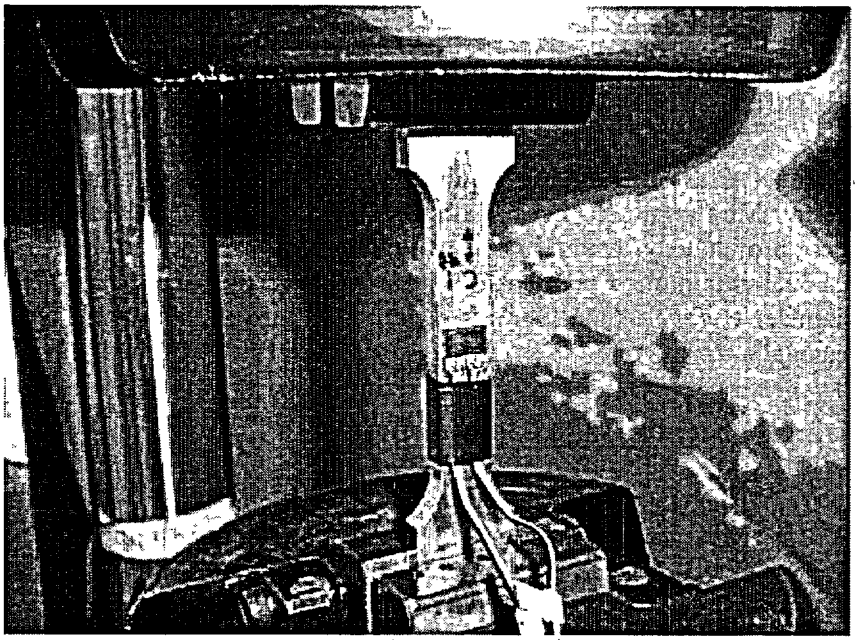

Figure 3- 1. Strain Gage Calibration Setup

Table 3- 1. Strain Gage Calibration Results for Lot A44AD805

Prepared by: Vincent Roy, Checked by: Thomas Service

Applied Load (lb_f)	Applied Axial Stress (psi)	Transverse		Axial Stress		
		Strain (με)	Calculated Stress (psi)	Strain (με)	Calculated Stress (psi)	Error (%)
1000	8171	-76	2204	277	8033	1.69
1500	12256	-111	3219	405	11745	4.17
1750	14299	-128	3712	476	13804	3.46

3.6.2 Diameter Measurements

The tube sample diameter was measured in four locations using a digital caliper. Measurements were made at two axial locations (each end of the tube sample) and at each 45° of rotation for a total of 8 diameter measurements per tube. Figure 3-2 illustrates the measurement scheme. These measurements were taken at the same locations both before and after the axial cut was made.

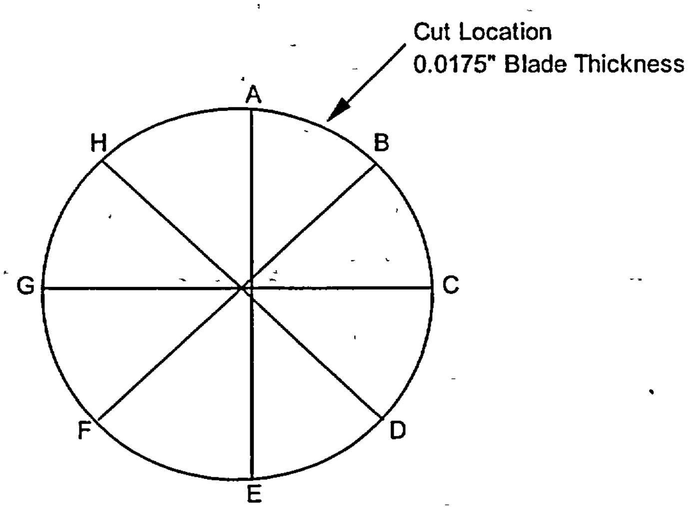

Figure 3- 2. Diameter Measurements and Saw Cut Location

3.7 Cracked Sample Analysis

3.7.1 Cracked Sample Deposit Collection

Deposits on the OD of the cracked tube sample were collected for chemical analysis. Special focus was placed on the interface between the deposit and the tube wall. To expose this interface, a short sample ring containing the deposit was wrapped with adhesive carbon tape and then mechanically expanded to dislodge the deposit. The tube wall side of the collected deposit was exposed for visual and microscopic examination and chemical analysis. Chemical analysis was performed using two complementary techniques, X-ray Photoelectron Spectroscopy (XPS) and Energy Dispersive Spectroscopy (EDS). XPS is a surface analytical technique that is the method of choice for the detection of Pb. EDS is a coarser tool that can penetrate the surface.

3.7.2 X-ray Photoelectron Spectroscopy (XPS) of Deposit

XPS was performed on the deposit at various locations. X-ray photoelectron spectroscopy, also referred to as electron spectroscopy for chemical analysis (ESCA), is a surface analysis technique that provides compositional and chemical bonding information from the near-surface region (approximately 2nm) of a sample. An argon sputter gun was utilized to remove surface layers from the deposit, providing information on compositional changes as a function of depth. All elements except hydrogen and helium can be detected with XPS.

3.7.3 SEM and EDS Analysis of Expanded Tube and Deposit

After the tube was expanded, a scanning electron microscope (SEM) was used to obtain high magnification images for analysis. Additionally, the instrument was equipped with an energy dispersive spectrometer (EDS) that allowed for the subsequent determination of the composition of features. Altran's EDS can detect elements as light as boron (atomic number 5). EDS was used to characterize both the expanded tube and deposit. Due to many parameters, such as sample size, surface condition, and orientation in the equipment, quantification of the elements present is considered to be semi-quantitative.

3.8 Gas Chromatography/Mass Spectroscopy (GC/MS) Analysis

Samples of a preservative (Tectyl 506G) used during the original manufacture and shipping of Seabrook station steam generator D, was analyzed by EDS (discussed in Section 3.7.3) and gas chromatography - mass spectroscopy to identify the constituent organic compounds.

The combined techniques of gas chromatography and mass spectrometry are applicable due to their wide analytical range for organic compounds, sensitivity to trace concentrations, and a large data base of materials previously characterized. The technique involves the introduction of a sample into a long, narrow column located within a temperature controlled enclosure. The compound to be analyzed is introduced into the column where it becomes physically separated into its constituent compounds. Large, complex molecules are impeded in their movement through the column due to interaction with the highly convoluted interior surface. Smaller molecules pass through more quickly. This interaction serves to separate the sample into its constituents. Preliminary identification of compounds is based on their retention time within the specific type of column being used. Components with specific retention times can be further analyzed with the mass spectrometer by diverting them as they exit the column. The mass spectrometer is then used to determine the molecular weight of a compound by measuring its angular deviation as it is accelerated through a strong magnetic field. Compounds are identified through a computer-based reference library.

4.0 Test Results and Discussion

This section presents the data from the freespan/unflawed and cracked tube analyses.

4.1 Freespan/Unflawed Analysis

The tests performed included:

- Bulk Chemical Analysis
- Microstructural Examination - Two-Step Etch
- Microhardness Measurements
- Modified Huey
- Residual Stress Measurements

Table 4-1 shows a summary of which tests were performed on which specimens for the freespan/unflawed analysis. In addition to the Seabrook service samples, testing was performed on other unflawed samples for comparative purposes and to establish baselines.

4.1.1 <u>Bulk Chemical Analysis</u>

The results of the chemical analysis are shown in Table 4-2. Limited analysis was performed on heat #1638 because the sample was received with a copy of its certified mill test report, Reference 15. For heats 1374, 1456 and 1457 only carbon and sulfur contents were determined. Appendix B shows the original test reports for all of the samples studied.

Table 4- 1. Summary Matrix of Tests Performed on Unflawed Samples

Sample	Bulk Chemical Analysis	Two-Step Etch	Microhardness	Modified Huey	Residual Stress Measurement
Seabrook Service R5C62 - As Received					
Seabrook Service R9C63 - As Received					
Seabrook Service R5C62 - Laboratory Thermal Treatment					
Seabrook Service R9C63 -Laboratory Thermal Treatment					
Seabrook Service R5C62 - As Received - Split Ring					
Seabrook Service R9C63 - As Received - Split Ring					
Heat 96845 - As Received - Mill Annealed					
Heat 96845 - Laboratory Thermal Treatment					
Heat 96845 - Laboratory Solution Treatment					
Heat 96845 - Laboratory Sensitization Treatment					
Seabrook Archived Heat TY9402 9993 B9579B - As Received					
Seabrook Archived Heat 1456 - As Received - Thermally Treated					
Seabrook Archived Heat 1457 - As Received - Thermally Treated					
Seabrook Archived Heat 1374 - As Received - Thermally Treated					
Heat 1638 - As Received - Mill Annealed					

Shaded block denotes test was run.

Table 4- 2. Bulk Chemical Analysis Data for Unflawed Samples (See Appendix B for Data Sheets)

Sample Description	[illegible]	[illegible]	[illegible]	P %	[illegible]	[illegible]	[illegible]	[illegible]	[illegible]	[illegible]	[illegible]	[illegible]	[illegible]
[illegible]	[illegible]	[illegible]	[illegible]	[illegible]	[illegible]	[illegible]	[illegible]	[illegible]	[illegible]	[illegible]	[illegible]	[illegible]	[illegible]
[illegible]	[illegible]	[illegible]	[illegible]	[illegible]	[illegible]	[illegible]	[illegible]	[illegible]	[illegible]	[illegible]	[illegible]	[illegible]	[illegible]
[illegible]	[illegible]	[illegible]	[illegible]	[illegible]	[illegible]	[illegible]	[illegible]	[illegible]	[illegible]	[illegible]	[illegible]	[illegible]	[illegible]
[illegible]	[illegible]	[illegible]	[illegible]	[illegible]	[illegible]	[illegible]	[illegible]	935	[illegible]	[illegible]	[illegible]	[illegible]	[illegible]
[illegible]	[illegible]	[illegible]	---	---	[illegible]	---	---	---	---	---	---	---	---
[illegible]	[illegible]	[illegible]	---	---	[illegible]	---	---	---	---	---	---	---	---
[illegible]	[illegible]	[illegible]	---	---	[illegible]	---	---	---	---	---	---	---	---
[illegible]	[illegible]	[illegible]	[illegible]	[illegible]	[illegible]	[illegible]	[illegible]	[illegible]	[illegible]	[illegible]	[illegible]	[illegible]	[illegible]

4.1.2 Microstructure Examination – Two-Step Etch

Appendix C contains the results of the two-step etch analysis. For illustrative purposes the microstructures for as received Seabrook service sample R5C62 have been reproduced from Appendix C and are presented below, Figures C-1 and C-2.

Unless noted images are from the longitudinal-circumferential plane. The Figures C-1, C-2, C-5 and C-6 show the Seabrook service samples R5C62 and R9C63 in the as received condition. The microstructures show heavy intragranular carbide precipitation and a small equiaxed ASTM grain size of 10-11. The grain boundaries are not well decorated with carbides. Reference 11 describes this type of microstructure as unacceptable. Figures C-3, C-4, C-7 and C-8 show the microstructure after a laboratory thermal treatment. The thermal treatment had little effect on the microstructure.

Figures C-9 and C-10 show the microstructure of heat 96845 in the as-received condition. The microstructure exhibits a combination of intragranular and grain boundary carbide precipitation, and an ASTM grain size of 6. Figures C-13 and C-14 show the microstructure after a thermal treatment (TT). The TT results in an increase in carbide density on the grain boundaries. Figures C-11 and C-12 show the microstructure after a solution anneal (SA) treatment. The resulting microstructure is homogenous with no carbide precipitation and a grain size of approximately ASTM 4-5.

The microstructure of Seabrook archive sample TY9402 9993 B9579B is shown in Figures C-15 and C-16 and consists of a combination of intragranular and grain boundary carbide precipitation, and an ASTM grain size of 6-7. Figures C-17 through C-22 show the microstructure of the archive heat 1374 material. The microstructure is very similar to that of the pulled tubes of the same heat. Figures C-23 through C-26 show the microstructure of the heat 1456 archived sample. The grain size (ASTM 8) is larger than for heat #1374 and the carbide distribution is more inter than intra-granular. The microstructure of the heat 1457 archive sample, shown in Figures C-27 to C-30, is similar to 1456 but with slightly larger grains.

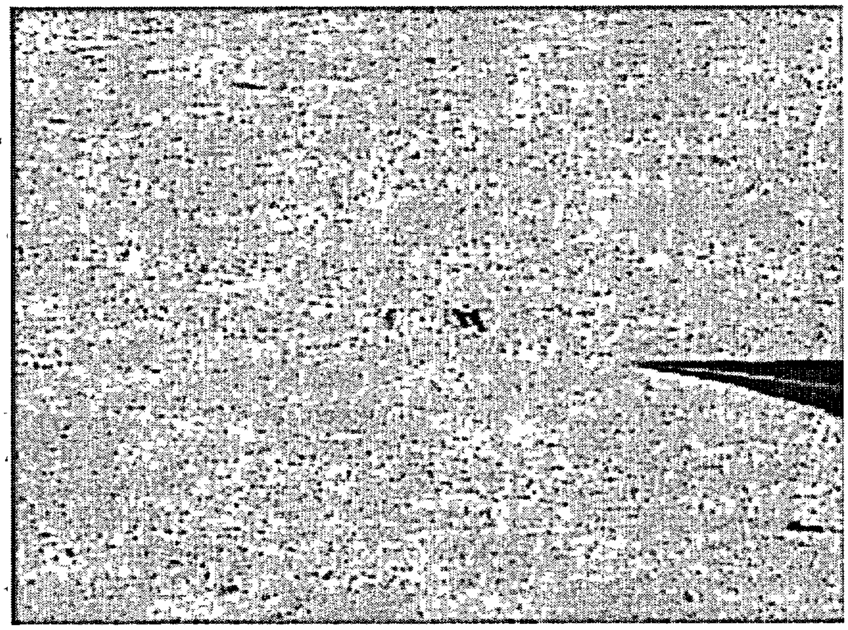

Figure C- 1. As Received Sample R5C62 – Carbide Etch

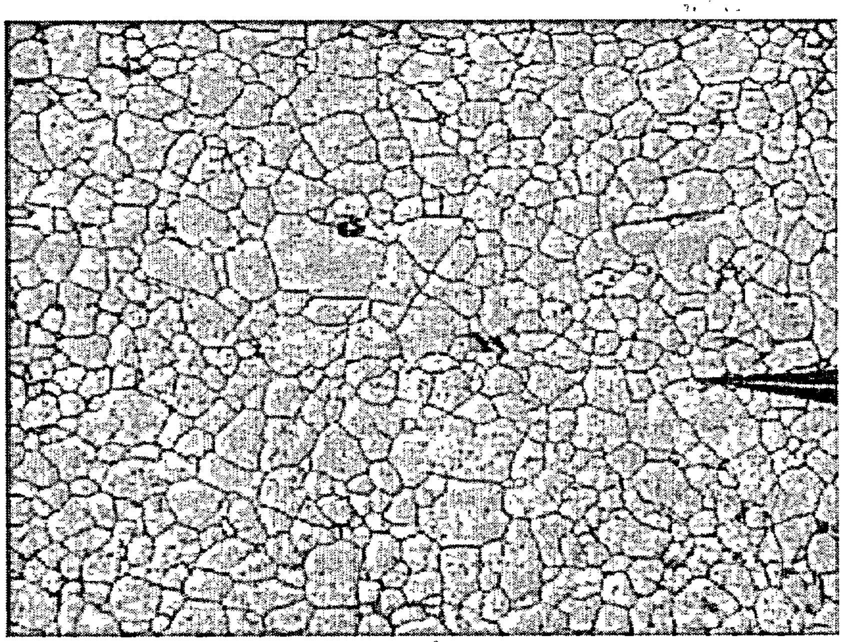

Figure C- 2. As Received Sample R5C62 – Grain Boundary Etch

4.1.3 Microhardness Measurements

Knoop microhardness measurements (100g load) were made on the transverse face of a Seabrook service R5C62 sample and on the longitudinal face of a Seabrook service R9C63 sample. Microhardness values with distance from the ID surface are shown in Figures 4-1 and 4-2. The results indicate an increase in hardness at the OD and ID faces of the tubes.

4.1.4 Modified Huey Testing

The results of the Huey testing are shown in Table 4-3. A shaded box indicates a high corrosion rate. Modified Huey testing was performed in both 25 volume percent and 25 weight percent nitric acid solutions. Testing at 25 volume percent, equivalent to 43 weight percent, provides for a more distinguishing test. Testing in a 43 weight percent solution allows for the detection of Cr depleted areas that would otherwise not be identified by the 25 weight percent solution. It is noted that the industry standard corrosion rate criteria for defining a sample as sensitized, 200 mdd, is measure in a 25 weight percent solution.

To obtain intermediate data points, some of the specimens were weighed at approximately 12-hour intervals during exposure. In comparing the continuous 48 hour tests to the 12 hour interrupted tests it is seen that removing the samples every 12 hours had little effect on overall behavior. Additionally, different sample sizes were tested, and were also shown to have little effect on overall behavior.

One important trend that was revealed by the 25 volume percent solution testing is that laboratory thermal treatment of the Seabrook service samples dramatically increased their corrosion resistance. Post Huey SEM images of Seabrook service R5C62 samples tested in the as received and laboratory thermal treated conditions are shown in Figures 4-3 and 4-4. The facetted surface of the as received sample clearly shows intergranular attack. Additionally, it should be noted that all of the archived Seabrook samples (TY9402 9993 B0579B and heats 1456, 1457 and 1374) performed satisfactorily in 25 volume percent solutions, as did the thermally treated and laboratory solutionized heat 96845 samples. Axially splitting the Seabrook service samples to partially relieve axial stresses prior to testing did not have a dramatic effect on their behavior.

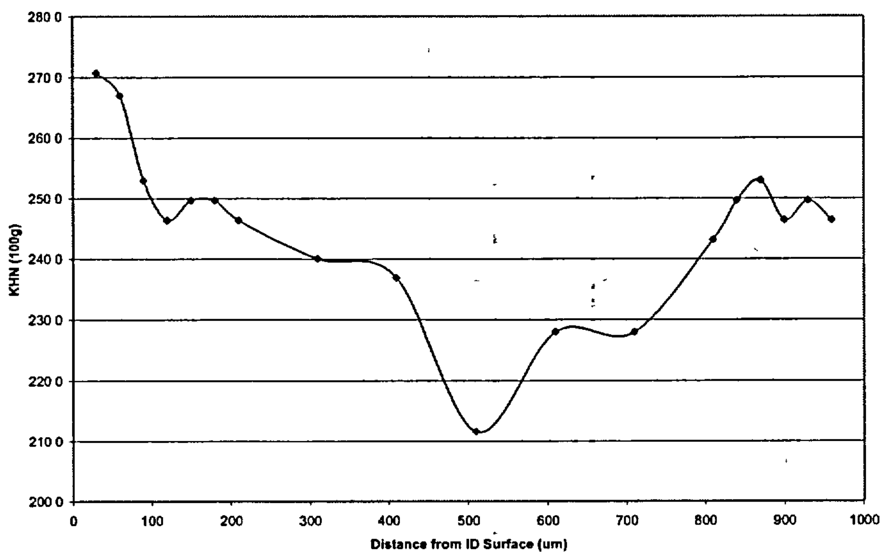

Figure 4- 1. Knoop Microhardness Measurements on the Transverse Face of a R5C62 Seabrook Service Sample

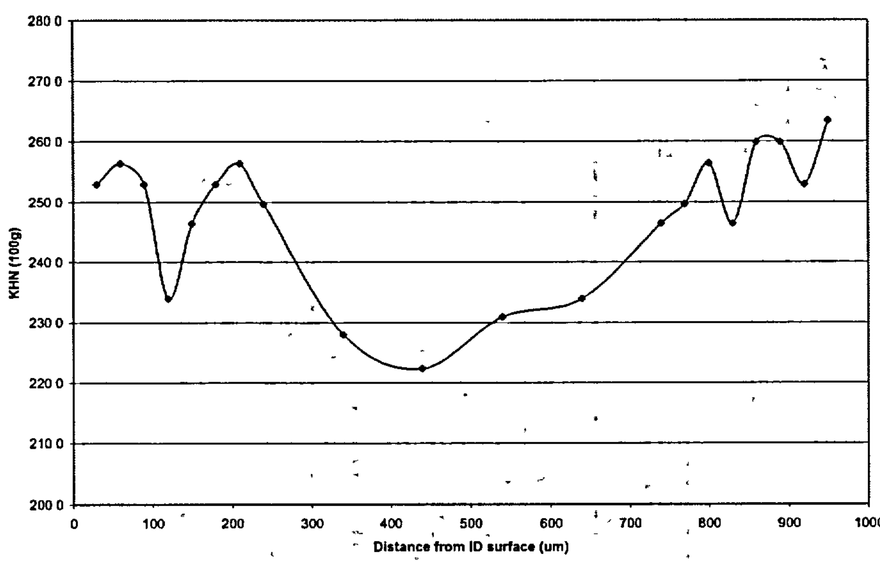

Figure 4- 2. Knoop Microhardness Measurements on the Longitudinal Face of a R9C63 Seabrook Service Sample Modified Huey Testing

Table 4- 3. Summary Matrix for Modified Huey Tests Performed

[illegible]	[illegible]	[illegible]	[illegible]	[illegible]	[illegible]
[illegible]	[illegible]				[illegible]
[illegible]	[illegible]				[illegible]
[illegible]	[illegible]				[illegible]
[illegible]	[illegible]				[illegible]
[illegible]		[illegible]			
[illegible]		[illegible]			
[illegible]	[illegible]	[illegible]	[illegible]	[illegible]	
[illegible]	[illegible]				
[illegible]	[illegible]				
[illegible]					[illegible]
[illegible]	[illegible]			[illegible]	
[illegible]		[illegible]			
[illegible]		[illegible]			
[illegible]		[illegible]			

NOTES:
[illegible]
[illegible]
[illegible]
[illegible]
[illegible]
[illegible]
[illegible]
[illegible]
[illegible]

[illegible]
[illegible]

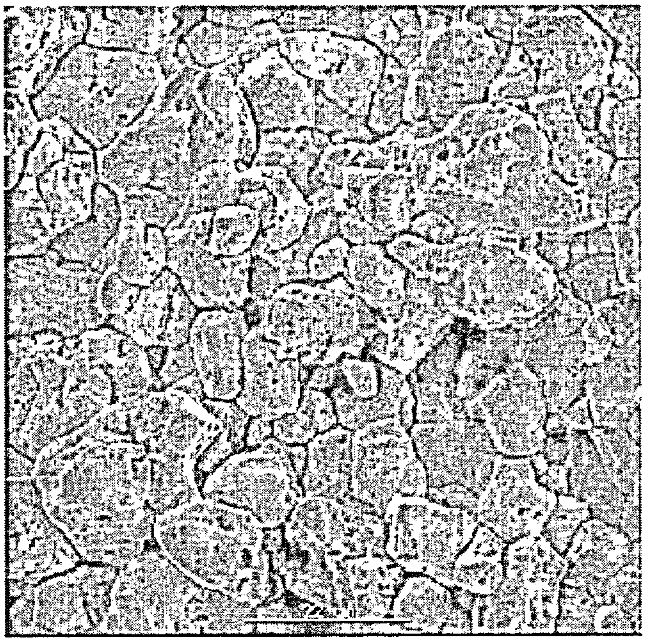

Figure 4- 3. Seabrook Service Sample R5C62 Post Modified Huey Testing

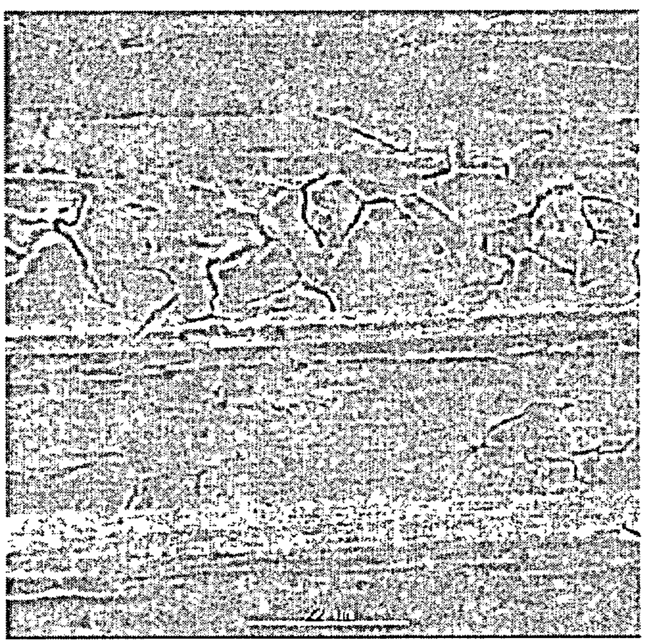

Figure 4- 4. Laboratory Thermally Treated Seabrook Service Sample R5C62 Post Modified Huey Testing

4.1.4 Residual Stress Measurements

Residual stress values were determined on tube samples that had been axially split using two methods: (1) Stresses were determined by measuring the change in strain, using strain gages attached to the tubing, resulting from the axial splitting process. Hoop strain measurements were converted to stress. (2) By measuring diameter changes upon tube splitting.

4.1.4.1 Strain Gage Residual Stress Analysis

The hoop and axial strains measured are presented in Tables 4-4 and 4-5. Also provided in these Tables are the residual stresses calculated from the residual strain measurements and an assumed elastic modulus of 31.1×10^6 psi, Reference 16. The measured residual stresses for the service tubing are higher than one would expect for thermally treated tubing, Reference 17.

Table 4- 4. Hoop Strain Measurements

Prepared by: Vincent Roy, Checked by: Thomas Service

Sample	Description	Residual Hoop Strain (με)		Calculated Residual Hoop Stress (psi)		Average Residual Stress (psi)
		Gage 1	Gage 2	Gage 1	Gage 2	
Heat 1638	MA		-240		7,464	7,464
Heat 1638	MA	-378	-218	11,756	6,780	9,268
Heat 96845	MA	-358	-167	11,134	5,194	8,164
Heat 96845	TT	-56	-121	1,742	3,763	2,752
Service R9C63	AR	-926	-762	28,799	23,698	26,248
Service R9C63	AR	-610	-496	18,971	15,426	17,198

Table 4- 5. Axial Strain Measurements

Prepared by: Vincent Roy, Checked by: Thomas Service

Sample	Description	Residual Hoop Strain (με)		Calculated Residual Hoop Stress (psi)		Average Residual Stress (psi)
		Gage 1	Gage 2	Gage 1	Gage 2	
Heat 1638	MA		10		-311	-311
Heat 1638	MA	-26	-7	809	218	513
Heat 96845	MA	-1	2	31	-62	-16
Heat 96845	TT	9	-9	-280	280	0
Service R9C63	AR	-18	24	560	-746	-93
Service R9C63	AR	-22	-18	684	560	622

4.1.4.2 Diameter Change Residual Stress Analysis

The diameter change of the tubes tested with the strain gages was also measured, and the results are shown in Table 4-6. As measurements were made on two tube diameters, the percent change in diameter was calculated. The tubes exhibited measurable increases in diameter after splitting, clearly demonstrating the presence of tensile residual hoop stresses on the OD of the tube prior to splitting. Two techniques were utilized to relate the measured changes in diameter to residual hoop stresses in the tubes. The first technique makes use of a relationship between bending stress and diameter change in a point loaded split tube. The second technique relies on Finite Element Analysis (FEA) to correlate the stress in a split tube to a change in diameter from an applied bending moment. A more detailed discussion of these analyses is given in Appendix D.

Bending Stress-Diameter Change Relationship

Equation 4.1 shows the analytical relationship between residual hoop bending stress, σ, and the change in diameter, Y_d, given by:

$$\sigma = 4.355 \times 10^6 \frac{Y_d\, h}{R^2} \qquad (4.1)$$

where R is the mean tube radius and h is the tube wall thickness. An elastic modulus of 31.1×10^6 psi is assumed for Inconel 600, Reference 16. This relationship is valid for different tube thickness and diameters.

Finite Element Technique

Finite element analysis resulted in the following relationships between diameter change and residual hoop stress on the tube exterior for 7/8" diameter 0.050" thick and 11/16" diameter 0.040" thick tubes:

$$\begin{aligned} \sigma &= 1.706 \times 10^6\, Y_d \quad \text{for } 11/16'' \\ \sigma &= 1.313 \times 10^6\, Y_d \quad \text{for } 7/8'' \end{aligned} \qquad (4.2)$$

These results also assume an elastic modulus of 31.1×10^6 psi for Inconel 600.

Knowing these relationships and the measured diameter changes, the corresponding hoop stress on the tube OD surface was calculated.

The measured diameter changes shown in Table 4-6 were input to the respective Equations (4.1) or (4.2) to estimate the residual stress. Table 4.7 presents the results of this analysis.

The results shown in Table 4-7 show agreement between the stress calculations obtained using the analytically derived relationship and the relationship obtained from the finite element analysis. The differences between the results calculated using the two different methods are less than 3%. The results also show that the residual stresses in the Seabrook service tubes are higher than the other tubes.

Table 4-8 compares the calculated residual stresses using the finite element analysis technique to the residual stresses obtained from strain gauge measurements. These results show that all of the stresses obtained using the strain gauge measurements are higher than the stresses calculated using the changes in diameters. This could be explained by the fact that the calculated stresses based on diameter changes assume essentially linear stress gradients through the tube wall thickness while the strain gauges measure the actual strain averaged over the area of the gauges. Work by EPRI has shown that the actual residual stress distributions can be far from linear and can have significantly higher residual stresses on the OD than the ID, Reference 17. Therefore, although the diameter change calculation provides a quick way to estimate differences in residual stresses, measuring the actual strains using strain gauges provides more accurate estimates of the strains on the surface of interest.

Table 4- 6. Percent Diameter Change

Prepared by: Vincent Roy, Checked by: Thomas Service

Sample	Description	Diameter Change (%)
Heat 1638	MA	0.5257
Heat 1638	MA	0.3543
Heat 96845	MA	0.3086
Heat 96845	TT	0.0114
Service R9C63	AR	1.3964
Service R9C63	AR	0.6836

Table 4- 7. Summary of Analytical Residual Stress Calculations

Prepared by: Thomas Service, Checked by: Jose Magalhaes

Sample	Description	Initial Dia. (in)	Thickness (in)	Diameter Change (in)	Diameter Change (%)	Stress Eq (4.1), (psi)	Stress FEA Eq (4.2), (psi)
Heat 1638	MA	0.8750	0.05	0.0046	0.5257	5,886	6,040
Heat 1638	MA	0.8750	0.05	0.0031	0.3543	3,967	4,070
Heat 96845	MA	0.8750	0.05	0.0027	0.3086	3,456	3,545
Heat 96845	TT	0.8750	0.05	0.0001	0.0114	128	131
Service R9C63	AR	0.6875	0.04	0.0096	1.3964	15,956	16,378
Service R9C63	AR	0.6875	0.04	0.0047	0.6836	7,811	8,018

Table 4- 8. Comparison of Hoop Stress Values

Prepared by: Thomas Service, Checked by: Jose Magalhaes

Sample	Description	Calculated Residual Stress (psi)	
		Strain Gauge	Diameter Change, FEA
Heat 1638	MA	7,464	6,040
Heat 1638	MA	9,268	4,070
Heat 96845	MA	8,164	3,545
Heat 96845	TT	2,752	131
Service R9C63	AR	26,248	16,378
Service R9C63	AR	17,198	8,018

4.2 Cracked Tube Analysis

Analysis of the cracked section involved:

- Visual/Microscopic Examination of the OD Surface
- Metallographic Examination
- XPS Analysis of Collected OD Deposit
- SEM Fractographic and EDS Analysis

The results of these analyses are described in detail below. The as-received cracked tubing sample was first characterized in detail using photographic techniques. Based on this characterization a sectioning map was derived. Figure 4-5 shows how the sample was sectioned to obtain the samples required for testing. Sectioning involved first identifying the land area, and then making the first cut at the midpoint of the land. One half of the sample was set aside for possible future testing and the other further sectioned to produce a section for metallography and another for deposit chemical analysis.

The scale/metal interface is the critical region for the definition of the crack initiation environment. The presence of Pb and/or Cu would be significant in the determination of the initiation environment and the root cause of the cracking. It was thus very important to preserve this interface and to be able to analyze the chemistry of this region. Samples from the deposit/metal interface region were obtained by wrapping a tube sample with conductive tape, after which the sample was mechanically expanded to free the deposit from the tube. In this manner a sample was obtained of the actual interface in a condition that was suitable for direct analysis using XPS, SEM and EDS techniques.

4.2.1 Visual/Microscopic Examination of the OD Surface

Figure 4-5 shows the OD surface of the cracked tube in the land area. The land area was characterized by the presence of thicker deposits than regions outside of this region. However, cracks could not be identified by visual means.

4.2.2 Metallographic Examination

The section containing the transverse face of the center of land cut was mounted and prepared in accordance with standard metallographic techniques. The sample was then photographed in the as-polished condition to show crack morphology. Figure 4-6 shows the transverse face of the sample at the 0 degree position. Note that two main cracks are present. In addition to the main cracks several smaller cracks were also observed. Next, the transverse face was etched using the grain boundary etch as described in Section 3.3. Figure 4-7 shows the resulting microstructure. The crack morphology is consistent with intergranular stress corrosion cracking. Further, Figure 4-7 shows intergranular attack (IGA) at the OD surface to a depth of a grain or two. This morphology is further illustrated in Figure 4-8.

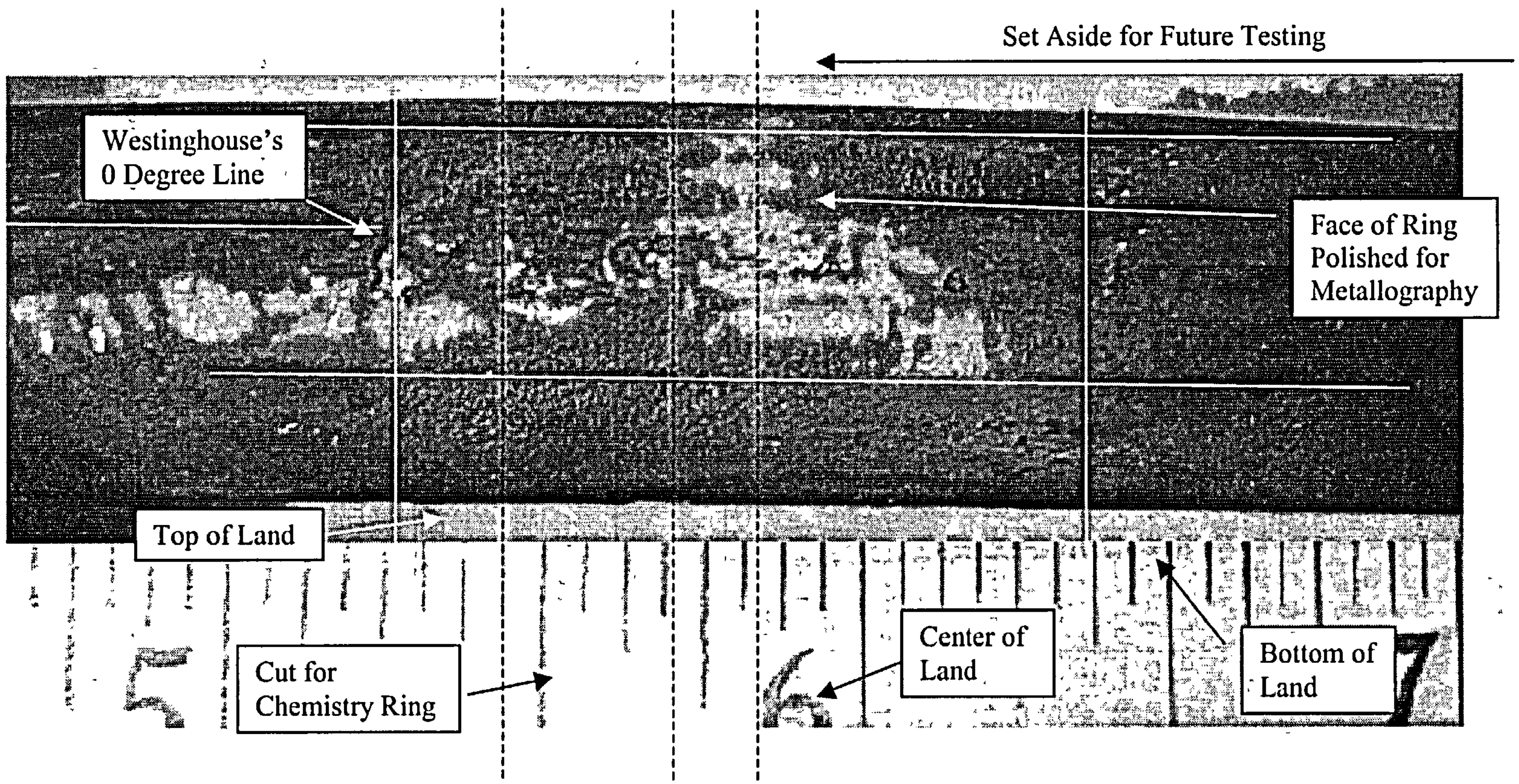

Figure 4- 5. Photograph of Land Area on Cracked Sample, Scale is in Inches

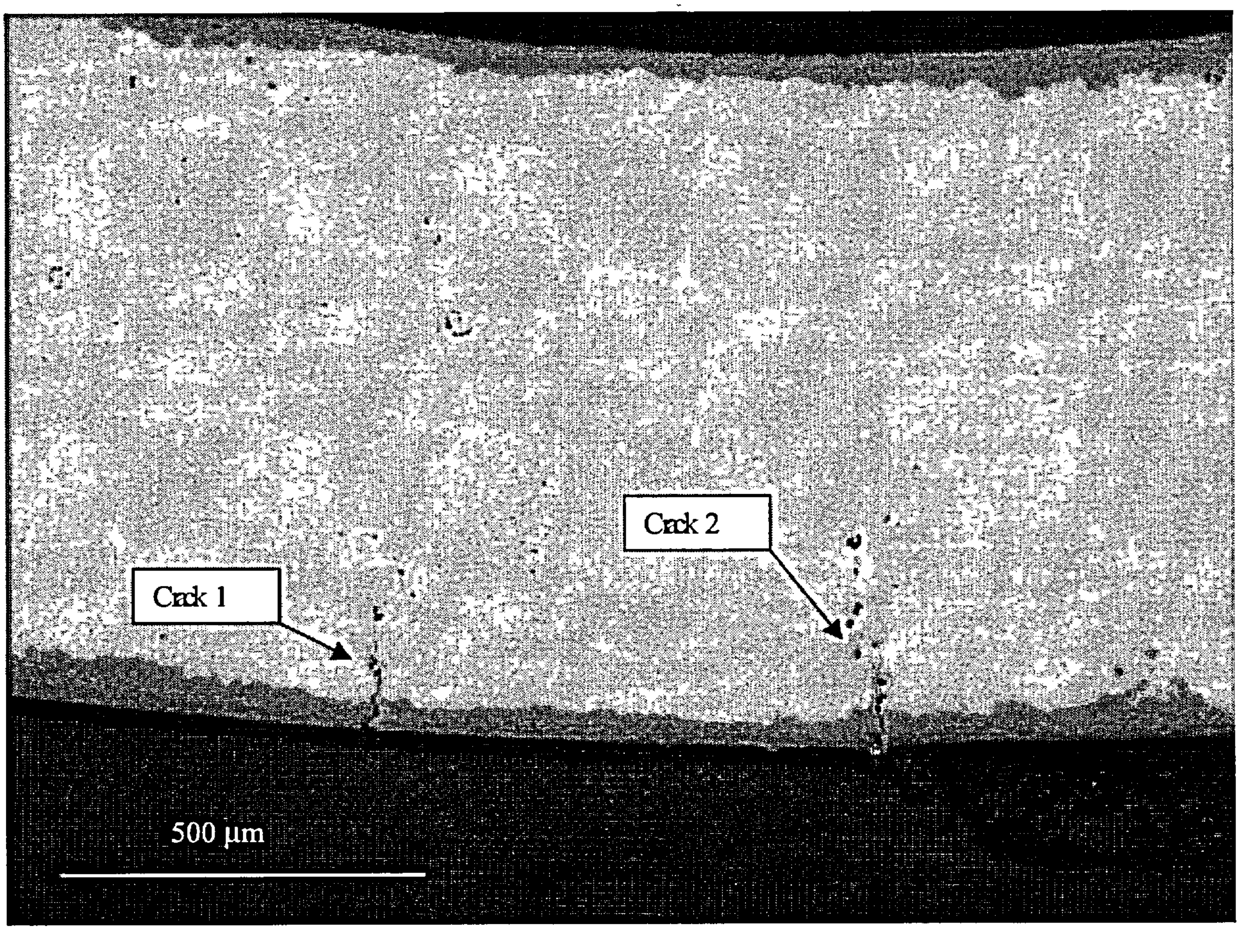

Figure 4- 6. Micrograph of Flawed Sample at the 0 Degree Position

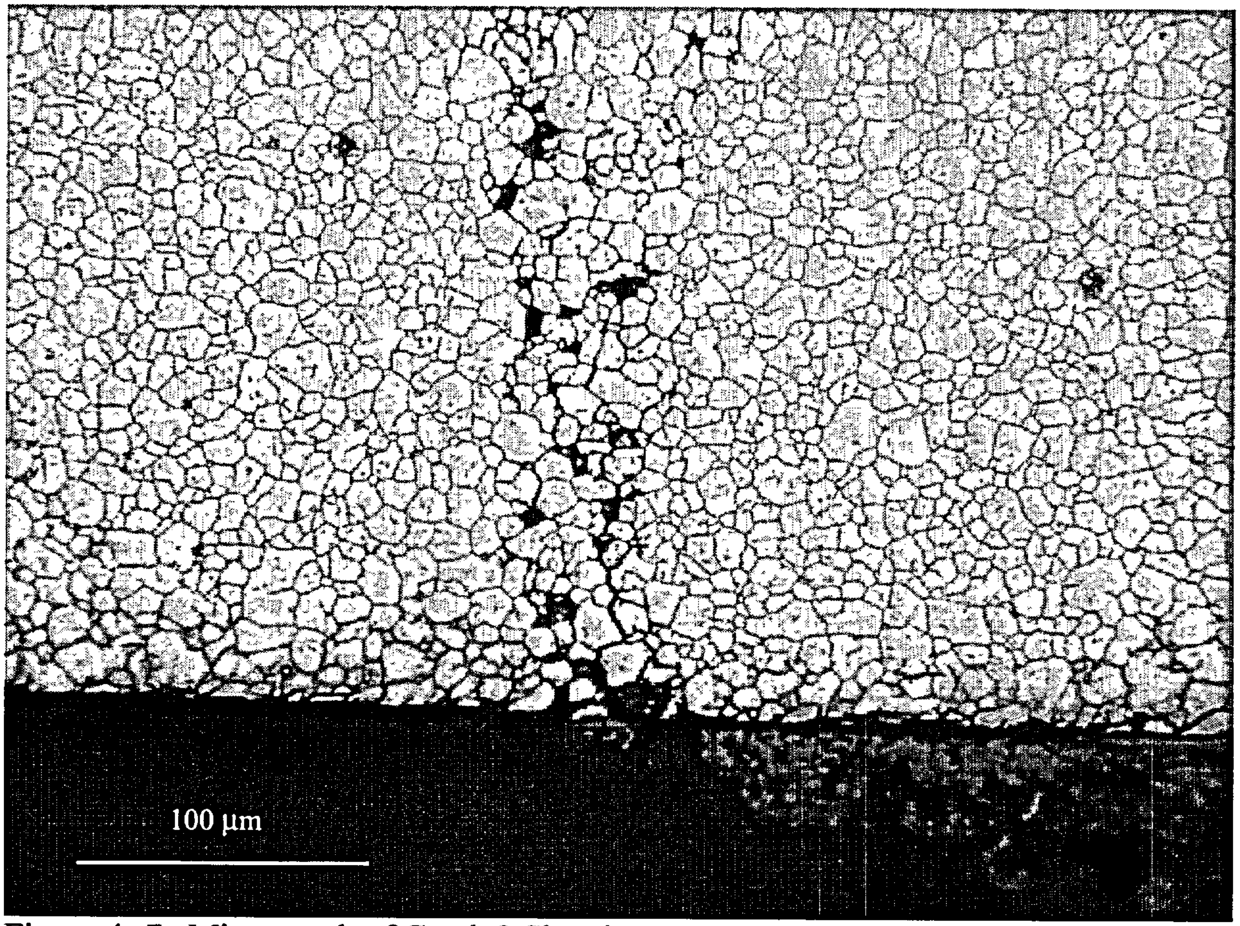

Figure 4- 7. Micrograph of Crack 2 Showing an Intergranular Crack Path

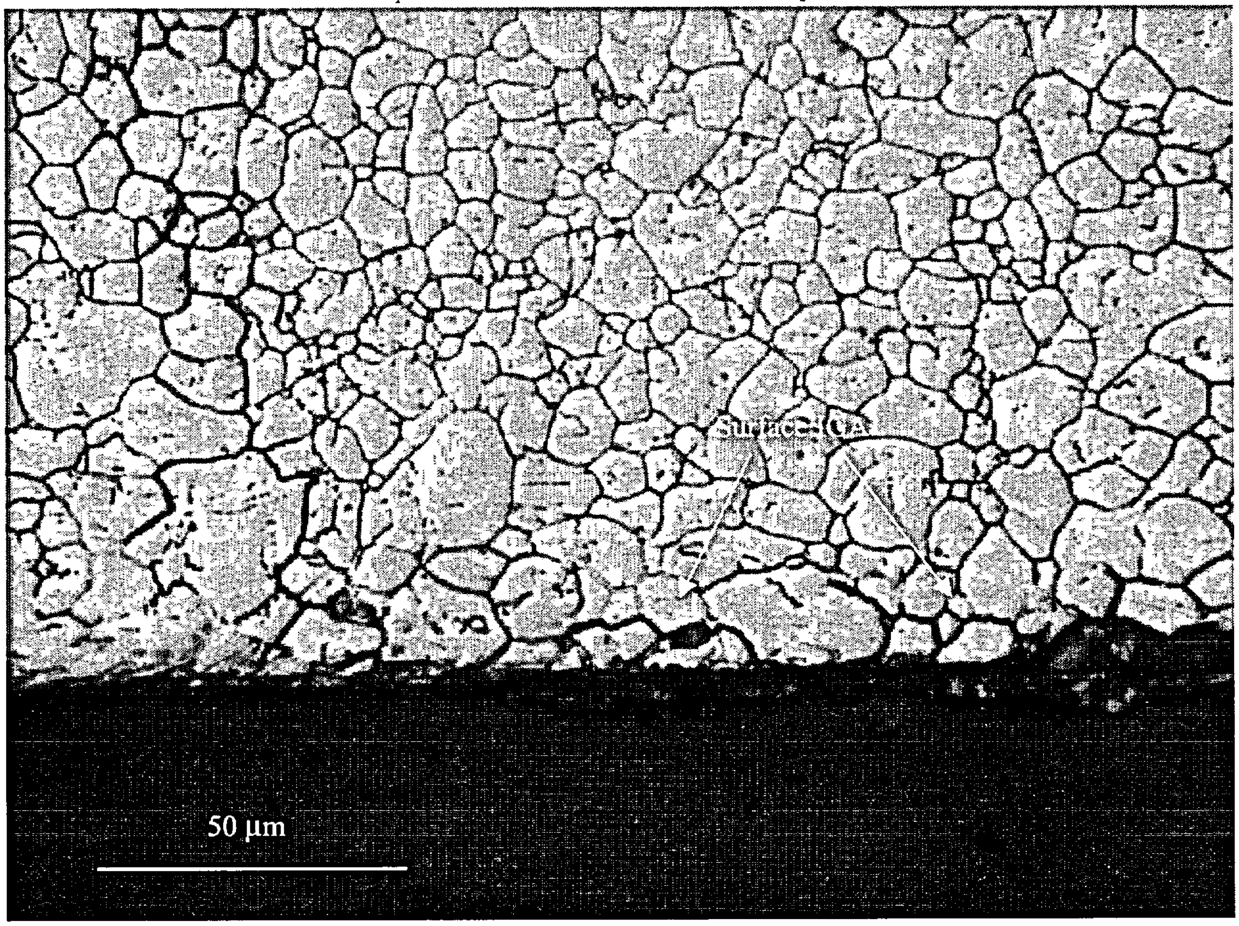

Figure 4- 8. Area on the OD Surface Showing Intergranular Attack, in Land Area

THIS PAGE
INTENTIONALLY
BLANK

4.2.3 X-ray Photoelectron Spectroscopy (XPS) of Cracked Tube Deposit

Figure 4-9 shows a photograph of the tape after removal from the expanded ring. The deposit/metal interface faces up and the mark, above the deposit and to the right, indicates the zero degree reference. Figure 4-10 shows a schematic of where XPS data was collected on the tape. In Figure 4-10 the area bounded by the dotted lines indicates the zero land position. The "V" shape indicates a relatively larger deposit accumulation that was removed from the crack locations on the tube. The locations of the numbered positions and the spot size used for analysis at these location are:

- Position 1 within zero land area (800 µm spot)
- Position 2 within zero land area (800 µm spot)
- Position 3 within zero land area (400 µm spot)
- Position 4 outside zero land area (800 µm spot)
- Position 5 on a new piece of tape (800 µm spot)

Appendix E shows the detailed XPS spectra for these locations as well as sputter depth profiles for positions 2 and 4. Table 4-9 summarizes the concentration of each element present with position. Position 2 showed the presence of Pb but at very low concentration. Trace amounts of copper were also found in some of the samples.

These results are considered to be non safety related, see Appendix E for details.

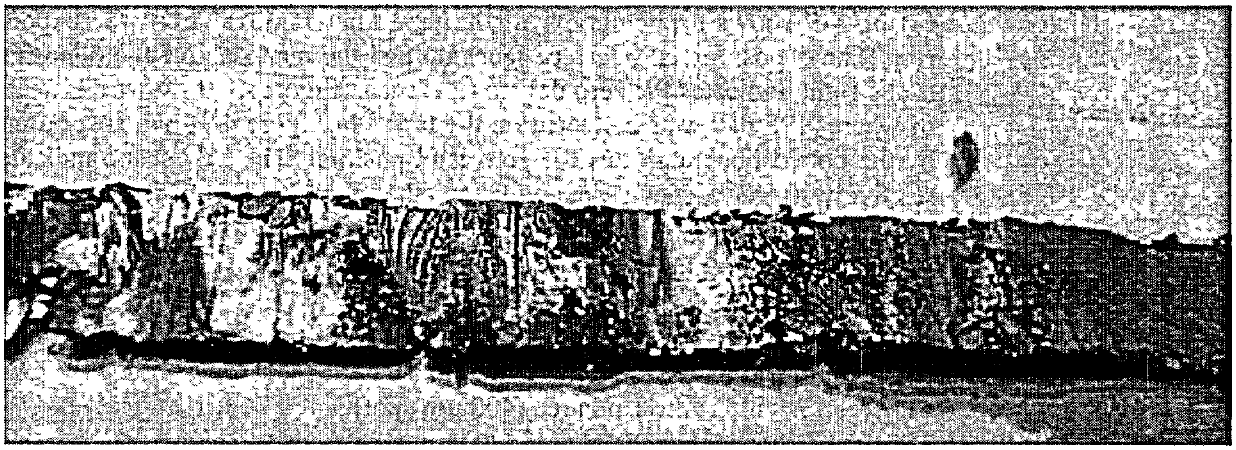

Figure 4- 9. Photograph of the Tape Containing the Deposit

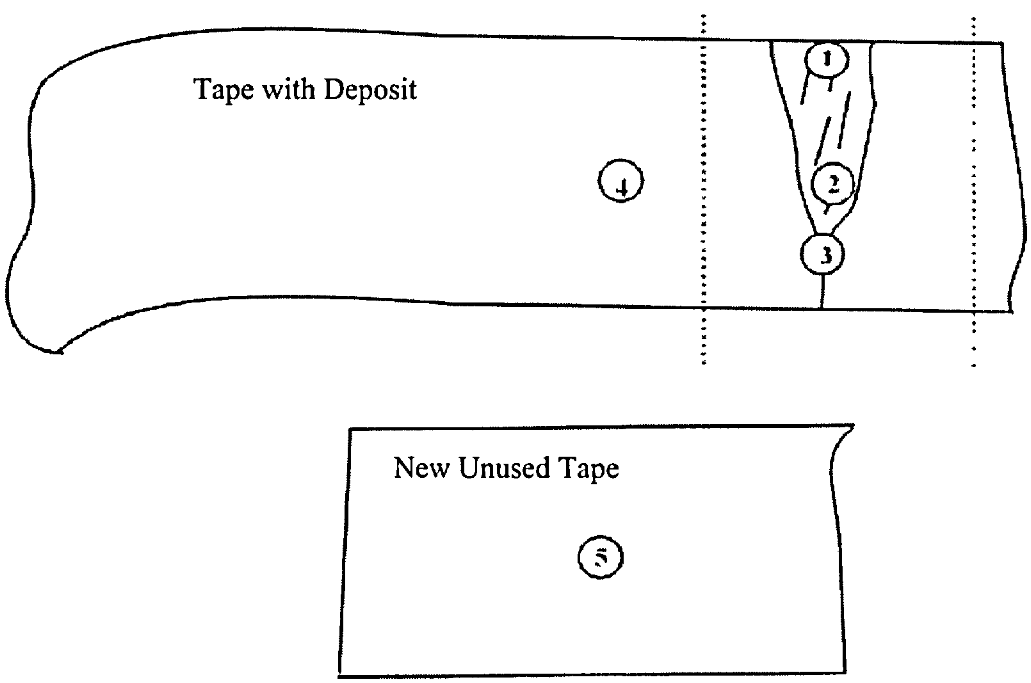

Figure 4- 10. Schematic Showing XPS Locations

Table 4- 9. XPS Summary Table

With Sputter Data

Position	[illegible]	[illegible]	Mg	Si	Al	P	[illegible]	Ce	[illegible]	Cu	[illegible]	[illegible]	Ti	[illegible]	Ni	[illegible]
1	[illegible]	35	23	33	61	26	34[illegible]	32	43[illegible]	1.4	0.3	ND	ND	ND	ND	ND
2	[illegible]	34	27	47	93	22	30[illegible]	11	43[illegible]	1.4	0.3	0.2	ND	ND	ND	ND
[illegible]	[illegible]	72	48	45	13.4	ND	29	61	[illegible]	1.4	ND	0.2	ND	ND	ND	ND
[illegible]	[illegible]	73	46	44	13.5	ND	24	61	[illegible]	1.5	ND	ND	ND	ND	ND	ND
[illegible]	[illegible]	84	48	42	13.8	ND	24	57	[illegible]	1.3	ND	ND	ND	ND	ND	ND
3	13.2	ND	ND	1.8	0.7	1.1	30[illegible]	0.2	[illegible]	3.4	ND	ND	1.4	[illegible]	32	ND
4	14.4	ND	ND	ND	0.8	ND	38[illegible]	ND	42[illegible]	1.2	ND	ND	1.4	63	0.3	1.4
[illegible]	38.6	ND	ND	ND	ND	ND	52	ND	[illegible]	1.4	ND	ND	1.3	10.5	11.4	ND
[illegible]	45.3	ND	ND	ND	ND	ND	25	ND	[illegible]	1.3	ND	ND	ND	[illegible]	85	ND
5	[illegible]	ND	5.9	ND	ND	ND	70[illegible]	ND	[illegible]	ND	ND	ND	ND	ND	ND	ND

ND = Not Detected

Without Sputter Data

Position	[illegible]	[illegible]	Mg	Si	Al	P	[illegible]	Ce	[illegible]	Cu	[illegible]	[illegible]	Ti	[illegible]	Ni	[illegible]
1	[illegible]	35	23	33	61	26	34[illegible]	32	43[illegible]	1.4	0.3	ND	ND	ND	ND	ND
2	[illegible]	34	27	47	93	22	30[illegible]	11	43[illegible]	1.4	0.3	0.2	ND	ND	ND	ND
3	13.2	ND	ND	1.8	0.7	1.1	30[illegible]	0.2	[illegible]	3.4	ND	ND	1.4	[illegible]	32	ND
4	14.4	ND	ND	ND	0.8	ND	38[illegible]	ND	42[illegible]	1.2	ND	ND	1.4	63	0.3	1.4
5	[illegible]	ND	5.9	ND	ND	ND	70[illegible]	ND	[illegible]	ND	ND	ND	ND	ND	ND	ND

ND = Not Detected

4.2.4 SEM and EDS Analysis

In addition to XPS analysis the expanded tube samples and scale were further analyzed using SEM and XPS techniques. The mechanical expansion of the tube resulted in an opening of any cracks or IGA that was present but not necessarily observed prior to this. SEM and EDS analysis were performed on the tube surfaces near and within the crack. Additionally, EDS analysis of the deposit removed from the tube was performed.

4.2.4.1 Expanded Tube Specimen

Figures 4.11 and 4.12 show micrographs of the edge of the expanded tube in the location of the land. The cracks are opened due to the expansion of the tube material and are shown to be axially oriented. The faceted surfaces of the cracks, Figure 4.13, shows the cracks to be intergranular as well. The exposed grains within the cracked areas shown in Figure 4.13 were selected for subsequent EDS analysis. The results of this analysis are shown in Figures 4.14 and 4.15. These spectra show elements typical of Inconel alloy 600. However, Figure 4-14 shows the presence of a small amount of lead.

Figure 4-16 shows an area on the OD surface of the specimen in the vicinity of a crack. This area shows regions where the deposit has been lifted and others where it is still intact. The spectra for an area where the deposit has been lifted, Figure 4-17, is similar to Figures 4-14 and 4-15. This spectrum shows the presence of the typical elements present in Inconel 600 and oxygen. The spectra for the area where the deposit still remained, Figure 4-18, shows the presence of a high concentration of oxygen and the typical base metal elements, particularly iron. The oxygen peak indicates the presence of metal oxides on the surface of the tube.

4.2.4.2 Tape removed from Expanded Tube Specimen

A small section of the tape containing the deposit was chemically analyzed using EDS. A typical spectra is shown in Figure 4-19. This spectra is similar to that shown in Figure 4-18, and shows predominantly iron and oxygen peaks typical for iron oxide.

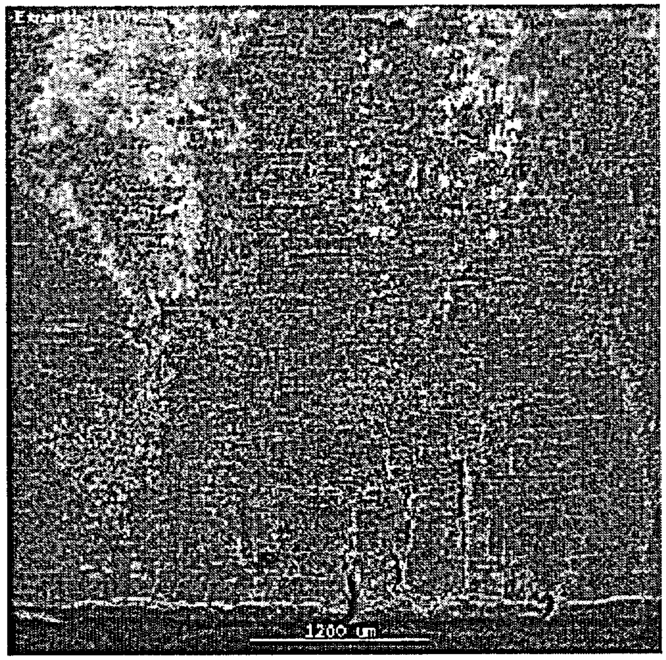

Figure 4- 11. Low Magnification SEM Image of Expanded Tube Edge in Land Area

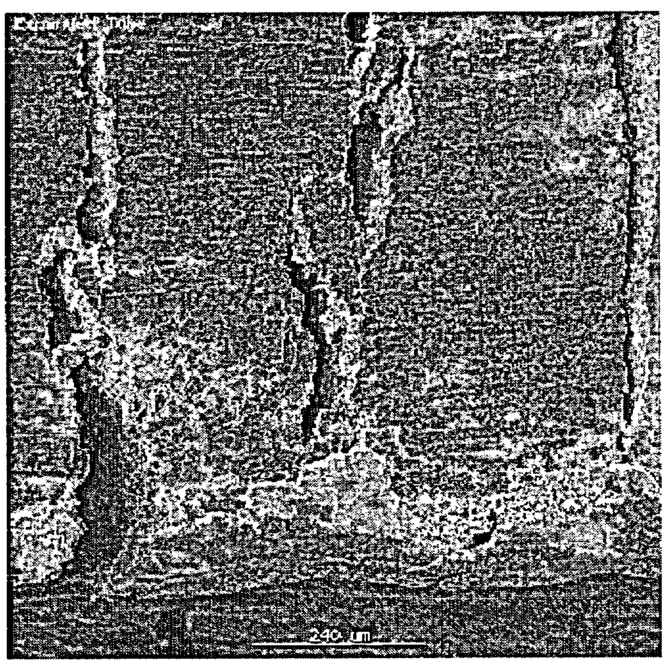

Figure 4- 12. High Magnification SEM Image of Expanded Tube Edge in Land Area

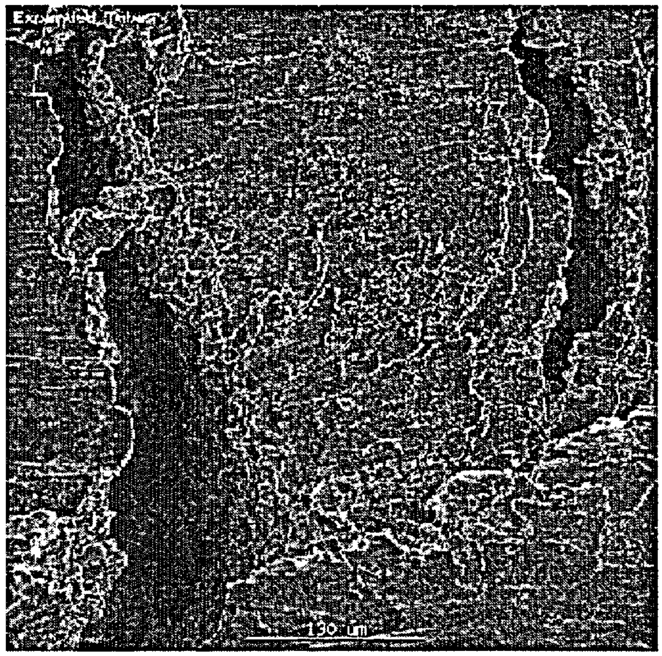

Figure 4- 13. High Magnification SEM Image of Cracks

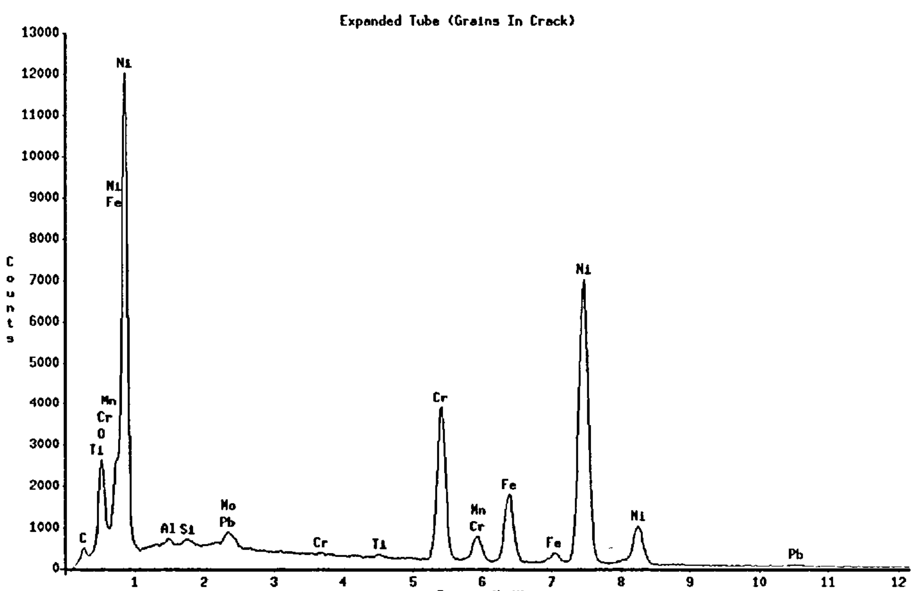

Figure 4- 14. EDS Analysis of Exposed Grains Shown in Figure 4-13

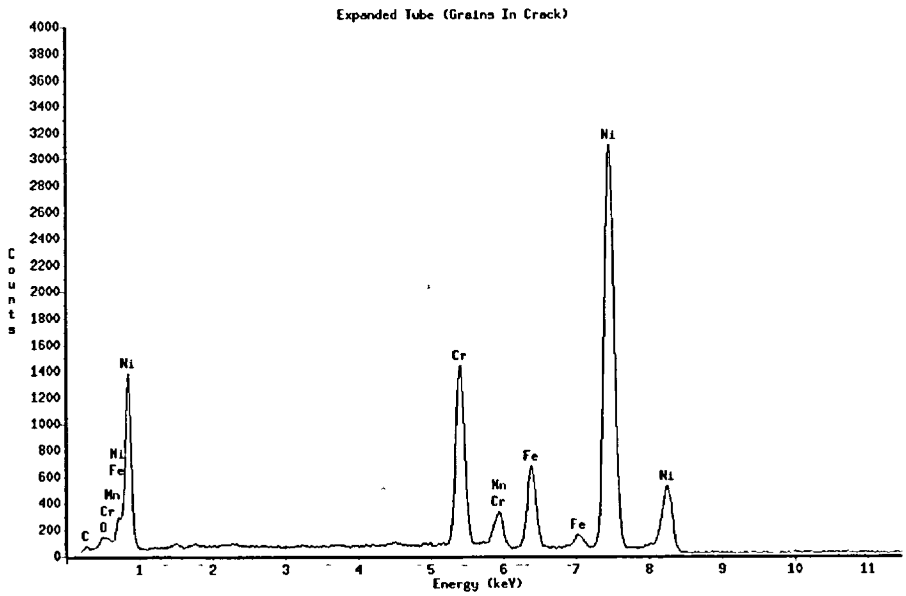

Figure 4- 15. EDS Analysis of Exposed Grains Shown in Figure 4-13

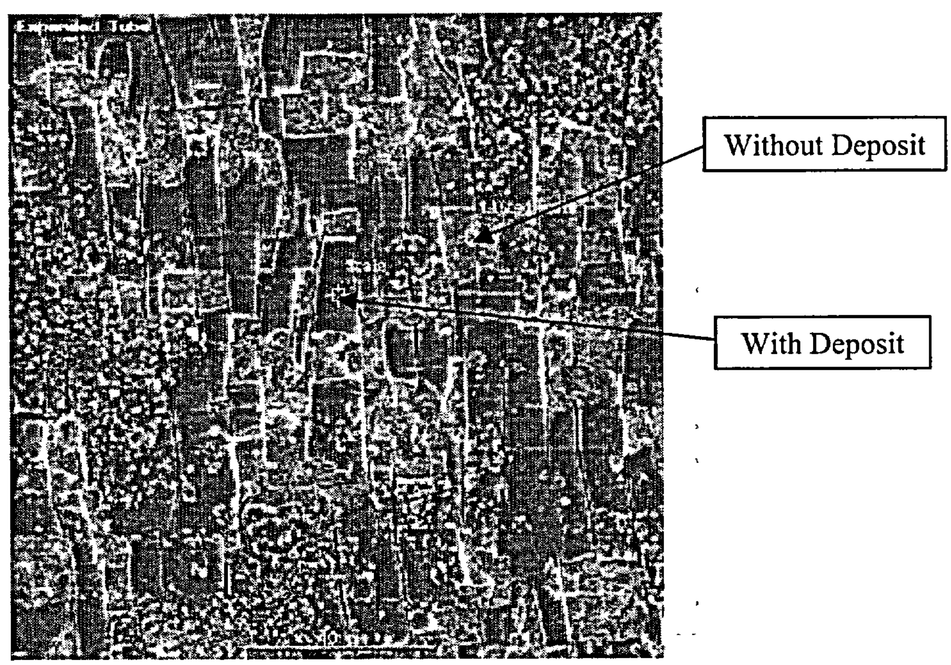

Figure 4- 16. SEM Image of OD Surface in Vicinity of a Crack, Showing Areas With and Without Deposit

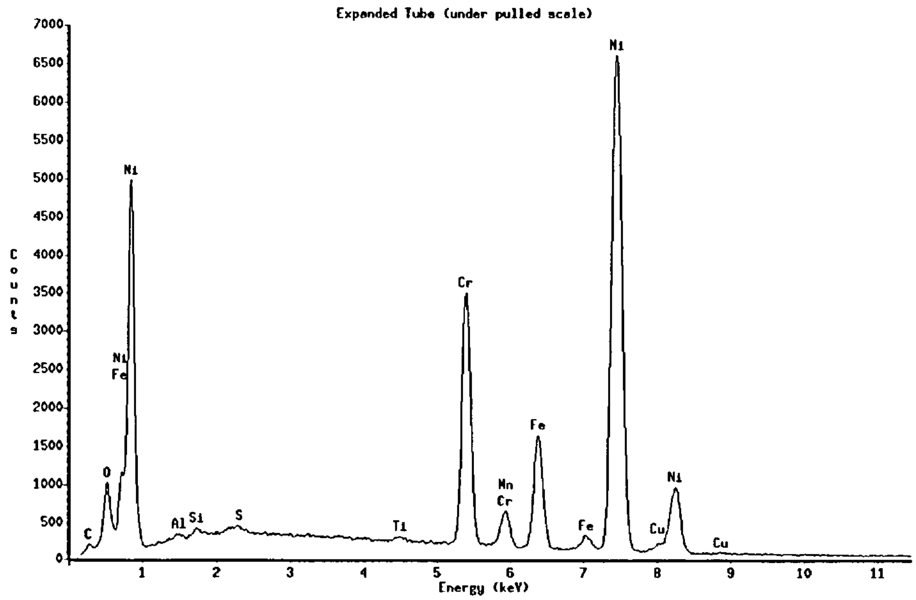

Figure 4- 17. EDS Spectra of Deposit Free Area Shown in Figure 4-16

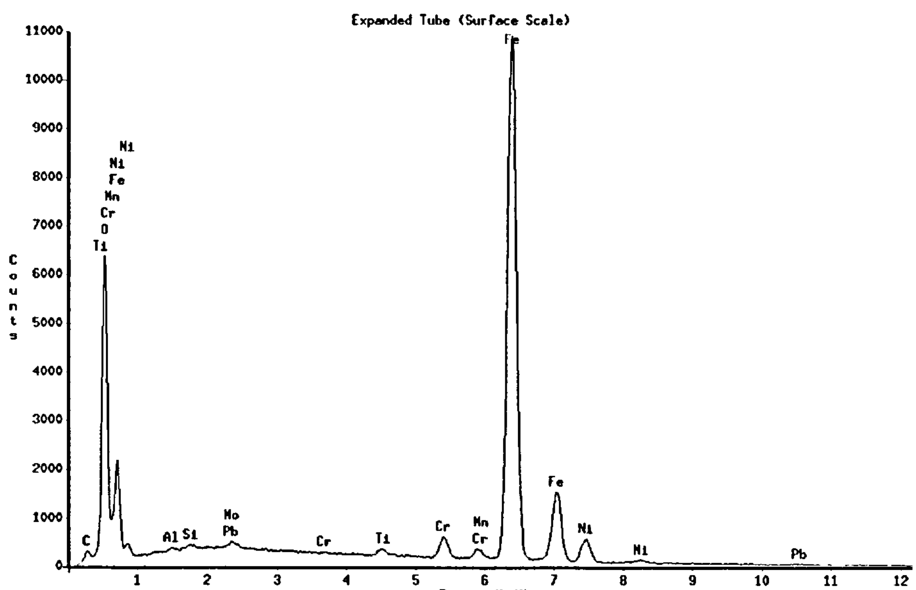

Figure 4- 18. EDS Spectra of Area Shown in Figure 4-16 Where Deposit is Still Present

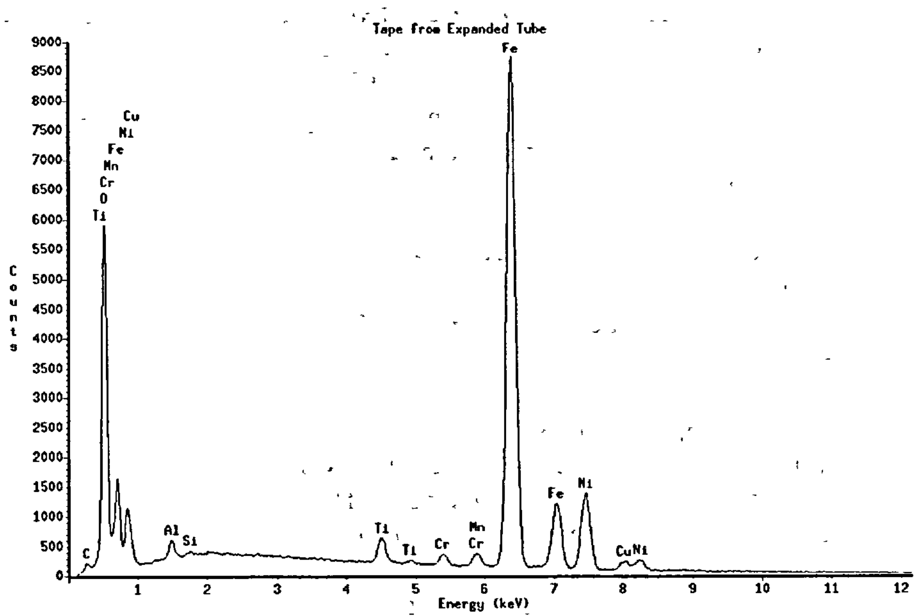

Figure 4- 19. Typical EDS Spectra of the Tape Containing the Deposit.

4.3 Analysis of Tectyl 506G Preservative

Samples of Tectyl 506G, a preservative used in the steam generator during original manufacture and shipping, were analyzed for chemical composition. The analytical methods included EDS for identification of elements, particularly inorganic, and gas chromatography/mass spectroscopy (GC/MS) for identification of organic compounds. Detection of lead or sulfur was of particular interest.

Results of the EDS analysis show a large organic component (carbon and oxygen) and inorganic elements that include sodium, magnesium, aluminum, silicon, sulfur, calcium and iron. The EDS spectrum is presented in Appendix F.

Samples subjected to GC/MS were first analyzed at 200°C. Results of this initial analysis showed the presence of volatiles such as alcohols, ketones, and straight and branched alkanes. However because any Tectyl 506G residuals that may have remained in the steam generator during operation would have been exposed to higher temperature, additional samples were analyzed 300°C. Results of this higher temperature analysis revealed significant changes in the Tectyl material. Lower temperature compounds such as the n-alkanes were converted to organic acids and the ketones appeared as amines. Also detected were propylene glycols, cyclohexanes, xylene isomers, cyclic hydrocarbons, diphenyl sulfides, alkanes, esters and possibly a phosphate compound. The GC/MS spectra are presented in Appendix F.

5.0 SUMMARY

The following summarizes the data presented in this report:

The microstructure of the Seabrook service samples showed heavy intragranular carbide precipitation and a small ASTM grain size of 10-11.
The service samples performed acceptably in the modified Huey test performed with a 25 weight percent HNO_3 solution. The material is not sensitized.
A modified Huey test with a 25 volume percent HNO_3 solution was shown to be a more discriminating test than the standard test with 25 weight percent solution.
As expected, the pulled Seabrook service samples showed higher corrosion rates in the 25 volume percent modified Huey tests than the 25 weight percent.
All Seabrook archived samples performed acceptably in the 25 volume percent modified Huey tests.
Subjecting the in-service tubing to an additional laboratory thermal treatment resulted in a significant improvement in performance in the 25 volume percent modified Huey test.

The Seabrook service samples contained large residual hoop stresses that are not consistent with a thermally treated material.
The cracking is predominantly intergranular, OD initiated within the land region and axially oriented.
A several grain region of IGA is present on the tube OD surface.
Chemical analysis within the expanded cracks, on the tube OD surface and at the deposit/metal interface reveal trace amounts of lead and copper.

6.0 References

1) See Appendix G Reference 1

2) See Appendix G Reference 2

3) See Appendix G Reference 3

4) See Appendix G Reference 4

5) See Appendix G Reference 5

6) See Appendix G Reference 6

7) See Appendix G Reference 7

8) See Appendix G Reference 8

9) R.C. Scarberry, S.C. Pearman and J.R. Crum, "Precipitation in Inconel Alloy 600 and Their Effect on Corrosion Behavior," Corrosion NACE, Vol. 32, No. 10, 1976, p. 401.

10) ASTM E3, Standard Practice for Preparation of Metallographic Specimens, American Society for Testing and Materials, West Conshohocken, PA.

11) EPRI NP-6743-L Guidelines for PWR Steam Generator Tubing Specifications and Repair, Volume 1: Specification for Alloy 600 Steam Generator Tubing, Electric Power Research Institute, Palo Alto, CA, February 1991.

12) ASTM A262, Standard Practices for Detecting Susceptibility to Intergranular Attack in Austenitic Stainless Steels, American Society for Testing and Materials, West Conshohocken, PA.

13) G.P. Airey, A.R. Vaia, N. Pessall and R.G. Aspden, "Detecting Grain-Boundary Chromium Depletion in Inconel 600," Journal of Metals, November 1981, p. 28.

14) Strain Gage Installation with M-Bond 200 Adhesive, Instruction Bulletin B-127-14, Vishay Measurements Group, October 2001.

15) See Appendix G Reference 15

16) Inconel 600 datasheet published on Special Metals Corporation's web site, www.specialmetals.com.

17) "Alloy 690 for Steam Generator Tubing Applications" EPRI Report NP-6997-SD Oct. 1990.

18) "Practical Stress Analysis in Engineering Design", Alexander Blake Marcel Dekker NY 1982.